

Oceanic Currents and Their Implications

Chapter Outline

| | | | |
|--|-----------|--|-----------|
| 1.1. Oceans' Thermohaline Conveyor Belt Circulation and Global Climate Change | 2 | 1.4.4.2. The Somali Current | 24 |
| 1.2. Meandering Currents, Eddies, Rings, and Hydrographic Fronts | 5 | 1.4.5. Equatorial Undercurrents | 24 |
| 1.2.1. Meandering Currents | 5 | 1.4.5.1. Equatorial Undercurrent in the Atlantic Ocean | 25 |
| 1.2.2. Eddies | 5 | 1.4.5.2. Equatorial Undercurrent in the Pacific Ocean | 27 |
| 1.2.3. Rings | 9 | 1.4.5.3. Equatorial Undercurrent in the Indian Ocean | 28 |
| 1.2.4. Hydrographic Fronts | 10 | | |
| 1.3. Influence of Eddies and Fronts on Fishery and Weather | 11 | 1.5. Currents of Different Origins | 29 |
| 1.4. Major Current Systems in the World Oceans | 12 | 1.5.1. Wind-Driven Current | 31 |
| 1.4.1. Antarctic Circumpolar Current | 13 | 1.5.1.1. Ekman Spiral | 31 |
| 1.4.2. Western Boundary Currents in the Atlantic Ocean | 15 | 1.5.1.2. Langmuir Circulation | 33 |
| 1.4.2.1. The Gulf Stream | 15 | 1.5.2. Inertia Current | 33 |
| 1.4.2.2. The Brazil Current | 17 | 1.5.3. Tidal Currents in Open Seas, Estuaries, and Ridge Valleys | 34 |
| 1.4.3. Western Boundary Current in the Pacific Ocean: The Kuroshio Current | 20 | 1.5.4. Rip Currents | 36 |
| 1.4.4. Western Boundary Currents in the Indian Ocean | 22 | 1.6. Implications of Ocean Currents | 40 |
| 1.4.4.1. The Agulhas Current | 22 | References | 42 |

Climate and oceanic researchers consider that one of the most important roles played by the planet's oceans is the regulation of the Earth's climate; naturally this has become the focus of the global approach to research in recent decades. We are increasingly concerned about global climate change (i.e., long-term fluctuations in temperature, precipitation, wind, and all other aspects of the Earth's climate) and its regional impacts. The sea ice extent in the Arctic Ocean has decreased to record minimums in recent years (e.g., Serreze et al., 2003; Comiso, 2006), and such Arctic processes might amplify changes in global climate.

An examination of autonomous drifting float observations collected during the 1990s and historical shipboard measurements suggests that the mid-depth (700–1,100 m) Southern Ocean temperatures have risen since the 1950s (Gille, 2002). This warming is faster than that of the global ocean and is concentrated in the *Antarctic Circumpolar Current* (ACC), where temperature rates of change are comparable with Southern Ocean atmospheric temperature increases (Gille, 2002). It has been found that the

warming is associated with a southward migration of the ACC since the 1950s of about 50 km in the Pacific (Swift, 1995) as well as the Atlantic and Indian oceans (Gille, 2002). A more recent analysis of 32 yr (1966–98) of subsurface layer (200–900 m) temperature observations in the Indian sector of the Southern Ocean similarly show a warming trend concentrated in the ACC, indicative of a southward shift of the ACC of about 50 km (Aoki et al., 2003).

These changes seem to be associated with long-term changes in the overlying atmospheric circulation (Thompson and Solomon, 2000; Fyfe, 2003; Marshall, 2003). From the global ocean modeling standpoint it is known that a change in the position of the surface wind stress over the Southern Ocean can affect a change in the position of the ACC (Hall and Visbeck, 2002; Oke and England, 2004). Transient climate-change simulations carried out by Fyfe and Saenko (2005) suggest that about half of the observed poleward shift of the ACC seen since the 1950s is the consequence of human activity. In the future the ACC is predicted to continue to shift poleward as well as

to accelerate. Based on theoretical studies, these changes appear to be indicative of the oceanic response to changing surface wind stress. The potential impacts of these changes on the global climate system merit investigation.

Global climate change continues to be a hot topic among scientists, climatologists, and the general public across the globe. It has become important to focus closely on the issue of climate change because the climate change is expected to increase the frequency and intensity of weather- and climate-related hazards (Goldenberg et al., 2001; Meehls et al., 2007; Ulbrich, et al., 2009) and will deplete and stress the planet's ecosystems, upon which we all depend (Holmes, 2009). Between 1980 and 2007, more than 8,000 natural disasters killed 2 million people, and more than 70% of casualties and 75% of economic losses were caused by extreme weather events (Jarraud, 2009). It is feared that there is an increased threat of future hurricanes as a result of climate change.

Analysis of the sea-level measurements made across the globe over the past several decades indicates that sea level is currently rising at an accelerating rate of 3 mm/year as a result of global warming. Arctic sea ice cover is shrinking and high-latitude areas are warming rapidly. Extreme weather events cause loss of life and place an enormous burden on the insurance industry. Globally, 8 of the 10 warmest years since 1860, when instrumental records began, occurred in the past decade. Their impacts are in some cases beneficial (e.g., opening of Arctic shipping routes) and in others adverse (increased coastal flooding, more extreme and frequent heat waves and weather events such as severe tropical cyclones). Likewise, the response of ocean boundary currents to climate change may directly affect marine ecosystems and regional climate (e.g., Stock et al., 2011).

1.1. OCEANS' THERMOHALINE CONVEYOR BELT CIRCULATION AND GLOBAL CLIMATE CHANGE

One of the ways the sun's energy is transported from the Earth's equator toward its poles is through the globally interconnected movement of ocean waters (i.e., ocean currents). Currents and countercurrents were first noticed in the oceans by ancient mariners. In understanding the system of oceanic circulation, they made a very simple assumption that from whatever part of the ocean a current is found to run, to the same part a current of equal volume is obliged to run. The whole system of ocean currents and countercurrents is based on this principle. Dr. Smith appears to have been the first to conjecture in 1683 (vide *Philosophical Transactions*) the existence of an undercurrent in the ocean. His conjecture was based on

the finding of a high-salinity surface current in the Mediterranean Sea. This current was found to carry an immense amount of salt into the Mediterranean from the Atlantic Ocean. Because the Mediterranean is not salting up (i.e., its salinity is not increasing day by day), it was logical to infer the existence of an undercurrent through which this salt finds its way out into the Atlantic Ocean again, thus preventing a perpetual increase of saltiness (i.e., salinity) in the Mediterranean Sea beyond that existing in the Atlantic. The proofs derived exclusively from reason and analogies were clearly in favor of an undercurrent from the Mediterranean to the Atlantic.

Seawater temperature and salinity together play an important role in the preservation of equilibrium in the ocean; thus there exists a special category of ocean currents known as *thermohaline circulation* (*thermo* for heat and *haline* for salt). This circulation, primarily driven by differences in heat and salt content, influences the net transport of mass in the ocean. Thermohaline circulation transports large quantities of warm water from the equator to the polar regions and cold water from the high-latitude regions to the low-latitude regions via various pathways and therefore plays an important role in distributing heat energy across the oceans and seas. The ocean currents can thus warm or cool a large region. The planet-spanning thermohaline circulation, also called *meridional overturning circulation* (MOC), is referred to as the oceans' thermohaline *conveyor belt* circulation (see the main image on the front cover of this book).

The wonderful conveyor system of global oceanic circulation consisting of a chain of surface, subsurface, and deep-ocean circulation paths and its role in controlling the global climate have attracted considerable attention in recent years. For maintenance of an efficient conveyor belt circulation system, there should be "sinking" regions as well as "rising" regions at diverse locations in the global oceans to connect them together as a closed circuit.

Careful observations by navigators in the 19th century brought to light the existence of an efficient *rising region* in the Arctic Ocean. The movement of right whales provided a reliable indicator in identifying such a region. Examination of the log books containing the records maintained by various ships for hundreds of thousands of days for preparation of mariner wind and current charts led to the interesting discovery that the tropical regions of the oceans are to right whales as a sea of fire, through which they cannot pass and into which they never enter. Note that whereas sperm whales are warm-water mammals, right whales are a special category of whale that delights in cold water. It was also found that the right whales of the northern hemisphere are a different species from those of the southern hemisphere (Maury, 1855).

It was the custom among the ancient whale hunters to have their harpoons marked with the date and the name of their ship before they fired the harpoons at whales. The presence of a region in the Arctic Ocean that was not covered by ice sheets was identified in the 19th century based on a very short travel time made by the harpoon-stricken right whales in traveling from the Atlantic side to the Pacific side of the Arctic Ocean. The calculation of the short travel time was arrived at based on the logic that the harpoon-stricken whale could not have traveled below the ice sheet for such a long distance, stretching across the entire Arctic path, nor could they have traveled around either Cape Horn (at the southern tip of South America) or the Cape of Good Hope (at the southern tip of South Africa) because of their proven dislike for warm waters. (Right whales are a class that cannot cross the equator because their habits are averse to the warm waters of the equatorial belt.) In this way circumstantial evidence afforded the most irrefragable and irrefutable proof that there is, at times at least, the presence of open water (i.e., water free from ice cover) in the Arctic Sea.

Further, based on rapid drifting of icebergs against a strong surface current, it was inferred that there is a powerful undercurrent through Davis Strait. The most dominant meridional overturning cross-equatorial thermohaline circulation, which traverses northward across the ocean surface all the way up from Antarctica (the return flow of cold water underneath traversing all the way into the middle of the Pacific), is found in the Atlantic Ocean (see the main image on the front cover of this book), and the climatic effect of this arm of the global thermohaline circulation is due to its large heat transport in the North Atlantic. It has been estimated that the amount of heat transported into the northern North Atlantic (north of 24°N) warms this region by ~5°K. This is indeed roughly the difference between sea surface temperatures (SST) in the North Atlantic compared to that in the North Pacific at similar latitudes (Rahmstorf, 2006). As a result of the existence of warmer surface currents in the North Atlantic sector compared to the North Pacific, the sea ice margins in the Atlantic sector are pushed back, which in turn leads to reduced reflection of sunlight and thus warming (albedo feedback).

In particular, it is recognized that since 1860 the net thermal effect of the northbound currents has caused a decrease in the extent of the ice cover in the Nordic Seas in spring. A continuation of this trend is predicted by global circulation models. If these predictions turn out to be correct, a permanent warming of the Arctic's climate and a decrease of the ice extent of the Barents Sea and the Arctic Ocean are likely to occur. Climate change will, in turn, affect large-scale circulation volume transport, which causes changes in water masses and subsequently affects

the Arctic marine ecosystem (Scottish Association for Marine Science [SAMS] report). Part of the cross-equatorial thermohaline circulation in the Atlantic Ocean is known as the *Gulf Stream*, providing some of the heat that keeps Europe warmer in winter than regions of North America at the same latitude.

The “conveyor belt” circulation spanning the world oceans is maintained primarily by the following four factors (Rahmstorf, 2006):

1. Downwelling (sinking) of water masses from the sea surface into the deep ocean in a few localized areas (e.g., the Greenland-Norwegian Sea, the Labrador Sea, the Mediterranean Sea, the Weddell Sea, and the Ross Sea)
2. Spreading of deep waters (e.g., North Atlantic Deep Water, and Antarctic Bottom Water) mainly as deep western boundary currents
3. Upwelling of deep waters into the sea surface (mainly in the Antarctic Circumpolar Current region)
4. Near-surface currents (required to close the flow)

It is feared that if the northern surface waters somehow become less salty (and therefore less dense)—as might happen if melting of ice sheets due to global warming diluted the upper ocean layer in this region with fresh water—then there would be no scope for the North Atlantic water to sink to the ocean bottom and thus maintain the continuity of the conveyor belt loop. Climate change could thus interfere with the formation of the cold, dense water that drives the thermohaline conveyor belt circulation and thus could bring about further changes in climate. Oceanic current circulation might, therefore, be crucial for climate change, not just over geological time but more immediately (Weart, 2009).

The Southern Ocean waters also play a role in climate change. For example, the ocean waters that move toward the Antarctic sink as their temperatures drop. Once this occurs, these waters then move northward. Water at greater depths has been found to have a significantly different impact than the high-nutrient waters that flow northward at intermediate depths. The circulation in the regions around Antarctica, where water sinks to depths greater than 1.5 km, was shown to be largely responsible for controlling the air-sea balance of carbon dioxide. The circulation in the sub-Antarctic regions that feeds water to depths between 0.5 and 1.5 km controls biological productivity. Further, the sinking water masses in the Southern Ocean are part of the overturning in this region and thus play a major role in the global climate. Interestingly, scientists from the National Aeronautics and Space Administration (NASA) and Columbia University in New York have used computer modeling (the Goddard Institute for Space Studies [GISS] climate model) to successfully reproduce an abrupt climate change that took place 8,200

years ago after the end of the last Ice Age. At that time, the beginning of the current warm period, climate changes were caused by a massive flood of freshwater into the North Atlantic Ocean. Scientists believe that the massive freshwater pulse interfered with the ocean's overturning circulation (the conveyor belt), which distributes heat around the globe. The GISS climate model is also being used for simulation by the Intergovernmental Panel on Climate Change (IPCC) to simulate the Earth's present and future climate.

One of the most persistent concerns among some climatologists is that with the collapse of the MOC or even catastrophic transitions in its structure, the climate system might lurch into a new state. These climatologists go even to the extent of fearing that a new glacial period could begin in the absence of the vast drift of the colossal amount of tropical warm waters northward, near the surface of the Atlantic, as a result of the collapse of the conveyer belt circulation. Some climate models have indicated that a shutdown of the conveyer belt is especially likely with rapid increase of greenhouse gas emissions, although a dramatic shift of the ocean circulation is expected to be very unlikely within the 21st century (International panel, 2007). Thus, the oceanic current circulation—together with the general circulation of the atmosphere—plays a very important role in global climate change.

Lack of sustained observations of the atmosphere, oceans, and land has hindered the development and validation of climate models, which are required to understand and eventually make predictions for changes in both the atmosphere and the ocean. Such predictions are needed to guide international actions, to optimize governments' policies, and to shape industrial strategies. An issue that has been debated in recent times is an example that came from a recent analysis, which concluded that the currents transporting heat northward in the Atlantic and influencing the western European climate had weakened by 30% in the past decade. This result had to be based on just five research measurements spread over 40 years. Questions have been asked as to whether this change could be part of a trend that might lead to a major change in the Atlantic circulation, or due to natural variability that will reverse in the future, or an artefact of the limited observations?

The Greenland Sea (a region that links the Arctic Ocean and the North Atlantic) has a unique worldwide impact on the properties of deep-ocean waters. The surface waters of the Greenland Sea area are sufficiently cold and salty in the winter that they become denser than the water below and then sink to great depths. This creates a source of cold water that can be traced around the globe through the deep oceans, extending from the north Atlantic to the south Atlantic around the tip of Africa through the Indian Ocean and up into the north Pacific.

Oceanographic research programs sponsored by multiple nations have evolved to observe in detail the movement of cold Arctic water as it travels through the Greenland Sea into all the world's oceans and to study the interactions of the atmosphere, ice, and ocean in the Greenland Sea. The deep-water current formed by conditions in the Greenland Sea is important to the processes of ocean mixing worldwide. This cold-water mixing has an effect on not only the physical properties of the global ocean but on biological activities as well because it affects the distribution of nutrients. Some atmospheric carbon dioxide is absorbed into the ocean, and the rate of deep-water mixing has an effect on the amount of that absorption.

The Atlantic Ocean has a prominent role among all other oceans in terms of its influence on climate, because this is the only ocean that provides a direct link between the equatorial warm waters and the cool waters of both the southern and the northern polar regions. The principal current system of the Atlantic Ocean is the Gulf Stream, which is often likened to a grand river in the ocean. There is no other such majestic flow of waters in the world. Its current is more rapid than the Mississippi or the Amazon. The Gulf of Mexico is well known for strong currents associated with the Loop Current and Loop Current eddies (LCE) and mesoscale (order 100 kilometers) features in near geostrophic balance. LCE currents usually extend to 400 m or deeper. The ancient sailors who navigated in simple wooden boats dreaded storms in the Gulf Stream more than they did in any other part of the ocean. It was not the fury of the storm alone that they dreaded, but it was the "ugly sea" that those storms raised. The current of the stream running in one direction and the wind blowing in another direction creates a sea that is often frightful. Lieutenant M. F. Maury ([Maury, 1855](#)) provides a telling account of how 179 officers and soldiers of a regiment of U.S. troops on board a fine new steamship, the *San Francisco*, were washed overboard and drowned after the ship was terribly crippled by a gale of wind in the Gulf Stream in December 1853.

The net transports of mass, heat, and salt through straits (i.e., narrow passages between basins of oceans or marginal seas) may represent a control for interior processes or forcing and thus is of interest for the functioning of a basin or as a boundary condition for modeling studies. Because straits give integrals of the fluxes over the interior basin, they potentially provide important observation sites for various applications. For example, monitoring the variability of the low-frequency transport through the Strait of Gibraltar is important for a wide range of problems. [Send et al. \(2002\)](#) has provided an overview of the water-current circulation studies on the Strait of Gibraltar in the context of climate change.

On the largest scale, the Mediterranean outflow plays an important role in the circulation of the North Atlantic

Ocean. The Mediterranean salt tongue is one of the main components of the Atlantic water mass system, extending across nearly the entire basin from the outflow at the Strait and strongly influencing the salinity budget of the Atlantic Ocean. Recent studies suggest that correct inclusion of the mass flow out of the Mediterranean (in Sverdrups) is necessary for a correct representation of the salt tongue in numerical models (Gerdes et al., 1999), as opposed to the frequently used salinity source at the Strait of Gibraltar.

The Mediterranean outflow and its intensity also may play a role in the dynamics of the North Atlantic. Reid (1979) speculated that the high-salinity Mediterranean Water (MW) may influence North Atlantic Deep Water formation and thus the global thermohaline circulation (THC). In a series of idealized global ocean models, Cox (1989) showed that the salty MW enabled the North Atlantic Deep Water to penetrate deeper and farther south in the Atlantic and into the Indian and Pacific Oceans. Rahmstorf (1998) used a simple coupled model to compare the THC with and without the Mediterranean outflow. He found that the THC intensifies by 1–2 Sverdrups ($1 \text{ Sv} \equiv 10^6 \text{ m}^3/\text{s}$) and that northern Atlantic surface temperatures increase by a few tenths of a degree if the outflow is included. The outflow from the Strait of Gibraltar even appears to be relevant for some large-scale, upper-layer current systems. There is a large flow of chilled polar waters into the Atlantic Ocean, and the preservation of the equilibrium of the Atlantic Ocean needs to be accounted for with the presence of undercurrents, which play an important part in the system of oceanic circulation.

It is interesting to note that probably the first observations of the penetration of Antarctic intermediate water into the North Atlantic were made in 1886 by the British oceanographer J. Y. Buchanan during the *Challenger* Expedition (December 1872–May 1876) for investigating “the physical and biological conditions of the great ocean basins.” His charts and vertical sections showed the global distribution of salinity for the first time and partially revealed the conveyor belt circulation, which was unheard of before that time.

1.2. MEANDERING CURRENTS, EDDIES, RINGS, AND HYDROGRAPHIC FRONTS

The complexity of the mesoscale ocean flow field has often been visualized as an evolving mosaic of eddies, rings, frontal systems, plumes, lenses, and filamentous jets.

1.2.1. Meandering Currents

Meandering currents (often called *meanders*) are those category of currents that “snake around,” exhibiting a characteristic wavy nature in the horizontal and vertical

planes. Under some conditions, the meanders grow exponentially, close upon themselves, and pinch off a closed loop with either cyclonic or anticyclonic circulation (depending on whether the meander is convex or concave, looking northward).

Trajectories of surface floats and subsurface floats over large areas in the oceans have shed much light on the complex motions of oceanic waters such as meandering currents, eddy motions, and rings. Several subsurface floats have been launched in the Gulf Stream (off the east coast of North America) since the beginning of 1983. Rossby et al. (1986) have provided an example of the space-time evolution of the meandering current, based on the trajectory of a subsurface float. The trajectory exhibited the characteristic wavy nature of the meandering Gulf Stream. In this example, the mean speed of the float was 55 cm/s. A striking aspect of this and all other float tracks in the Gulf Stream was found to be the tendency for floats to shoal from meander trough to crest and to deepen from a meander crest to the next trough. It was observed that during the float’s 2,100 km journey to the east, its lateral displacements relative to the current were less than 100 km. From the pressure record it was noticed that these motions are not random but were clearly a result of the dynamics of curvilinear motion. For example, Figure 1.1 shows an artist’s rendition of a multiscale circulation of the Gulf Stream (GS) meander and ring region. Large-scale meandering of oceanic currents results in shedding of mesoscale eddies and rings.

Apart from the most stable meander found in the Gulf Stream, meanders are commonly also found in the other major western boundary current systems. For example, the Kuroshio Current south of Japan exists in one of two stable paths, a zonal path and a meander path, each lasting for a period of years. Mizuno and White (1983) reported identification of a quasi-stationary meander pattern (Kuroshio Meander) in the Kuroshio Extension in the vicinity of the Shatsky Rise (160°E). The Kuroshio Meander becomes unstable as a consequence of increased eddy activity and ring production.

1.2.2. Eddies

The term *eddy* refers to rotation (vortex motion) of water mass. The motion of an eddy can be likened to that of a spinning top, having both rotary and translatory motions. The horizontal cross-section of most eddies is essentially circular in shape, whereas others are much more elongated (both these types of eddies have been noticed in the vicinity of Sugarloaf Point off the east coast of Australia; see Tilburg et al., 2001). Twin eddies have also been noticed in some regions. Eddies usually taper toward the bottom, but cylindrical-shaped eddies are not uncommon. In the case of essentially elliptical eddies, the swiftness of the current in

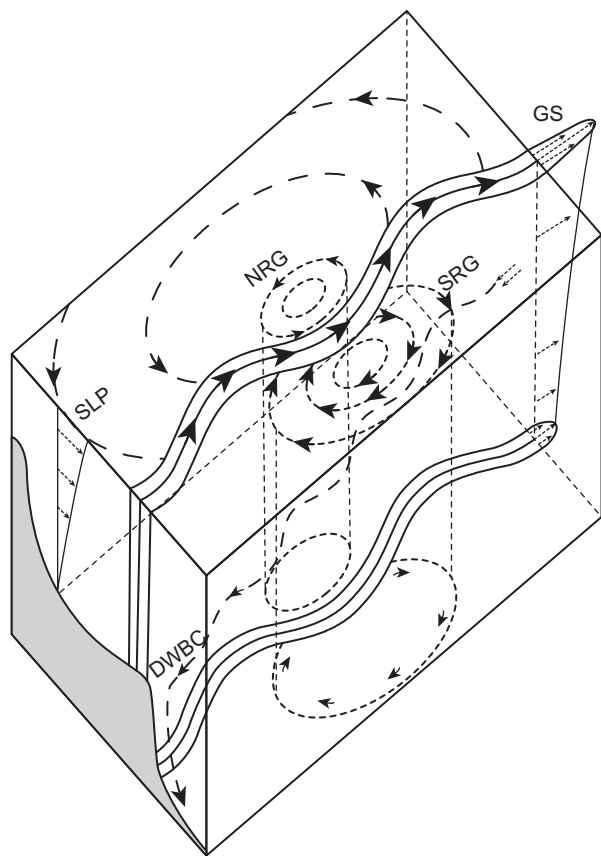


FIGURE 1.1 Artist's rendition of a multiscale circulation of the Gulf Stream (GS) meander and ring region. The large-scale meandering of the Gulf Stream results in mesoscale eddies while interacting with the subbasin-scale gyres (NRG and SRG). The deep western boundary current flows along the 3,400 m isobath and crosses under the Gulf Stream near Cape Hatteras to flow further southward. (Source: Gangopadhyay et al., 1997. © American Meteorological Society. Reprinted with permission.)

certain portions of the eddy can be much different from the other portions. Eddy diameters are in the tens and hundreds of kilometers. Some are warm-core eddies; others are cold-core eddies.

Cold-core eddies cause transport of nutrient-rich water from ocean depths to the sea surface, thereby providing them a low-temperature signature. A horizontal spatial gradient in nutrient-rich water relative to the vertical axis of the core results in a corresponding spatial gradient in chlorophyll concentration. Whereas the spatial gradient in temperature relative to the core allows remote detection of eddies using satellite-borne thermal radiometers, a spatial gradient in chlorophyll concentration relative to the core allows remote detection of eddies using satellite-borne visible wavelength radiometers. Whereas cold-core eddies have their centers depressed, *warm-core eddies* have elevated centers. This enables their detection by satellite-borne altimeters. *In situ* hydrographic measurements

are often employed for detailed examination of eddy structure. The core of the eddy current is defined as the region of fastest-flowing surface current (Andrews and Scully-Power, 1976).

The mechanisms that generate eddies in the open ocean include baroclinic (i.e., surface of equal hydrostatic pressure crossing surface of equal water density) instability of large-scale currents, topographic steering, and direct atmospheric forcing (Kamenkovich et al., 1986, Ikeda et al., 1989). In general, Antarctic Circumpolar Current and western boundary currents (i.e., currents flowing in the vicinity of the western boundaries of oceans) such as the Gulf Stream and the Brazil Current in the Atlantic, Kuroshio and East Australian Currents in the Pacific, and the Agulhas Current in the southern Indian Ocean have the potential for generating warm- or cold-core eddies, which are an integral part of the general circulation (see descriptions of these currents in section 1.4 (Major Current Systems in the World Oceans)).

With the deployment and monitoring of increasing numbers of subsurface floats at various depths, oceanographers have gained increased knowledge of some facets of the extremely complex oceanic circulation features in the interior of the ocean basins. An illuminating account of the complex movements of a cluster of subsurface floats at a depth of about 1,300 meters is provided by Rossby et al. (1975) and Rossby (1983). They described a variety of exciting time-dependent events such as a chain of eddy lenses, each about 600 m thick and 100 km in diameter. Some floats exhibited striking anticyclonic motions with time periods as large as eight months. In fact, Rossby and co-researchers observed repeated cyclonic and anticyclonic oscillations of a cluster of some floats in direct response to the effect of the Earth's rotation, exhibiting perhaps "the simplest and most explicit geophysical demonstration of the conservation of angular momentum to date." These interesting effects indicate that eddies not only command considerable interest in their own right but are also a key to our understanding of the general oceanic circulation (Rossby, 1983). New and unexpected findings will certainly help develop appropriate theories to support the observed facts. Hopefully, such theories will permit oceanographers to unravel, at least partially, the hidden secrets of nature.

Eddies are found in several parts of the world oceans. Davis (2005) conducted a comprehensive analysis of the voluminous dataset obtained from Argo floats, using various methods. He found that well-developed strong subtropical gyres feed western boundary currents. It was also found that tropical gyres are separated by eastward flow along the equator in both hemispheres of both the Indian Ocean and the South Pacific Ocean basins, although the Indian subcontinent splits the North Indian tropical gyre. The Indian Ocean's subtropical gyre, and perhaps

part of the South Atlantic's, reaches east to a retroflexion just upstream of the Campbell Plateau, south of New Zealand. It was found that encounter between two different currents gives rise to the generation of eddies. It was also noticed that several Argo floats went from speeds of a few centimeters per second north of the Agulhas (which is the strongest flow, exceeding 50 cm/s, observed off the South African coast in the Indian Ocean), passed through the boundary current in one or two submergence cycles of 25 days, and, after clearing the tip of Africa, decelerated again to a few cm/s where the Agulhas encounters the eastward-flowing South Atlantic Current and apparently breaks up into eddies. In fact, the eddy motion is so vigorous that it clouds the general ocean circulation patterns. In the face of ubiquitous eddy variability, averaging is often required to describe patterns of mean circulation.

Another piece of information obtained from analyses of Argo float datasets is that outside the equatorial zone ($\pm 10^\circ$) seawater circulation is dominated by subtropical gyres bounded by strong eastward flow in the ACC and the South Indian Current (SIC) or South Pacific Current (SPC). It was found that the Indian Ocean's subtropical gyre is at least twice as strong as the South Pacific's, thereby making the powerful intermediate-depth Agulhas Current much stronger than the East Australia Current. Remarkably, the eastern limbs of the southern subtropical gyres in all three basins occur away from land.

Based on satellite-derived data, hydrographic data, and data obtained from moored current meters, Lee et al. (1981) found that on the Georgia continental shelf the Gulf Stream frontal eddies control the residence time of the outer shelf waters, defined as the mean separation time between eddy events. Upwelling in the cold core extends into the euphotic (i.e., light penetrating) zone (~45 m) and shoreward (35 to 40 km) beneath the southward-flowing warm filament in a 20-m-thick bottom intrusion layer. The annual nitrogen input to the shelf waters by this process is estimated at 55,000 tons each year, about twice all other estimated nitrogen sources combined.

Long-term seawater temperature observations have also shed ample light on the presence and lifetimes of several eddies in the world oceans. Such measurements indicated that the Kuroshio Current region in the China Sea is well known for prevalence of cold-core eddies. Stommel and Yoshida (1971) examined the subsurface temperature arranged chronologically for a selected region (Enshunada) in the Kuroshio to clearly document the bimodal state of the Kuroshio in this area. The great Cold Eddy in the Kuroshio, often referred to as the Cold Water Mass, appears from time to time south of Enshunada. Surveys carried out for a decade from 1955 to 1964 by the Maritime Safety Agency have shown the appearance and disappearance of this cold eddy very convincingly. It was found that there exists

a pronounced bimodality between 150 m and 600 m, thus verifying the on and off nature of the eddy. Interestingly, the stream passes through intermediate states quite quickly. The Cold Eddy was present from mid-1934 until the beginning of 1941. The eddy was present also during the last half of 1941 and all of 1942. Stommel and Yoshida (1971) found that the Cold Eddy remained absent until mid-1959, when it abruptly appeared again and stayed turned on for three and a half years until early 1963, when it disappeared once more.

Depending on the local topography and proximity to islands, eddies demonstrate varying characteristics. For example, Robinson and Lobel (1985) report that the ocean eddies that form off the Island of Hawaii can remain in the lee for weeks before moving or dissolving.

Eddies are frequently found in western boundary currents, but they are also found in eastern boundary currents. In fact, eddies are considered to be a general feature of the general circulation. In the Gulf Stream, eddies can form within a week of meander generation and then persist for another one to two weeks (see Lee and Mayer, 1977; Legeckis, 1979). They appear to form all along the Gulf Stream boundary at any time of year, and at times they serve to dissipate kinetic energy from the mean flow (Lee, 1975). They also serve as an effective mechanism for exchange of shelf and Gulf Stream waters. In the Florida Straits, vortex diameters are in the order of 10–30 km, with downstream axes two to three times the cross-stream dimension (Lee, 1975; Lee and Mayer, 1977). The vortex travels northward along the shelf break at speeds less than the mean speed of the Gulf Stream. The vortex occurs on the average of one per week in the Florida Straits and results in large-amplitude, cyclonic flow reversals over the shelf that distort the temperature and salinity fields to a depth of approx. 200 m (Lee, 1975; Lee and Mayer, 1977). In the case of the Brazil Current, eddies are spun off from its northern end as it moves up the north coast of South America. These eddies generate speeds of up to three knots. Lee et al. (1981) investigated the eddy-induced sea surface temperature (SST) features in the Florida Straits and termed them “spin-off eddies” due to their cyclonic rotation, cold core, and exchange of heat and salt with adjacent shelf waters. However, that terminology has been discontinued in favor of a more general definition of the features as *frontal eddies*.

Warm-core eddies off East Australia have been observed from time to time. Wyrtki (1962) produced dynamic topographies of the southwest Pacific that suggested that these eddies are separated from the main current and drift south down the coast. In this study, eddy diameters were found to be in the range 200–250 km, whereas drift rates were estimated to lie within about 5–8 km/day. Hamon (1965) and Boland and Hamon (1970) have also noticed the dynamic height maps of this region usually

showing several intense anticyclonic eddies just offshore. Hynd (1969) tracked a “pool of warm water” with an airborne radiation thermometer for a month in mid-summer, finding a drift rate of 5.5 km/day. The pool was about 50–70 km in diameter and was surrounded by marked temperature fronts. Boland (1973) found that the average time between the appearances of successive eddy structure in the Tasman Sea off the southeast coast of Australia at about 33.5°S is about 73 days and that strong currents appear and disappear within 40-day intervals. Hamon and Cresswell (1972) deduced a dominant length scale (distance between like eddies) of 500 km. Andrews and Scully-Power (1976) examined the structure of an intense, anticyclonic, warm-core winter eddy off the east coast of Australia and found that the eddy had a diameter of 250 km and a mixed layer depth extending to over 300 m in the core. Such deep mixed layer is the most pronounced feature that makes the warm-core eddies off east Australia somewhat unique.

The East Australian Current seems to consist of strong anticyclonic eddies, which tend to move irregularly southward along the coast. In particular, the eddies south of Sugarloaf Point are not separate entities but probably form by the pinching off of current loops that start near Sugarloaf Point (Godfrey et al., 1980). An excellent graphical presentation of a multitude of eddies generated off the southeast coast of Sydney during 1977–1979 has been reported by Godfrey et al. (1980). In the Agulhas Current System, eddies in the Mozambique Channel have spatial scales of approximately 300–350 km and propagate southward at speeds of approximately 3–6 km/day (Schouten et al., 2002, 2003). In the North Pacific, Bernstein and White (1981) found eddy activity in the Kuroshio Extension to be intensified over the abyssal plane between the Izu Ridge and the Shatsky Rise.

Seafloor topography exerts an important role in the generation of eddies. For example, the circulation in the coastal region of the Gulf of Maine and Georges Bank (GOMGB) is associated with features such as the buoyancy-driven Maine Coastal Current (MCC), Georges Bank anticyclonic frontal circulation system, the basin-scale cyclonic gyres, the deep inflow through northeast channel, and the shallow outflow via the great south channel (Gangopadhyay and Robinson, 2002). A schematic of the surface circulation of this coastal region with the features identified is presented in Figure 1.2a; Figure 1.2b shows various processes and the topographic pathways that the coastal features tend to follow. In addition to processes that govern the deep regional dynamics (large-scale wind-driven, barotropic and baroclinic instabilities, meandering and eddy-mean flow interaction), significant variability in the shallow region is determined from water mass formation, topography, freshwater influence, tides, winds, and heating/cooling.

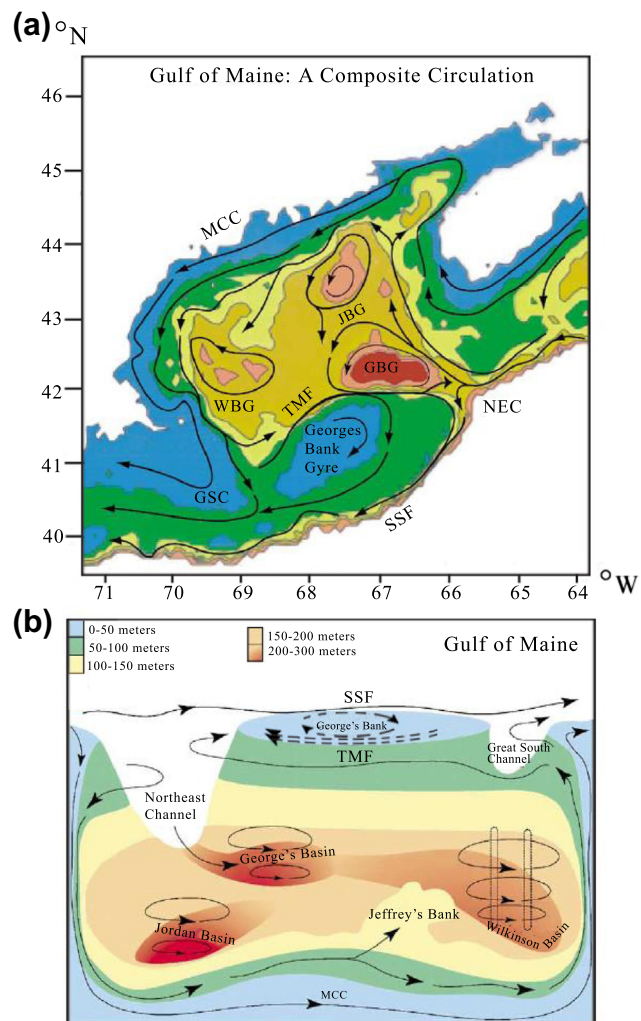


FIGURE 1.2 (a) A schematic of circulation features in the Gulf of Maine: The great south channel (GSC); shelf-slope front (SSF); northeast channel (NEC); Georges basin gyre (GBG); tidal mixing front (TMF); Wilkinson basin gyre (WBG); Maine coastal current (MCC); Jordan basin gyre (JBG). (b) A three-dimensional bathymetric perspective of the regional circulation features. The basins are the three deep regions in the interior gulf. The vertical mixing region is predominantly in the Wilkinson basin. (Source: Gangopadhyay and Robinson, 2002.)

Subsurface eddies that do not reach up to the sea surface have also been reported. For example, based on hydrographic measurements, Babu et al. (1991) reported identification of a cold-core subsurface eddy in the Bay of Bengal (in the Indian Ocean). The thermal structure observed across the eddy (Figure 1.3a) indicates that it was confined to a level well below the mixed layer, between 50 m and 300 m, and that it had a diameter of about 200 km. A temperature drop of 4–5°C relative to the periphery was observed at the center of the eddy. The surface dynamic topography derived from the conductivity, temperature, depth (CTD) data, relative to 500 db, showed that the eddy

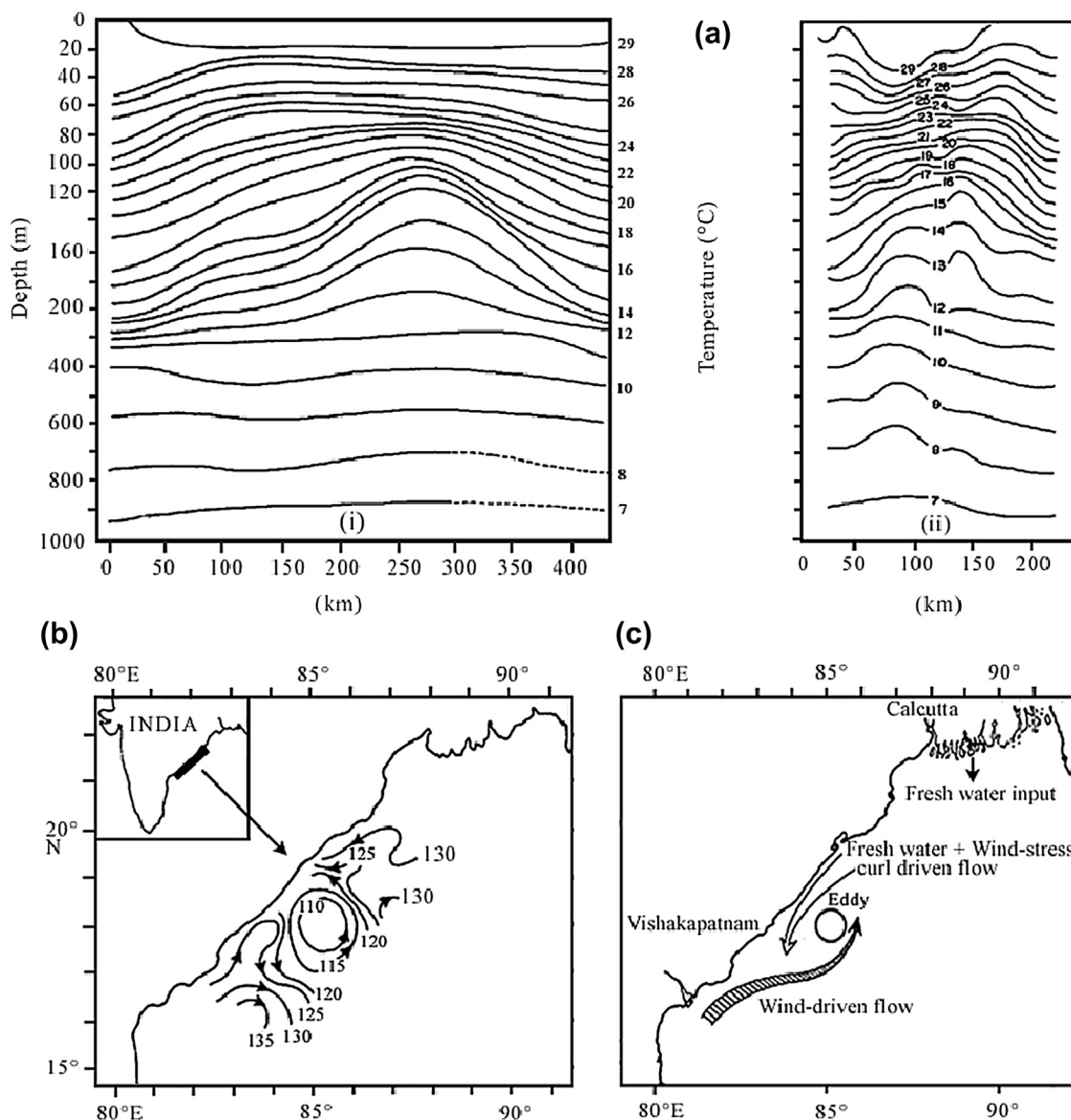


FIGURE 1.3 (a) Vertical distribution of water temperature ($^{\circ}\text{C}$) across a subsurface eddy in the Bay of Bengal off the east coast of India along transects (i) parallel and (ii) normal to the coast (note break in scale at 200 m depth). (b) Surface dynamic topography (in dynamic cm) relative to 500 db. (c) Schematic representation of the eddy and associated currents. (Source: Babu et al., 1991. Reproduced with kind permission from the lead author.)

center was depressed by approximately 10 dynamic cm compared with the waters adjacent to the 200-km-wide eddy (Figure 1.3b), thus indicating cyclonic circulation. Just below the mixed layer, the eddy was elliptical in shape, with a major axis of about 400 km and a minor axis of 200 km. Figure 1.3c gives a schematic view of the eddy and the regional currents. The eddy was apparently generated at the interface of two opposing currents along the western boundary of the Bay of Bengal. High stratification caused by freshwater influx prevented the eddy from being detected at the surface.

1.2.3. Rings

Rings are that category of eddy that exhibits very definitive annulus characteristics; therefore rings can be identified by their distinctive thermal characteristics at the sea surface. Rings are usually identified by a closed contour line, the temperature amplitude size of which is distinctly different relative to the mean background temperature field. For example, Kawai (1979) defined cold rings in the North Pacific characteristically as having water colder than 16°C at a depth of 200 m in the area south of the Kuroshio

Current. The temperature difference is usually greater than 0.5°C. Ring formation usually takes two weeks to one month, as observed by Fuglister and Worthington (1951). But Kawai (1972) showed an example of ring formation that took place more slowly, over a six-month period. Ring shedding is not unusual for western boundary currents. For example, ring shedding from the Gulf Stream, the Kuroshio, the East Australian Current, and the Brazil Current are either well known or have been recognized. The Kuroshio Extension east of Japan is known as a highly variable current, with cold and warm rings generated from the season-to-season unstable growth of meander.

The generation of rings is a fascinating process. Because there is open water on both sides of the jets, the rings are free to meander and snake around. Ring formation is one of the important processes of mesoscale activity in the Kuroshio Extension. Cold/warm rings can be found over the entire Kuroshio Current System, west of 170°E. The warm rings in the Kuroshio Extension adjacent to Japan have been examined by several researchers (for example, see Kawai, 1972; Hata, 1974; Kitano, 1975; Tomosada, 1978). Kawai (1979) studied the geographical distribution of cold rings, finding them to occupy the area southeast of Japan. In the North Atlantic, Richardson (1981) found Gulf Stream meander activity and ring generation intensification by the presence of the New England Seamounts. The upstream or downstream drift of rings and their subsequent reabsorption by the mother current has been observed in the Gulf Stream, the Kuroshio, and the East Australian Current. The coalescence of cast-off rings has also been observed. In the case of the East Australia Current, closed rings are the rule and not the exception.

Lai and Richardson (1977) estimated an average lifetime of 650 days for Gulf Stream Rings, which compares favorably with that estimated for East Australian Current eddies by Nilsson and Cresswell (1981). The Ring Group (1981) estimates an even longer lifetime of up to four years, suggested by the decay rate. The distribution of Gulf Stream rings in the North Atlantic has been studied in some detail by Richardson (1980) and Richardson et al. (1978) and has been shown to be extensive. The drift of eddies cast off from the East Australian Current (Nilsson and Cresswell, 1981) as well as the Brazil Current (Legeckis and Gordon, 1982) has been shown to be small. In many cases the effect of mid-ocean or other ridges on the area in which rings or eddies are to be found is significant (Dantzer, 1976; Roden et al., 1982; Bernstein and White, 1981). This is found to be true in the Agulhas Current rings as well. For example, the ring-shedding area of the Agulhas retroflection is bordered by the Atlantic-Indian mid-ocean ridge to the south, the Atlantic mid-ocean ridge to the west, and the Walvis Ridge to the north. However, it is difficult to find a clear relation between bottom bathymetry and the location of ring

generation, as was shown by Richardson (1981) for the North Atlantic.

The location of maximum ring population probably coincides with the location of maximum generation. Interestingly, warm rings are generated more uniformly along the Kuroshio Extension from 140–170°E, whereas cold-ring generation is concentrated between 140–150°E. Rings of both types propagate to the west at an average speed of 1 cm/s. Whereas cold rings move consistently southward, at about 0.6 cm/s, warm rings move generally northward, at about 0.4 cm/s, but less consistently.

1.2.4. Hydrographic Fronts

Hydrographic fronts in the ocean have always attracted oceanographers' attention. *Ocean fronts* are narrow zones of enhanced gradients separating different water masses. The frontal structure of seawater motion is defined by steeply sloping isopycnals (equal density contour). Fronts, across which there are large horizontal variations of temperature and salinity, are known for the presence of prominent oceanic fine structures (down to a meter-scale wavelength) and microstructures (down to a centimeter-scale wavelength). A front operates to block exchange across it (in the absence of diapycnic mixing). Strong western boundary currents (WBCs) such as the Gulf Stream, Kuroshio, and Brazil Currents are well known for large-scale meandering frontal systems. The Kuroshio warm current and the Oyashio cold current meet in the Kuroshio Extension, east of Japan and form a high gradient frontal structure.

Along-front length scales vary from 100 m to 10,000 km; cross-front length scales from 10 m to 100 km; vertical scales, from 10 to 1000 m; and time scales as short as 1 h. The cross-frontal temperature/salinity changes sometimes exceed 10°C/1 ppt over an order 100 m distance. Ocean fronts are associated with, or accompanied by, strong mixing and stirring, current jets, water mass boundaries, bioproductivity maxima, acoustical wave guides, and atmospheric boundary layer fronts. Subduction, upwelling, and phytoplankton blooms are commonly observed features at oceanic fronts.

Fronts, where two different water masses meet, are ubiquitous features in the ocean and have long been known to be sites of elevated primary production and fertile fishing grounds. The elevated primary production in the frontal regions is supported by the nutrient supply from lower layers associated with the frontal circulation that consists of a primary circulation, the motions of which are mostly directed parallel to the front, and a secondary circulation, the motions of which are orthogonal to the front. The subduction near fronts is a major mechanism for the transmission of atmospheric and near-surface properties, such as heat and carbon dioxide, into the ocean's interior.

Therefore, a proper understanding and proper representation of the subduction process near fronts are necessary to quantify the role of the ocean as a reservoir and sink of heat and carbon in the climate system.

Eddies and rings, which have unique water masses, are considered to be circular fronts. With the availability of satellite data, the unique signature of fronts is now identifiable in the gradients of SST, sea surface height, and sea surface color. SST images derived from satellite infrared radiometers consistently show folded-wave patterns in the western boundary of the Gulf Stream from Cape Canaveral to Cape Hatteras (see Lee et al., 1981). Frontal eddies of this type manifest in the surface waters as warm, tongue-like extrusions of the Gulf Stream oriented toward the south around cold upwelled cores. They were first measured as a succession of overlapping thermal segments termed *shingles* in the pioneering mapping of the Gulf Stream cyclonic front off the southeast United States by Von Arx et al. (1955). The shingle shapes of frontal eddies are more similar to *roll vortices*, which are produced by wave-like rolling up of a shear zone (Rouse, 1963), or *wake vortices*, which are formed in the wake of islands as Karman vortex streets (Wille, 1960). Sailing captains were probably the first to be aware of the transient southward flow generated on the shoreward side of the Gulf Stream by these events. In 1590 it was reported (White, 1590) that a sailing vessel bound from Florida to Virginia had to stand far out to sea to avoid “eddy currents setting to the south and southwest.” It has been suggested that atmospheric forcing can trigger a disturbance in the front that travels with the stream as an unstable wave, eventually evolving into a cyclonic edge-eddy (see Lee and Mayer, 1977; Duing et al., 1977; Lee and Brooks, 1979).

It is important to recognize the role of fronts in describing regional seawater circulation. For example, a large-scale Gulf Stream meandering frontal system also defines the boundaries of unique water masses, which in turn defines the boundary of the basin and subbasin-scale gyres in a synoptic state (see Gangopadhyay et al., 1997). A list of different kinds of fronts that are observed in the eastern boundaries of the world ocean is presented in the first table of Hill et al. (1998) and discussed by many authors in *The Sea* (Robinson and Brink, 1998). These front types include upwelling fronts, equatorial fronts, water mass fronts, plume fronts, coastal current fronts, and shelf-break fronts. It may be noted that the large-scale, wind-driven current transport and its interaction with the adjacent gyres play important roles in the dynamics of the western boundary current fronts (in addition to their role as the boundary of two distinct water masses). The constituent water masses and buoyancy forcing primarily contribute to the formation and maintenance of the coastal and water mass fronts (Hill et al., 1998; Church et al., 1998).

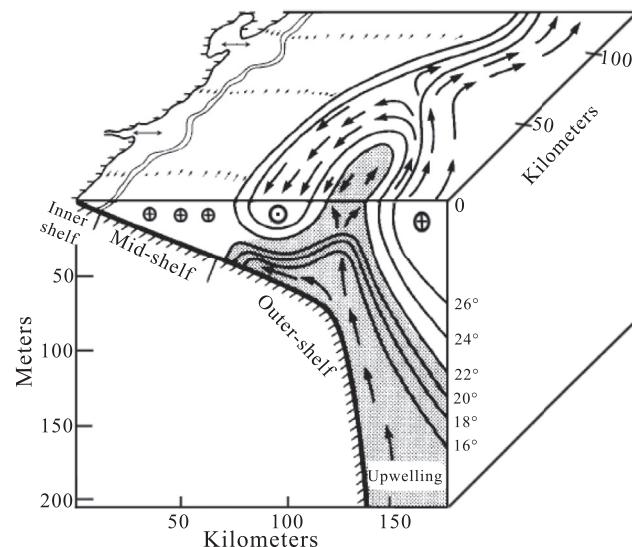


FIGURE 1.4 Schematic characterization of a Gulf Stream frontal eddy on the Georgia shelf. (Source: Lee et al., 1981.)

The deep Gulf Stream Meandering and Ring (GSMR) region has the large-scale meandering Gulf Stream front, which interacts with the subbasin-scale gyres and generates mesoscale eddies, the deep western boundary current, and other mesoscale and submesoscale transients. Schematic characterization of a Gulf Stream frontal eddy on the Georgia shelf is shown in Figure 1.4. Perturbations of the Gulf Stream cyclonic front are commonly observed as folded wave patterns in routine satellite-derived analyses of the western boundary of the Gulf Stream between Cape Hatteras and Miami. The features are defined as cyclonic, cold-core frontal eddies due to their flow and water mass properties (Lee et al., 1981).

1.3. INFLUENCE OF EDDIES AND FRONTS ON FISHERY AND WEATHER

Eddies have vital influence on biological productivity and fishery. Cold-core eddies are associated with *upwelling*, which is an outstanding phenomenon in the ocean whereby cold and nutrient-rich deep water is displaced toward the surface, exerting widespread influence on the ecology, regional climate, and meteorological conditions of the adjacent land (La Fond, 1980). Estimates of speeds of vertical motions in regions of upwelling are from 10–20 m/month to about 80 m/month. Because the upwelled water is rich in nutrients, it could contribute significantly to the biological productivity of the area. There are examples where eddies and associated features in the ocean enhanced plankton and primary productivity, resulting in concentration of large fish schools (Cram and Hanson, 1974; Tranter

et al., 1986). Robinson and Lobel (1985) investigated the role of seasonal low-frequency oscillations of mesoscale currents (eddies) on the dispersal and recruitment of reef fishes in the early 1980s. Many coral reef fishes possess a pelagic larval phase that ranges from several days to several months in duration, depending on the species. Early discoveries of Lobel and co-researchers at Boston University have revealed mesoscale eddies as one of the physical oceanographic mechanisms that can function in favor of the local retention of the pelagic larvae from coastal marine species. Lobel and Robinson (1983, 1986, 1988) proposed that reef fish larvae could be entrained and retained near natal reefs on the basis of the structure and movement of an ocean eddy and the trajectory of current. It was found that the peak seasonality of fishes spawning in Hawaii coincided with a seasonal oceanographic regime that included frequent eddies (Lobel, 1978, 1989).

It has been hypothesized that the larvae during an eddy event would benefit from passive drift by favorable currents, which would bring them regularly near the coastline. Once near the coast, fish larvae would be able to transition (metamorphosis during the settlement process) at the youngest competent ages. Reef fish larvae that are adrift when eddies are absent may spend longer periods at sea due to the less predictable and more chaotic patterns of advection that would bring larvae within range of the shorelines. Studies conducted by Lobel (2011) indicate that mesoscale ocean currents can influence the recruitment pattern of coral reef fishes. For example, the cyclonic ocean eddy off Hawaii that remained in one general area for 70 days from July to September 1982 allowed many reef fish larvae to complete their planktonic development from an embryo to a settlement-stage larva. There are indications suggesting that the rotating stationary eddy (i.e., an eddy having no translatory motion) could be bringing larvae near reefs more regularly than at other times when such eddies are absent. It has also been suggested that ocean currents can be influential in the recruitment process. The frequency with which larval fishes could be transported past a coast is a function of an eddy's swirl speed. An eddy is predicted to act as a major entrapment and near-island retention mechanism. Lobel (2011) found that eddies can enhance local replenishment of populations as well as being a mechanism for transport away. If an eddy develops and remains in a given area adjacent to a coast and thereby retains larvae in local waters, recruitment may be enhanced. Alternatively, if an eddy develops and entrains a quantity of larvae but moves far offshore quickly, it will likely have a diminished effect on recruitment back to the natal area but may result in enhanced recruitment elsewhere.

Links between oceanic fronts in the mid-latitude North Atlantic and North Pacific and the large-scale atmospheric circulation in the Northern Hemisphere have been a subject of study over the last few decades. Efforts to

study the impact of oceanic fronts on the large-scale atmospheric circulations, using various data products and atmospheric general circulation models with high spatial resolutions, have revealed that the oceanic fronts do play a major role in the large-scale atmospheric circulations. It has been found that SST anomalies in the vicinity of the fronts can generate at least local response in the atmosphere (see Kwon et al., 2010; Kelly et al., 2010; Nakamura, 2012). The variations in the Gulf Stream and the Kuroshio—Oyashio Extension exert major impacts on the storm tracks and low-frequency flow in the Northern Hemisphere.

1.4. MAJOR CURRENT SYSTEMS IN THE WORLD OCEANS

Water circulation in the oceans results from a number of primary forcing mechanisms such as thermohaline driving, surface wind stress, tide-generating forces, and so on. Other major influences include the piling-up effect occurring at the western boundaries of the ocean and the presence of ocean ridges, gorges, sandbanks, islands, and the proximity of the seabed. The just-mentioned forces and perturbations produce a spectrum of water motions, with temporal and spatial scale variations spanning from turbulent motions at millimeter scales to interbasin exchanges and large-scale boundary currents that have representative distance scales up to several hundred km and perturbations at time scales of months or longer.

Oceanic water circulation can be broadly classified into steady or irregular motions. In any turbulent flow, heat, chemical components, and dispersed materials are transported not only by the mean currents but also by the turbulent components. Surface waves and shear flows induced by wind stress are the main sources of small-scale turbulence in the upper few meters of the ocean, whereas internal waves and eddies cause turbulent motions at depths. A turbulent motion is made up of a large number of components with different frequencies and length scales. In some cases instantaneous current supplies energy to the mean current. The resolution of the large-scale turbulence problem is especially important in the oceanographic context because the fluctuating turbulent motions are normally much stronger than the velocity of the mean circulation (Zenk et al. 1988). Measurements of turbulent velocity pulsations permit evaluation of energy dissipation rates in the near-surface layer. It is, therefore, important to measure not only the mean currents but also their fluctuations with sufficient accuracy and resolution. To study the dynamics of the prevalent eddies in the ocean, precision instruments capable of measuring current fluctuations become necessary. Air-sea interaction studies of momentum, heat, and salt fluxes in the upper ocean

require a detailed knowledge of the mean and fluctuating components of near-surface flows, whereas bottom turbulence measurements are required to describe the benthic boundary layer dynamics and for sediment transport studies near the ocean floor. Flow sensors used for such studies must respond fast enough to capture the signals of interest and must be small enough to resolve their spatial variations. Such measurements hold out the promise of collection of useful information that will throw some light on the mechanisms of many strong ocean currents.

The global ocean current circulation is strongly structured in terms of dynamically distinct regions. In particular, the western boundary regions of the oceans are dominated by large-scale meandering currents (Loder et al., 1998). Thus there exist major currents such as the *Antarctic Circumpolar Current* in the Antarctic Ocean, the *Gulf Stream* and the *Brazil Current* in the Atlantic Ocean, the *Kuroshio Current* in the Pacific Ocean, the *Agulhas Current* and the *Somali Current* in the Indian Ocean, and the *Equatorial Undercurrent* beneath the equator in the Atlantic Ocean, Pacific Ocean, and Indian Ocean.

With the observation that most of the kinetic energy of the ocean circulation is associated with mesoscale variabilities, namely major ocean gyres, the general circulation is broadly regarded as ocean climatology and the mesoscale variability as the ocean weather (Munk et al., 1979). Mesoscale variabilities are ocean variabilities on a 100-km scale. It is now known that, at any given time, a snapshot of the ocean circulation is dominated by the mesoscale eddies, which can be regarded as “ocean storms” (Monk, 1983). Near-monochromatic anticyclonic oscillations in the ocean have been reported, and no atmospheric counterparts to these eddies are known to exist (Rossby, 1983). The variety of oceanic motion that falls under the general title of eddy motion is enormous. Interestingly, theoretical model studies indicate (Burkov et al., 1981) that the horizontal structure of the general oceanic circulation can be represented mainly by a system of semi-enclosed gyres non-geostrophically connected to each other through their boundary fronts. In fact, the earlier notion of the ocean as a steady-state system of large-scale, wind-driven currents and a weaker thermohaline abyssal circulation, and the hitherto classical view of the ocean circulation as a climatological mean taken over several years, have been overhauled with the discovery of these mesoscale variabilities supported by theoretical model studies of global circulation patterns. It is now known that several well-known coastal currents of the world oceans are influenced by these mesoscale variabilities.

Western boundary currents generally exhibit different modes such as large meander, straight path, and short meander. It is now well recognized that western boundary coastal currents are merely the limbs of one or more

gigantic whirls referred to as *gyres*. The water mass structures across the deep-sea free inertial jets can be rather complex. For the Gulf Stream, the high-transport jet core is situated at the boundary between two distinct water masses (slope and Sargasso). Additionally, the core of the stream carries several different water masses from outside this region, which is usually originated during its inertial and wind-driven regime further south (Gangopadhyay and Robinson, 2002). Similar situations must be anticipated in other regions of the world oceans.

1.4.1. Antarctic Circumpolar Current

In terms of the mean ocean circulation, the Southern Ocean is distinguished from all other oceans by the presence of a strong eastward-flowing circumpolar current, namely the *Antarctic Circumpolar Current* (ACC). The ACC is the only current that circumnavigates the globe unimpeded by continental barriers and coastlines (see Figure 1.5). The ACC connects the three major ocean basins (Atlantic, Pacific, and Indian) and redistributes active and passive oceanic tracers such as heat, salt, and nutrients. Thus, anomalies created by atmospheric forcing in one basin can be carried around the globe, affecting the global oceanic mass balance, ocean stratification, circulation, and consequently heat transport and climate.

The ACC encircles the Antarctic continent, flowing eastward through the southern portions of the Pacific, Atlantic, and Indian oceans. It is the world’s largest, and arguably most influential, ocean current (Nowlin and Klinck, 1986; Rintoul et al., 2001). Although the speed of the ACC is not extraordinary (about 50 cm/s at the surface), its depth (about 4 km) and width (500–1,000 km) result in a massive transport of about 140×10^6 m³ of water per second, equivalent to about 150 times the flow of all the world’s rivers combined. Because the Pacific, Atlantic, and Indian ocean basins are almost entirely surrounded by land except at their southern boundaries, the ACC is the primary means by which water, heat, and other properties are exchanged between ocean basins. At the latitudes of the Drake Passage there are no barriers to zonal flow (i.e., current flow parallel to the equator) in the upper ocean. Water from abyssal depths in the ocean at low latitudes rises along the sloping density surfaces associated with the ACC and toward the surface in the Southern Ocean, helping to sustain the conveyor belt circulation. In fact, the characteristics of more than 50% of the world ocean volume reflect the air–sea ice interactions taking place in the Southern Ocean.

The ACC forms the northern boundary for the Southern Ocean, which represents an important component of the climate system. Antarctic bottom water, one of the coldest and densest water masses, is formed in the Southern Ocean. It is this water mass that cools and ventilates most of the volume of the deep oceans (Schmitz, 1995). There is

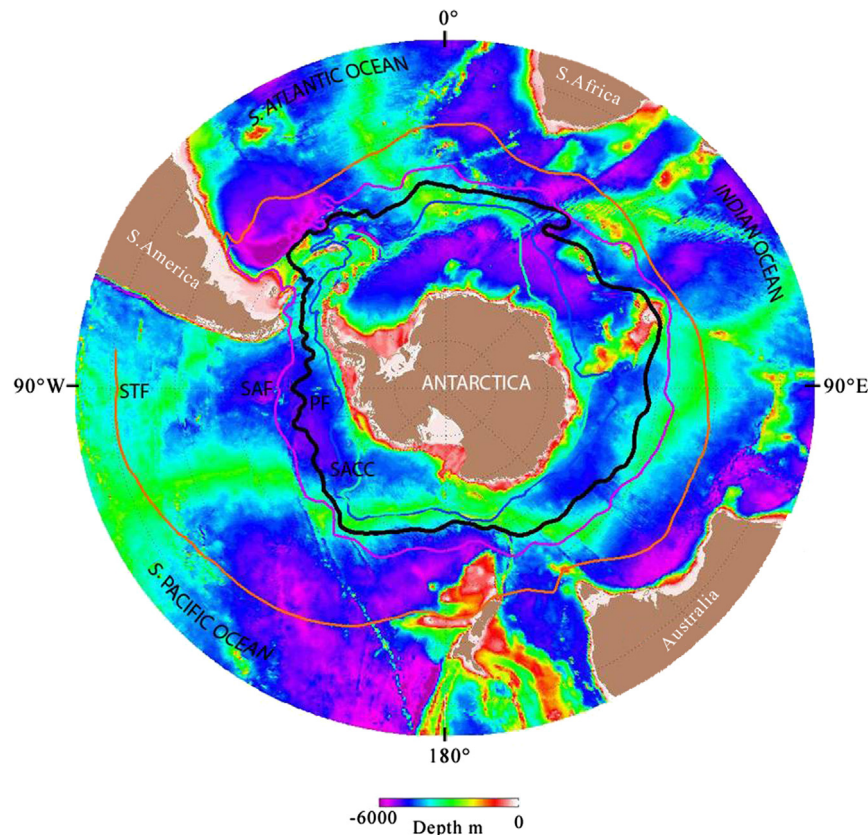


FIGURE 1.5 Trajectory of the eastward flowing Antarctic Circumpolar Current that circumnavigates the globe unimpeded by continental barriers and coastlines and connecting the three major ocean basins (Atlantic, Pacific, and Indian). (Source: Orsi et al., 1995.)

considerable interannual and decadal variability at high southern latitudes, and these features tend to propagate along the ACC. The anomalies circle around Antarctica in roughly 8–10 years at an average speed of 6–8 cm/s (White and Peterson, 1996). The coupling of the atmosphere and the ocean takes place via anomalous wind stresses and heat fluxes. In short, the ACC profoundly influences, and is influenced by, the regional and global climate (Fyfe and Saenko, 2005).

The absence of land barriers in the ACC results in distinct dynamical features that have no direct counterpart in the theory of mid-latitude ocean gyres. Sverdrup dynamics, the cornerstone of subtropical thermocline theory (Rhines and Young, 1982; Luyten et al., 1983), do not apply here. Both wind and buoyancy forcing play a role, as do geostrophic eddies, which appear to be crucial in determining the stratification and transport of the ACC. Recently, however, residual-mean theories have been applied (see Karsten et al., 2002; Marshall and Radko, 2003) that appear to capture the essence of the zonally averaged circulation and stratification of the Southern Ocean and fully embrace the central role of eddies. It is assumed that the Eulerian meridional circulation driven by the westerly winds (the Deacon cell), tending to overturn

isopycnals, is largely balanced by the geostrophic eddies that act in the opposite sense.

It is generally believed that wind stress is the main source of zonal momentum for the current, although thermohaline processes may also be important in driving the ACC (Olbers and Wubben, 1991). The dynamics of the ACC are complex and strongly depend on interactions among mesoscale eddies, topography, and the mean flow (Gouretski et al., 1987; Wolff et al., 1990, 1991). Munk and Palmev (1951) were the first to show that the flow can establish a pressure difference across meridional ridges, with the high pressure on the western side of the ridge. A necessary ingredient of the flow is the presence of mesoscale eddies that transfer the surface stress to the bottom, where it is dissipated by the topographic form stress. Marshall (1995) investigated the topographic steering of the ACC. He found that the ACC is partially steered by bottom topography and therefore does not exactly follow latitude circles. As a result, the surface heat flux into the ocean increases (relative to the streamline average) where the ACC meanders equatorward into warmer regions downstream of Drake Passage and decreases when the ACC drifts poleward in the Pacific sector. Wind stress also varies along the path of

the ACC, being significantly larger in the Atlantic-Indian sector. Marshall (1995) found that transient eddies are important in the general maintenance of the current. Ivchenko et al. (1996) investigated the dynamics of the ACC in a near-eddy-resolving model of the Southern Ocean (FRAM) and found that the topographic form drag is the main sink of the momentum that is input by the wind.

The ACC is traditionally thought to be composed of a series of hydrographic fronts associated with sloping isopycnals and relatively strong meridional property gradients. Fronts are strongly steered by the topography. Sallee et al. (2008) found three typical frontal regimes, namely merging, shoaling, and lee meandering, depending on their position relative to the bathymetry. Thus topography influences the pathway of the fronts, as seen in several previous studies, but also influences the mean intensity of the jet.

1.4.2. Western Boundary Currents in the Atlantic Ocean

Two major currents in the Atlantic Ocean are the *Gulf Stream* and the *Brazil Current*. Of these two currents, the former commands more prominence.

1.4.2.1. The Gulf Stream

The GS originates in the Gulf of Mexico and then follows the North American continental shelf until the shelf takes a major bend at Cape Hatteras (35°N , 75°W), where it turns eastward away from the coast and flows straight out to sea, rather than following the bend (see Figure 1.6). Eventually the current breaks up in several directions south and east of the Grand Banks. The surface currents have typical maximum speeds of about 200 cm/s (4 knots). Except in summer, the current is conspicuously warmer at the surface than in the surrounding waters.

The GS System is a complex of currents in the western and northern North Atlantic Ocean. Based on the outcome of an extensive survey reported by Fuglister (1960), it is found that the GS occupies an extensive area on the western and northern edges of the relatively warm, saline, central Atlantic water mass where the main thermocline layer rises toward the sea surface. The principal part of the GS lies off the east coast of North America between Florida and Newfoundland. To the east of Newfoundland, the GS is separated from the continental shelf by the cold, southward-flowing Labrador Current. The currents of the GS System generally contain a core of water at the surface that is warmer than the surroundings, suggesting a transport from lower latitudes. Consequently, the westward flow of

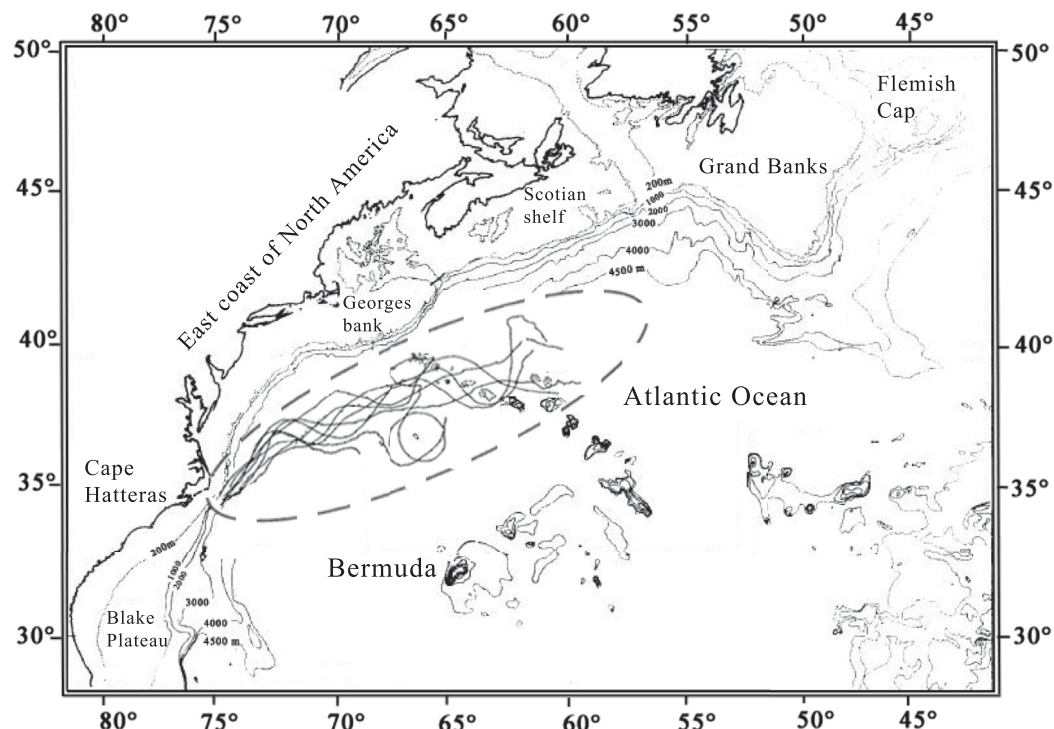
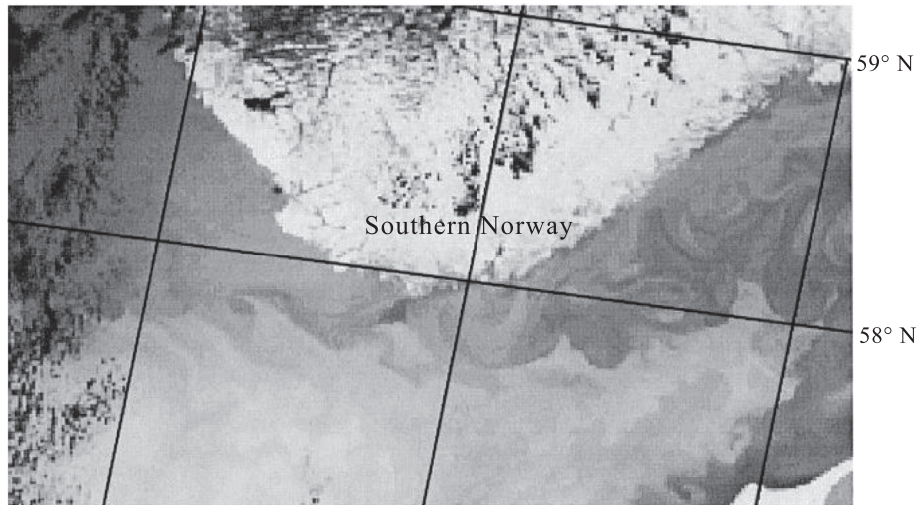


FIGURE 1.6 A portion of the Gulf Stream depicted by a composite of subsurface drifting float trajectories (shown inside broken elliptical boundary). The float trajectories clearly reveal the meandering character of the Gulf Stream and the formation of circular eddies. (Source: In part from Rossby et al., 1985, © American Meteorological Society. Reprinted with permission.)

FIGURE 1.7 Thermal infrared image of the Norwegian Current hugging the coast of Southern Norway. (Source: Johannessen et al., 2000.)



relatively warm water south of Iceland (the Irminger Current) and the northward flow off Norway (see the thermal infrared image of the Norwegian Current in Figure 1.7) are considered to be parts of the system. The Bay of Biscay and the Azores (see Figure 1.8 for the Azores Current region) are two regions into which some of the currents in the central Atlantic Ocean flow.

South of Cape Hatteras (see Figure 1.6), the GS System presses against the western boundary of the ocean basin. This boundary is not a vertical wall but consists, at the

surface, of the shore line, then a shelf roughly 60 miles wide out to the 200-m depth contour, then a broad plateau averaging 800 m in depth (the Blake Plateau), and, finally, a relatively steep slope down to the floor of the basin 5,000 m below. Flowing northward on the plateau, close to the shelf, is the strong current sometimes referred to as the Florida Current but more generally called the Gulf Stream. This current meanders, the amplitude of the meanders being about equal to the width of the stream (Webster, 1961), and it reaches to the bottom as evidenced by ripple

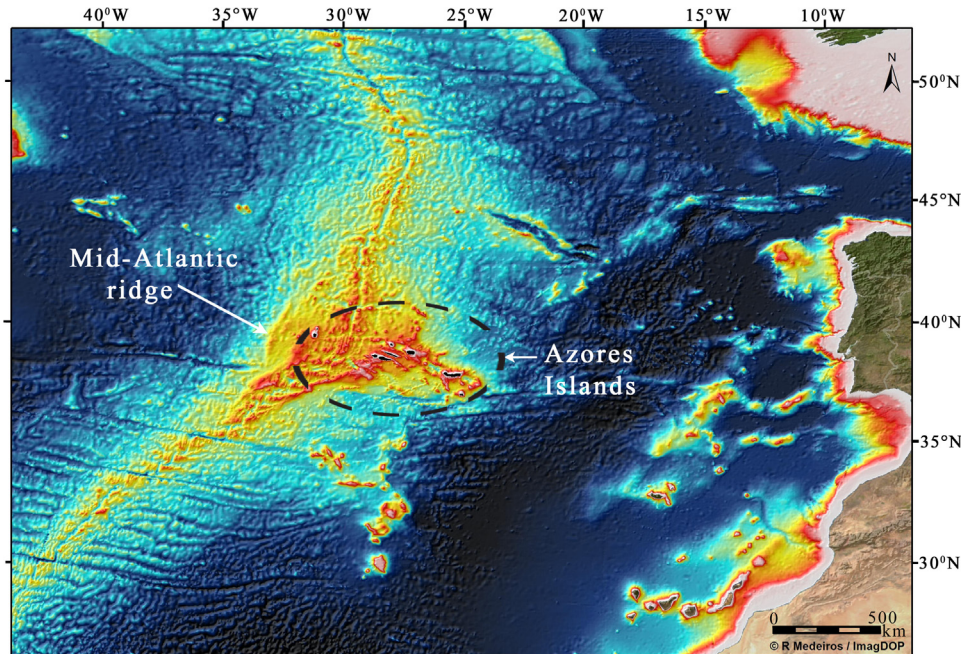


FIGURE 1.8 The Mid-Atlantic Ridge across which the Azores Current (a meandering jet 60–100 km wide with an eastward velocity of 25–50 cm/s) heads southeastward to the south of the Azores Islands chain and then flows mainly eastward at a latitude of about 35°N to the Gulf of Cadiz. (Source: Courtesy of Dr. Ricardo S. Santos, University of Azores, Portugal.)

marks and current observations. Stommel (1957) hypothesized a deep southward current along this boundary, and Swallow and Worthington (1961) observed a southward flow at depths near 2,800 m off Charleston, South Carolina. This flow has been referred to as a *deep countercurrent* to the Gulf Stream, although it is not actually beneath the stream in this area.

The Gulf Stream south of Hatteras is known to extend to the ocean bottom, i.e., to about 800 m. Profiles across this current show a horizontal density gradient at great depths, even near the bottom in 5,000 m of water. North of the principal current of the GS System, the main thermocline again rises abruptly toward the surface. This latter horizontal temperature gradient, or current, is not always present just north of Cape Hatteras but is a permanent and quite pronounced feature to the eastward, south of the Laurentian Channel. Based on the results of extensive surveys, Fuglister (1955) suggested that the Gulf Stream may not be a single continuous current between Cape Hatteras and the Grand Banks. It is generally agreed that the Gulf Stream forms the boundary zone between the Sargasso Sea and the slope water. At the surface it contains the warm core of the stream, which is characteristically fresher than the water at the same level in the Sargasso Sea and has less dissolved oxygen than the water to either side. The Slope Water Current and the Gulf Stream are both parts of the GS System, but the interrelationship between the two currents is not clear. Measurements have indicated that the subsurface currents in the GS are essentially in the same direction as the surface flow.

Detailed surface- and subsurface-temperature measurements made in the western area showed a banded structure parallel to the GS, which was undoubtedly associated with the streaky, “discontinuous edge” of the stream as observed from the air (Von Arx et al., 1955). The 1960 survey revealed the presence of an eddy, which was moving slowly toward the north along an anticyclonic curve. The eddy was found to have been circling in the area over a period of a month apparently before it moved again downstream.

The GS is well known for meander activity. Sudden change in the pattern of meanders is a permanent feature of the Gulf Stream. Consequently, the GS is perceived as a giant conduit wiggling about in the ocean. The meander pattern of the current exhibits a sharp line of demarcation near 65°W longitude, the longitude of Bermuda, separating the area of relatively small amplitude meanders in the west from the eastern area of much larger north-south meanders. The shapes of these large meanders may be influenced by the various geographical obstacles such as sea mounts in this area. For example, the GS path is deflected and curved around by Kelvin Sea Mount and the New England Seamounts. Ring generation is intensified by the presence of such Seamounts (Richardson, 1981). Lai and Richardson (1977) identified

cold rings in the North Atlantic characteristically as having greater than a 150-m upward displacement in the thermocline isotherms. They investigated the movement of GS rings and obtained a mean distance of 250 km during a season. The GS separates into two branches at the southeast of the Grand Banks of Newfoundland. The northern branch turns northeastward and becomes the North Atlantic Current (NAC). The southern branch, which becomes the Azores Current (AC), heads southeastward across the Mid-Atlantic Ridge to the south of the Azores (see Figure 1.8), then flows mainly eastward at a latitude of about 35°N to the Gulf of Cadiz (GoC).

Jia (2000) has provided an analysis of the Azores Current and shows that its existence and strength depends critically on the volume flow out of the Mediterranean Sea. Associated with AC is a front with significant temperature and salinity contrasts. The eastward flow of the AC extends all the way to the African coast, with southward branches in the Canary Basin as part of the subtropical gyre recirculation (Stramma 1984; Olbers et al., 1985; Klein and Siedler, 1989). The hydrographic database of Lozier et al. (1995) reveals a coherent AC that stretches across the eastern half of the basin, with divergences to the south and convergences from the north such that the downstream transport does not change much. Hydrographic surveys also indicate the eastward extension of the AC to the Moroccan continental slopes (Fernandez and Pingree, 1996; Pingree, 1997). Drifting buoys deployed in the AC are found to travel eastward and reach the western side of the GoC, then move northward or southward along the continental slopes. Based on the just-mentioned surveys, the AC is observed to be a meandering jet 60–100 km wide with an eastward velocity of 25–50 cm/s. The eastward flow is mostly in the upper few hundred meters but can reach as deep as 2,000 m. The current carries a large fraction of the water entering the eastern recirculation region of the Canary Basin. The estimates of the AC transport are in the range of 10–15 Sv (1 Sv ≡ 10⁶ m³/s). The surface temperature and salinity changes across the front can be as large as 2°C and 0.3 psu. The front marks the northern boundary of the 18°C Sargasso Sea water in the central North Atlantic. Both drifter data (Richardson, 1983; Krauss and Kase, 1994; Brugge, 1995) and satellite altimetry data (e.g., Le Traon et al., 1990; Wunsch and Stammer, 1995; Stammer, 1997) show a band of high eddy kinetic energy (EKE) associated with the AC. Kase and Siedler (1982) observed considerable meandering of the front southeast of the Azores with mesoscale eddies on both sides of the front.

1.4.2.2. The Brazil Current

The Brazil Current (BC) was a great bugbear to ancient mariners, principally on account of the difficulties that

a few dull vessels falling to leeward of St. Roque found in beating up against it. It was said to have caused the loss of some English transports in the 18th century; they fell to leeward of the cape on a voyage to the other hemisphere, and navigators, accordingly, were advised to shun it as a danger.

The BC is a highly baroclinic western boundary current. This current has a southern segment and a northern segment. The formation region of the North Brazil Current (NBC) is generally agreed to be near 10°S, where waters flowing westward in the South Equatorial Current (SEC) first begin to concentrate into a northward boundary current. The bulk of the volume transport of the BC is concentrated between 25 and 40 Sv, in the top 500 m of the water column. The collision of the Brazil Current and the Malvinas Current (which is a swift, barotropic, and narrow branch of the Antarctic Circumpolar Current that flows north along the continental slope of Argentina up to approximately 38°S), known as the Brazil/Malvinas Confluence, occurs near the mouth of the La Plata River, where it creates a region of intense mesoscale variability (Figure 1.9). The interaction between the poleward flow of the BC and the bottom topography greatly influences the nearshore circulation, particularly in the bottom boundary layer.

Temporally growing frontal meandering and occasional eddy shedding are observed in the BC as it flows adjacent to the Brazilian Coast. Silveira et al. (2008) reported a study of the dynamics of this phenomenon in the region between

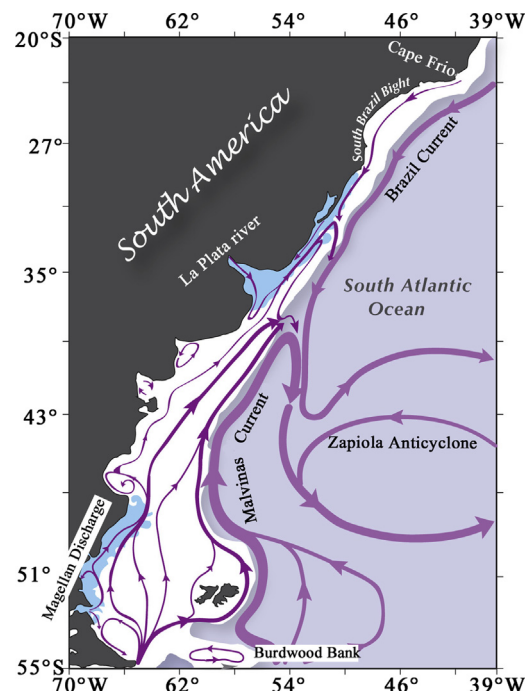


FIGURE 1.9 Schematic representation of the depth-averaged circulation including Brazil Current and Malvinas Current in the southwestern Atlantic region. The shelf (depths smaller than 200 m) is marked by a white background. (Source: Matano et al., 2010.)

22°S and 25°S. Large frontal meanders and intense mesoscale activity are often observed off the southeastern Brazilian coast (Mascarenhas et al., 1971; Signorini, 1978; Schmid et al., 1995; Silveira et al., 2004). The vertical structure of the BC system between 20°S and 25°S presents a unique regime in terms of a subtropical western boundary current. From the surface down to intermediate depths (400–500 m), the BC flows south–southwestward. The BC has maximum surface speeds of 40–70 cm/s and a width of about 100–120 km. It transports two water masses: Tropical Water (TW) at surface levels and South Atlantic Central Water (SACW) at pycnocline levels (Silveira et al., 2008). The BC transport ranges from 5 to 10 Sv in this region. Below 500 m, there is a direction reversion associated with the Intermediate Western Boundary Current (IWBC) flow toward the north–northeast (Boebel et al., 1999). The IWBC transports 2–4 Sv of Antarctic Intermediate Water (AAIW) and has its core centered between 800 and 1,000 m, with maximum speeds of about 30 cm/s. The frontal meander growth inferred from thermal satellite images (Figure 1.10) suggests that a mechanism of geophysical instability occurs in the region.

The NBC is an intense low-latitude western boundary current in the western tropical Atlantic Ocean that transports upper-ocean waters northward across the equator (Figure 1.11). Near 6–8°N the NBC separates sharply from the South American coastline and curves back on itself (retroflects) to feed the eastward North Equatorial Countercurrent (e.g., Csanady, 1985; Ou and DeRuijter, 1986; Johns et al., 1990, 1998; Garzoli et al., 2003). The NBC retroreflection is present year-round but is most intense in boreal autumn. The NBC occasionally retroflects so severely as to pinch off large, isolated warm-core rings exceeding 450 km in overall diameter. The anticyclonic rings, with azimuthal speeds approaching 100 cm/s, move northwestward toward the Caribbean Sea on a course parallel to the South American coastline (Goni and Johns, 2003). After translating northwestward for three to four months, the rings decompose in the vicinity of the Lesser Antilles. During their brief lifetime, and especially upon encountering the islands of the eastern Caribbean, the strong and transient velocities associated with NBC rings episodically disrupt regional circulation patterns, impact the distributions of near-surface salinity and ichthyoplankton (e.g., Cowen et al., 2003), and pose a physical threat to expanding deep-water oil and gas exploration on the South American continental slope (e.g., Summerhayes and Rayner, 2002).

In the Atlantic the NBC plays a dual role, first in closing the wind-driven equatorial gyre circulation and feeding a system of zonal countercurrents and second in providing a conduit for cross-equatorial transport of South Atlantic upper-ocean waters as part of the Atlantic meridional overturning cell (Johns et al., 1998). Seasonal variability of the NBC between 10°S and the equator appears to be quite small.

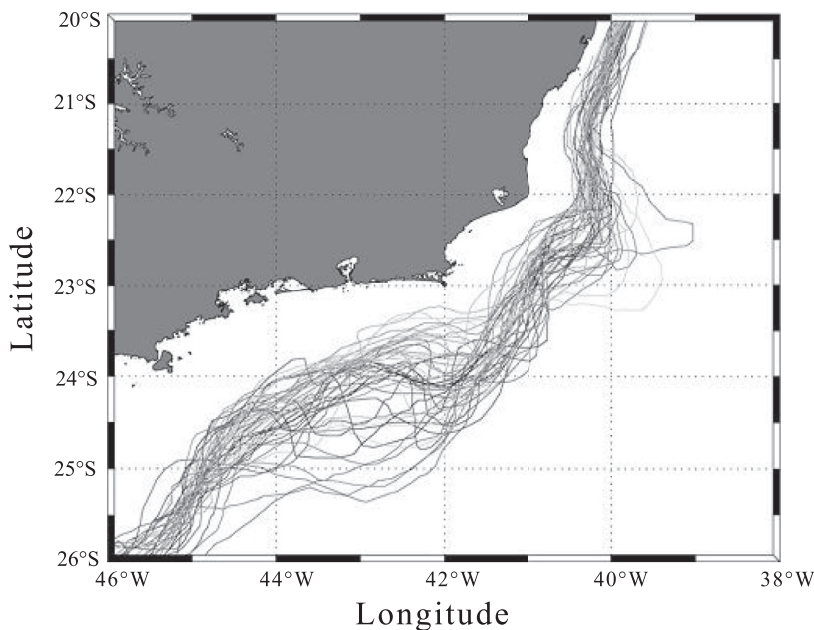


FIGURE 1.10 Thermal front patterns representing a section of the Brazil Current meander based on AVHRR images obtained at the Brazilian National Institute for Space Research, INPE. (Source: *Silveira et al., 2008*.)

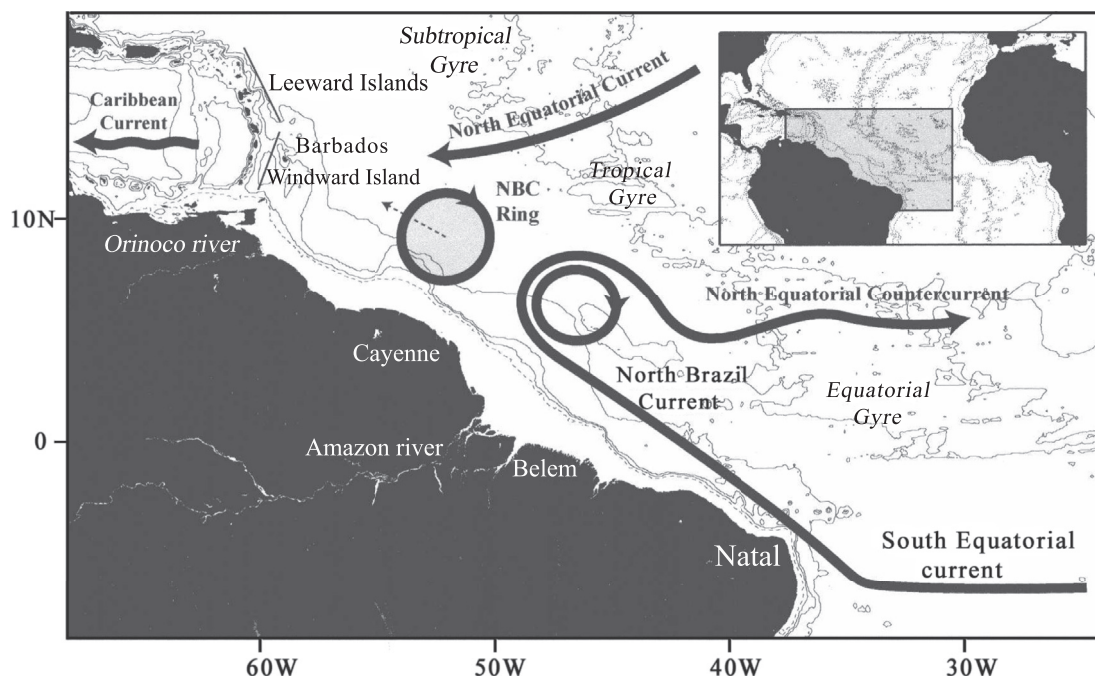


FIGURE 1.11 Schematic depiction of circulation in the western tropical Atlantic Ocean showing the North Brazil Current (NBC) retroflecting into the North Equatorial Countercurrent near 6°N. The NBC retroflexion occasionally collapses upon itself, resulting in the generation of anticyclonic NBC rings that translate northwestward toward the Caribbean and the arc of the Lesser Antilles. (Source: *Fratantoni and Richardson, 2006*, © American Meteorological Society. Reprinted with permission.)

However, models (e.g., Philander and Pacanowski, 1986) indicate that the NBC has a large seasonal cycle north of the equator, related to the seasonal migration of the intertropical convergence zone (ITCZ) and associated changes in the wind stress curl across the interior of the basin.

In contrast to the BC, the NBC regularly sheds rings primarily because of the small inclination of coastline between 5° and 8°N (Zharkov and Nof, 2010). Both the NBC and its rings contribute to the dispersal of fresh, nutrient-rich outflow from the Amazon River and provide

a mechanism for transport of this water northwestward toward Tobago and Barbados (e.g., Muller-Karger et al., 1988; Johns et al., 1990; Fratantoni and Glickson, 2002). As described by Fratantoni and Glickson (2002), NBC rings undergo a rapid evolution, driven primarily by interaction with topography and neighboring rings. Fratantoni and Richardson (2006) have reported a detailed account of the evolution and demise of North Brazil Current rings.

1.4.3. Western Boundary Current in the Pacific Ocean: The Kuroshio Current

The major boundary current in the Pacific Ocean is the *Kuroshio Current* flowing along and off the Japan coast. The other current in the Pacific Ocean is the southward-flowing East Australian Current (EAC). Extending from the Coral Sea to the Tasman Sea, the EAC system generates numerous eddies and has several branches including the Tasman Front, the East Auckland Current (EAUC), the East Cape Current (ECC), and the EAC extension. Unlike other western boundary currents such as the Gulf Stream and the Kuroshio, the strength of the EAC varies substantially with time. The mass transport within eddies spawned by the EAC can be much larger than its mean flow (Ridgway and Godfrey, 1997; Lilley et al., 1986). The flow patterns in the EAC are so complex and variable that it is often difficult even to decide whether a single, continuous current exists (Godfrey et al., 1980). In the light of the preceding description of the EAC, this current is not considered in this book. Instead, some general ideas on the Kuroshio Current System are given here.

In recent years, much curiosity has been generated concerning the quasi-stationary meander in the Kuroshio Current System in the North Pacific as it flows eastward past the Japanese islands. When the meander is absent, the Kuroshio flows along the continental slope near the 1000-m isobath, but when it is well formed, the Kuroshio bends away from the slope near Shikoku and enters deep water (see Figure 1.12). As just mentioned, the Kuroshio Current System consists of two limbs: the Kuroshio south of Japan and the Kuroshio Extension east of Japan. The Kuroshio and its variations may exert great influence on the climate of East Asia, particularly China, Japan, and Korea. On the other hand, it may respond to some big oceanic/climatic events such as El Nino. Great efforts have been made to describe Kuroshio and its relationship with some variations of marine environment and atmosphere. The Kuroshio south of Japan exists in one of two stable paths, a zonal path (i.e., path parallel to the equator) and a meander path, each lasting for a period of years. Taft (1972) has shown that the meander may remain in evidence for a number of years, disappear for some years, and then reappear. Past studies of the temporal and spatial variability of the Kuroshio Current System have revealed the presence of both annual and

interannual variability (Taft, 1972; Shoji, 1972). Their studies can be summarized as follows:

- The amplitude of the Kuroshio meander is as large (250 km) as Kyushu Island and its adjacent shelf and slope region.
- When the meander is present, its wavelength seems directly related to the magnitude of the transport.
- The transport of the Kuroshio downstream from Kyushu is generally about 30% greater than the transport upstream from Kyushu, this being the result of recirculation of some kind. In addition, the maximum surface speed of the Kuroshio (generally in the vicinity of the Kii Peninsula) can increase by a factor of two or more from speeds measured off Kyushu, indicating that the Kuroshio downstream from Kyushu can be both faster and narrower than upstream.
- There is an inverse relationship between the transport of the Kuroshio and the presence of the meander; below the critical transport (i.e., $\sim 40 \times 10^6 \text{ m}^3/\text{s}$) the meander is present, above the critical transport the meander disappears, leading to an apparent bimodal character of the Kuroshio meander.

These conclusions have been corroborated by White and McCreary (1976) in their studies.

Based on a numerical study, Chao and McCreary (1982) showed three separate paths that arise from Rossby wave resonance with the coastline topography; two of these were similar to the observed paths. According to the studies carried out by Mizuno and White (1983), the Kuroshio Extension bifurcates near the Shatsky Rise. One of the branches, represented by the 7–8°C isotherm, consistently goes northeastward along the Shatsky Rise, while the main branch extends eastward along 36°N, encountering the Emperor Seamounts. After the regional change, this bifurcation occurs much farther to the west, near 150°E.

The Kuroshio Extension east of Japan is known as a highly variable current, with cold and warm rings generated from unstable meander growth. Ring formation is usually a fast process, taking two weeks to one month as observed by Fuglister and Worthington (1951). However, Kawai (1972) showed an example of ring formation that took place more slowly over a six-month period. Kitano (1975) observed warm rings in the Kuroshio Current System to move 50–250 km during a season in the northeast direction. Hata (1974) observed one warm ring almost continuously for 21 months, moving also in the northeast direction 110 km during a season on average. The typical speed of translatory movement of rings is $<2 \text{ km/day}$ (i.e., $<2.3 \text{ cm/s}$); and due to their relatively slow speed the detection of ring movement is much easier. According to a study of Mizuno and White (1983), both warm and cold rings in the Kuroshio Current System propagate to the west

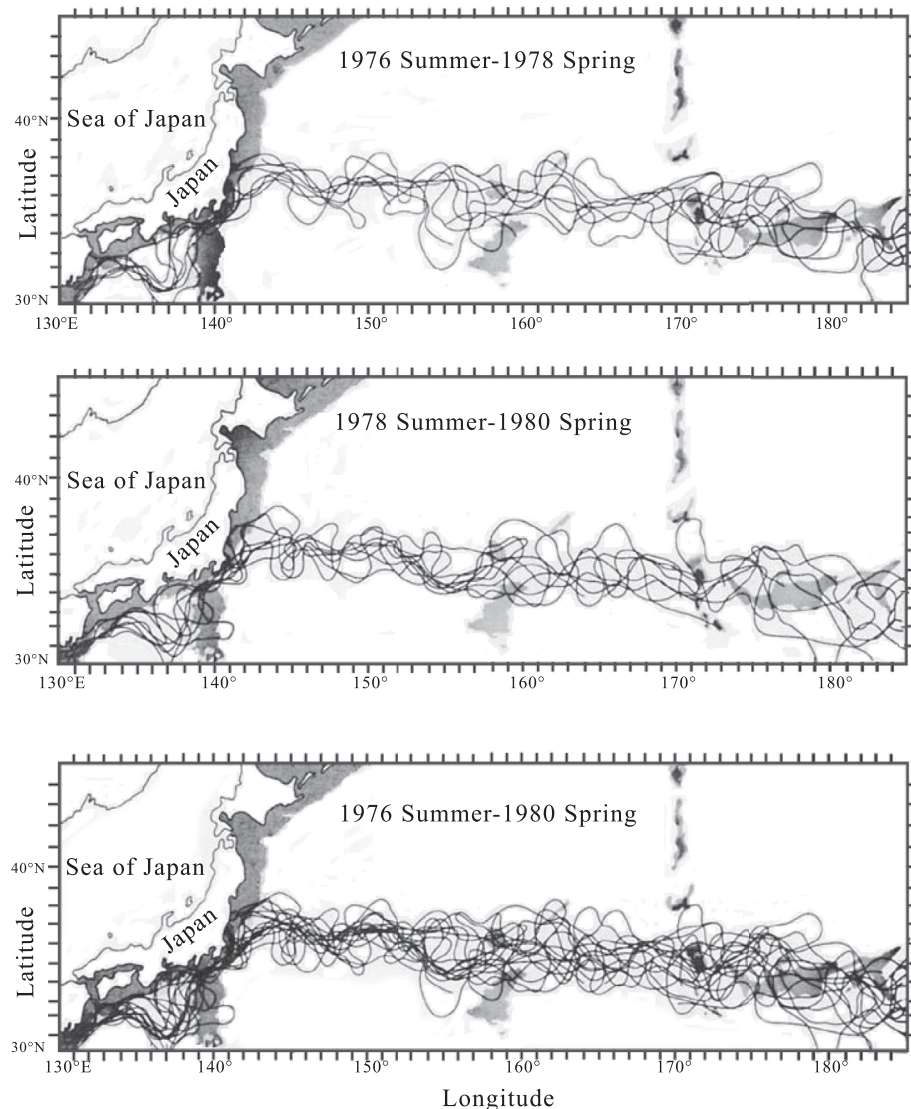


FIGURE 1.12 Path of the Kuroshio Current System during various years. (Source: Mizuno and White, 1983, © American Meteorological Society. Reprinted with permission.)

at an average speed of 1 cm/s. Cold rings were observed to have moved consistently southward, at about 0.6 cm/s, whereas warm rings moved generally northward, at about 0.4 cm/s, but less consistently. The fact that warm rings tend to have moved poleward while cold rings tend to have moved equatorward indicates that a net flux of heat is being conducted poleward by the meridional movement of rings in the Kuroshio Current System.

The Kuroshio Current System is characterized by the quasi-stationary existence of meanders (Kawai, 1972). Bernstein and White (1977) first observed the eastward extension of intense meander and eddy activity in the Kuroshio Extension. It extended eastward from the coast of Japan to at least 175°W, which is much farther east than had previously been realized. The quasi-stationary meander pattern in the Kuroshio Extension becomes

unstable, associated with increased eddy activity and ring production.

Using a series of multiple-ship expendable bathythermograph (XBT) surveys, Wilson and Dugan (1978) and Bernstein and White (1981) produced a series of thermal maps of the eddy activity in the Kuroshio Extension and showed westward propagation of meanders and eddies over this region. Ring formation is one of the important processes of mesoscale activity in the Kuroshio Extension. Whereas warm rings occupy the Kuroshio Extension adjacent to Japan (Kawai, 1972; Hata, 1974; Kitano, 1975; Tomosada, 1978), cold rings occupy the area southeast of Japan (Kawai, 1979).

Bathymetric perturbations such as the Izu Ridge, the Shatsky Rise, and the Emperor Seamounts and their valleys have been found to deflect the Kuroshio Current System (see Taft, 1972; Bernstein and White, 1981).

Abyssal plane also plays a role in the eddy activity. For example, Bernstein and White (1981) found eddy activity in the Kuroshio Extension to be intensified over the abyssal plane between the Izu Ridge and the Shatsky Rise. According to the studies conducted by Mizuno and White (1983), the Kuroshio Extension east of Japan can be traced as a high-gradient frontal feature.

1.4.4. Western Boundary Currents in the Indian Ocean

Two major boundary currents in the Indian Ocean are the *Agulhas Current* and the *Somali Current*, both flowing along the east coast of the African continent. In other regions in the Indian Ocean (except the equatorial undercurrent), the general patterns of circulation are found to be masked by eddy variability, and some form of averaging is needed to define patterns of general circulation.

1.4.4.1. The Agulhas Current

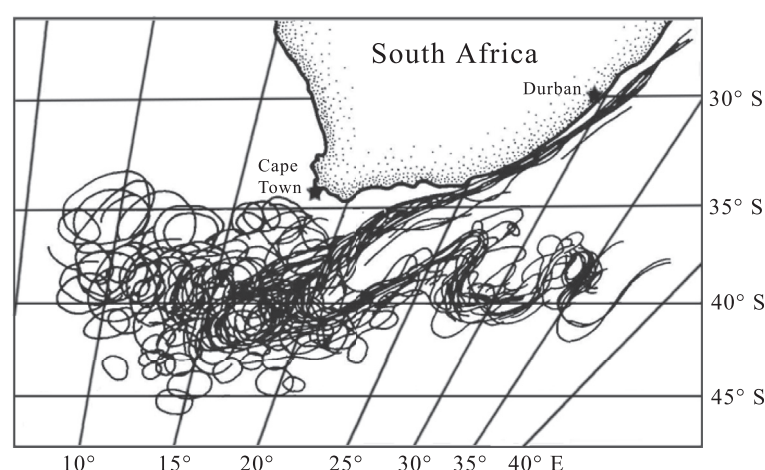
The Agulhas Current is the strongest western boundary current in the Southern Hemisphere. It transports about 65 Sverdrup (Sv , $1 \text{ Sv} \equiv 10^6 \text{ m}^3/\text{s}$) of warm tropical water southward along the southeast coast of Africa (Stramma and Lutjeharms, 1997). This is also one of the strongest western boundary currents in the world's oceans (Lutjeharms, 2007). The water movement in the southwest Indian Ocean is largely dominated by the anticyclonic sweep of the Agulhas System (Barlow, 1935). Figure 1.13 shows trajectories of the Agulhas Current and eddies constructed from thermal infrared images for a period from December 1984 to December 1985. The three major sources in the south Indian Ocean for the Agulhas Current are considered to be: (1) recirculation in the southwest Indian Ocean, (2) flow through the Mozambique Channel, and (3) the East Madagascar Current. This interrelation is also subject to seasonal variation due to direction changes in the monsoon winds (Barlow, 1935; Darbyshire,

1964). The flow in the Mozambique Channel is dominated by southward-moving anticyclonic eddies (Sætre and da Silva, 1984; Biastoch and Krauss, 1999; de Ruijter et al., 2002). As a major western boundary current, the Agulhas Current, which rushes toward the south pole in the southwest Indian Ocean, exhibits a unique and prominent turnabout near 20°E , at which the current direction is more or less reversed back eastward; this is known as the *Agulhas retroflection* (Gordon et al., 1987; Jacobs and Georgi, 1977; Lutjeharms and van Ballegooyen, 1988). It retroflects and flows back into the mid-latitude South Indian Ocean as the Agulhas return current (Lutjeharms and van Ballegooyen, 1988) before eventually becoming the South Indian Ocean current (Stramma, 1992).

Figure 1.14 shows a conceptual image based on seven years of thermal data of the Agulhas retroflection and environment. Thus, forming part of the Southwest Indian Ocean subgyre, the Agulhas Current flows poleward along the southeastern coast of Southern Africa from 27°S , eventually retroreflecting and flowing eastward back into the South Indian Ocean south of Africa between 40°S and 42°S (Gordon, 1985; Stramma and Lutjeharms, 1997). Although the Mozambique Channel eddies and the East Madagascar Current do not form a continuum with the Agulhas Current, they both affect its dynamics (Lutjeharms, 2007) and contribute to the fluxes of volume, heat, and salt. For example, interaction of the Mozambique Channel eddies with the Agulhas Current has been shown to influence the timing and frequency of Agulhas ring-shedding events at the retroflection.

The terminal region of the Agulhas Current is also populated by a range of eddies. During the flow of the relatively warm waters of the retroflection and the Agulhas return current in the east-southeastward direction across the southern mid-latitudes, they release large amounts of heat to the overlying atmosphere. Each year, a number of Agulhas rings are shed off the retroflection region and track northwest into the southeast Atlantic Ocean, again with

FIGURE 1.13 Trajectories of Agulhas Current and eddies constructed from thermal infrared images for a period from December 1984 to December 1985. (Source: Lutjeharms and Van Ballegooyen, 1988, © American Meteorological Society. Reprinted with permission.)



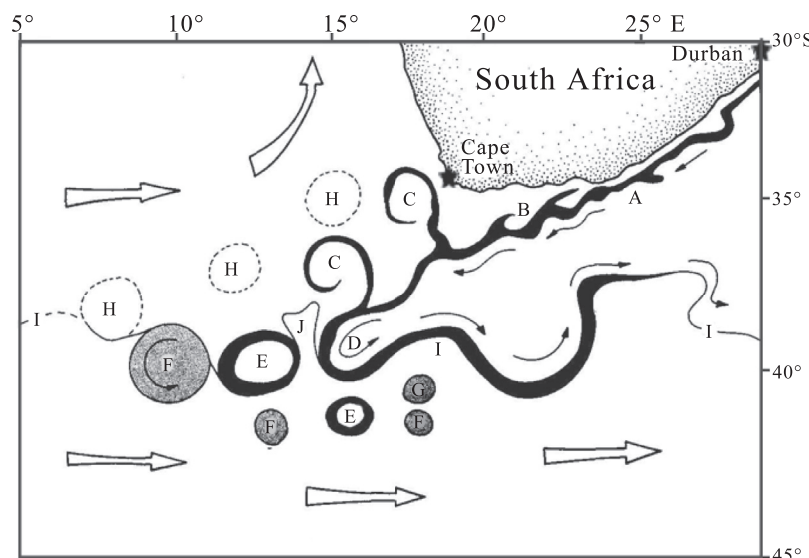


FIGURE 1.14 A conceptual image based on seven years of thermal data on the Agulhas retroflection and environment. (Source: Lutjeharms and Van Ballegooyen, 1988, © American Meteorological Society. Reprinted with permission.)

substantial heat fluxes to the atmosphere. It is likely that such large fluxes may have a significant impact on the regional atmospheric circulation and help to enhance the intensity of transient weather disturbances passing across southern Agulhas waters (e.g., Walker, 1990). It is also conceivable that heat transfer over the Agulhas return and South Indian Ocean currents may influence the intensity and track of mid-latitude depressions that contribute significantly to winter rainfall downstream in southern Australia (Reason, 2001). A number of studies have linked the variability in the greater Agulhas Current region with rainfall over large areas of South Africa (e.g., Walker, 1990; Jury et al., 1993; Mason, 1995).

The Agulhas retroflection is unstable, and it can coalesce and form Agulhas rings (Lutjeharms, 1981a) with an average diameter of 320 km (Lutjeharms, 1981b). The factor responsible for the singular current behavior manifested in the retroflection may stem from the principle of conservation of potential vorticity. The exchange process of water south of Africa depends to a large extent on ring shedding at the Agulhas retroflection (Lutjeharms and Gordon, 1987; Olson and Evans, 1986). A narrow filament of much colder water lies directly to the west of the retroflection, spreading laterally north of the current. The narrow, warm ribbon of the Agulhas Current (about 90 km wide, on average) exhibits a number of meanders south of Africa.

Because of retroflection, the volume exchange between the Indian Ocean and the Atlantic Ocean due to the Agulhas Current is relatively small, that is, about 10% of the Agulhas transport. Within the Agulhas retroflection region, the flow has a strong variability, and about six times every year a large ring is separated from the main current that propagates westward into the South Atlantic. Although the

exchange due to the rings is small, it may be sufficiently large to cause changes in the Atlantic thermohaline circulation because the properties of the Indian Ocean water are substantially different from those in the Atlantic (Gordon, 1985). Paleoceanographic studies have indicated that this exchange has varied significantly in the past, although a “supergyre” that fully connected the Indian and Atlantic Oceans probably never existed. The physics of the Agulhas Current, particularly its retroflection, has been examined by Dijkstra and de Ruijter (2001).

Because the Agulhas Current experiences strong topographic control, first by the continental slope of Africa, then by the Agulhas Bank, it does not exhibit the continuous meandering of the detached, eastward-flowing Gulf Stream. As a result, such a distinct steering level within the Agulhas is not expected. However, solitary meanders, often referred to as *Natal pulses* (owing to their apparent origin over an area of wide shelf known as the *Natal Bight* offshore of Port Elizabeth) propagate downstream in the Agulhas Current about six times per year (Lutjeharms and Van Ballegooyen, 1988; Lutjeharms and Roberts, 1988). The gentler continental slope and wider shelf at Natal Bight, between 29°S and 30°S, present favorable conditions for the occurrence of instabilities and subsequent growth of meanders (de Ruijter et al., 1999). Thus, mesoscale variability in the northern Agulhas Current occurs in the form of *Natal pulses* (intermittent cyclonic meanders). *Natal pulses* propagate downstream at rates of 10 km/day (Lutjeharms and Roberts, 1988).

Using current-meter time series measurements, Bryden et al. (2005) showed that solitary meanders are the dominant mode of variability in the Agulhas Current. Van Leeuwen et al. (2000) demonstrated that solitary meanders (i.e., *Natal pulses*) on the trajectory of the Agulhas Current

are responsible for the timing of ring shedding at the Agulhas retroflection. These Natal pulses in turn are triggered by offshore eddies. Schouten et al. (2002) demonstrated a case in which an eddy from the Mozambique Channel triggered a Natal pulse that was subsequently responsible for the occlusion of an Agulhas ring at the Agulhas retroflection. It is believed that a Natal pulse event enables cross-frontal mixing within the Agulhas Current in addition to causing straightforward path variability. The shedding of nine rings per year, even if not all of them were to drift northward, has significant implications for the energy contribution of these features to the total kinetic energy balance of the South Atlantic Ocean. A detailed study by Lutjeharms and Van Ballegooyen (1988) of this ring-spawning process shows that in almost all cases the shedding of a ring is preceded by the genesis and growth of a cold wedge of Sub-Antarctic Surface Water at the subtropical convergence. It is believed that the spawning of rings may be influenced or precipitated directly by perturbations in the Agulhas Current itself.

A major feature of the Agulhas Current is a very sharp meander in the Agulhas Return Current at about 27°E. It has been identified as a cold-core eddy being spawned at the subtropical convergence. Another feature is a large eddy southwest of Cape Town, centered at 15°E. A distinctive wedge of cold sub-Antarctic water separates the ring from the retroflection loop. The ring has an elliptical configuration with evidence of some shear-edge features. According to some estimates, the Agulhas rings have diameters of ~250 km and circular velocities of 90–100 cm/s and move at an average speed of 7 cm/s. Olson and Evans (1986) have shown that these rings translate at speeds of 4.8–8.5 cm/s. Sarukhanyan (1982) identified intense and less intense mesoscale eddy-like features south of the subtropical convergence; Lutjeharms (1988) has described the budding off of warm eddy across the convergence and its subsequent drift in the Sub-Antarctic zone. Some satellite images of the area show warm-water features with undifferentiated surface temperatures, i.e., discs with more or less the same surface temperature throughout, as well as distinct rings of warmer water with higher temperatures in an annulus shape, i.e., with slightly cooler water in the center. Although exceptional in its complete retroflection, the ring shedding from the Agulhas Current is not unusual for a western boundary current. However, the rate of ring shedding by the Agulhas Current seems high.

The average diameter for the retroflection loop (~342 km) does not vary dramatically from year to year. It has been suggested that the westward protrusion of warm Agulhas Current water may extend far into the South Atlantic.

Observations by Beal et al. (2006) suggest that the water mass properties on either side of the dynamical core of the Agulhas Current are significantly different. Inshore of its velocity core are found waters of predominantly Arabian

Sea, Red Sea, and equatorial Indian Ocean origin, but the offshore waters are generally from the Atlantic Ocean, the Southern Ocean, and the southeast Indian Ocean.

1.4.4.2. The Somali Current

The Somali Current system is well known to be forced significantly by the wind field along and off the coast of Somalia. This current system is made up of two gyres. There is a northern gyre slightly to the north of the equator and a southern gyre a little to the south of the equator, and the Indian monsoon is related to the movements of these gyres (Anderson and Rowlands, 1976). As the monsoon sets over India, the southern gyre begins to move northward, and eventually the two gyres coalesce. The two-gyre configuration is most prominent during good monsoon years, but in years of weak monsoons the southern gyre is hardly perceptible. The alongshore winds over the Somalia coast are generally of a jet-like structure and can be very strong, and they reverse direction seasonally with the monsoons. In rapid response to the changing winds, the Somali Current also reverses seasonally. Soon after the onset of the Indian Southwest Monsoon, an intense coastal circulation exists north of 5°N. Cold water appears all along the coast of Somalia, although it is concentrated in wedges (Brown et al., 1980). The surface poleward flow is very strong (~100–200 cm/s) and forms one or two quasi-stationary eddies (Duing et al., 1980). There is an undercurrent with an instantaneous maximum speed as large as 60 cm/s (Leetmaa et al., 1982), although the monthly average speed has a maximum of only about 20 cm/s (Schott and Quadfasel, 1982; Quadfasel and Schott, 1983). The width scale of both currents is of the order of 50–100 km. The wind at this time is in the form of an alongshore jet, which reaches a maximum speed near 10–15°N, well north of the region of the undercurrent (Luther and O'Brien, 1985; Knox and Anderson, 1985). One western-boundary upwelling region that has been studied extensively is the coast of Somalia; it is found that this current system is a classic upwelling regime (Schott, 1983; Knox and Anderson, 1985). Based on model studies, McCreary and Kundu (1985) found the existence of an undercurrent in the south, which is in agreement with observations off Somalia, where a southward undercurrent has been observed at 5°N during the Southwest Monsoon.

1.4.5. Equatorial Undercurrents

The *Equatorial Undercurrent* (EUC), which is one of the most outstanding branches in the equatorial current system, is a narrow ribbon of eastward flow (termed *jet*) centered on the equator in the upper thermocline. It is a permanent feature of the general circulation in the Atlantic and Pacific oceans and is present in the Indian Ocean in northern winter

and spring during the northeast monsoon. It reaches speeds of 50–100 cm/s below the westward flow of the South Equatorial Current, and in the Pacific the jet transports as much mass on average ($40 \times 10^6 \text{ m}^3/\text{s}$) as the Florida Current, which feeds the Gulf Stream. Intense vertical shear of the undercurrent both above and below its core produces turbulent mixing. Turbulence tends to homogenize the thermal structure near the equator and so works in concert with the field of vertical velocity to weaken the thermocline. McPhaden (1986) has provided an interesting review of the chronology of historical events surrounding the “multiple discoveries” of the Equatorial Undercurrent.

It is now generally agreed that the driving force of the Equatorial Undercurrent is primarily the horizontal pressure gradient along the equator, given by the downward slope from west to east of the sea surface and of isobaric surfaces in the upper strata of the ocean. Among other reasons, speed variations along the course of the current have to be expected as a result of slope variations in zonal direction. The eastward zonal pressure gradient along the equator is generated by prevailing easterly wind distribution (i.e., wind blowing from the east) over the tropical and subtropical regions of the ocean. In general, the trade winds on both sides of the equator produce a westward transport of water in the upper strata of the sea. This water piles up along the western boundaries of the equatorial ocean basin, and the general slope of the sea surface in a zonal direction is downward from west to east.

An equatorial zonal slope downward from west to east, comparable to that in the Atlantic Ocean, is also found in the Pacific Ocean and in the Indian Ocean during the period of existence of an Equatorial Undercurrent. If the zonal slope downward to the east is a necessary requirement for the development of the Undercurrent, this current should be missing in the region where the slope is reversed. A peculiar physical-chemical structure, typical for the Equatorial Undercurrents in all three equatorial oceans, is a pronounced weakening of the vertical temperature gradient in the thermocline and water with a high oxygen content reaching down from the surface to a depth of 200 m and more (Neumann, 1966).

1.4.5.1. Equatorial Undercurrent in the Atlantic Ocean

The first observations of the Equatorial Undercurrent were made in 1886 by the British oceanographer J. Y. Buchanan in the Gulf of Guinea in the eastern Atlantic Ocean (Figure 1.15) during the *Challenger* Expedition. While making subsurface seawater temperature measurements, Buchanan found that the surface water had a very slight westerly set, and the water below 30 fathoms (180 ft) was running so strongly to the southeast direction that it was impossible to make temperature observations, since the

heavily loaded lines drifted straight out and could not be sunk by any weight of which they could bear the strain. By using a makeshift current drogue composed of a surface buoy and a weighted biological sampling tow net suspended at about 55 m depth, Buchanan estimated the speed of this “very remarkable undercurrent” at more than 50 cm/s at three equatorial stations. He observed a weakening of the thermocline within 2° of the equator, a feature now commonly associated with equatorial upwelling and enhanced vertical mixing in the undercurrent.

On a later submarine cable-laying cruise from Senegal to the island of Fernando Noronha, Buchanan again observed the undercurrent in the western Atlantic and noted that the equatorial undercurrent is a constant and important factor of the oceanic circulation. Subsequent to the first current-meter measurements of the undercurrent in the Atlantic Ocean by Soviet oceanographers from on board the *R. V. Mikhail Lomonosov*, the eastward subsurface equatorial current in the Atlantic Ocean basin has frequently been referred to as the *Lomonosov Current* (Philander, 1973).

The Equatorial Undercurrent in the Atlantic Ocean received considerable attention in the years since 1960 (Neumann, 1960; Metcalf et al., 1962). It was found that the Atlantic Equatorial Undercurrent is a thin, swift, and relatively narrow current flowing from west to east at, or in close proximity to, the geographical equator. Its thickness is between 150 and 250 meters and its lateral extent 250 to 300 kilometers. The maximum speed in the core of the current is found at depths between 50 and 100 meters. In general, this core is deeper in the western part of the ocean and rises toward the east. The speed of the Equatorial Undercurrent varies along its course and with time at a given longitude. The average speed is probably near 70 cm/s. However, maximum speeds as high at 130 cm/s have been observed by Metcalf et al. (1962). They suggested that the high-salinity core of the Undercurrent has as its source region the high-salinity shallow water south of the equator off the east coast of Brazil. Cochrane (1963) described the Undercurrent as being an equatorial extension of a narrow saline current setting east-southeast at the surface near (2°N , 42°W), combined near 38°W with a retroverse branch of the northwesterly flowing Guiana Current along the South American coast.

Vertical oscillations of the core of maximum speed at a fixed location have been noted by several investigators. Evidence for lateral oscillations and lateral current displacements to the north and south of the equator, respectively, have been reported by Metcalf et al. (1962), Stalcup and Metcalf (1966), and Sturm and Voigt (1966). There is evidence that the current may sometimes split into two cores flowing just a little north and a little south of the equator (Sturm and Voigt, 1966). The temperature/oxygen relationship indicates that most of the Undercurrent water comes from the South Atlantic by way of the North

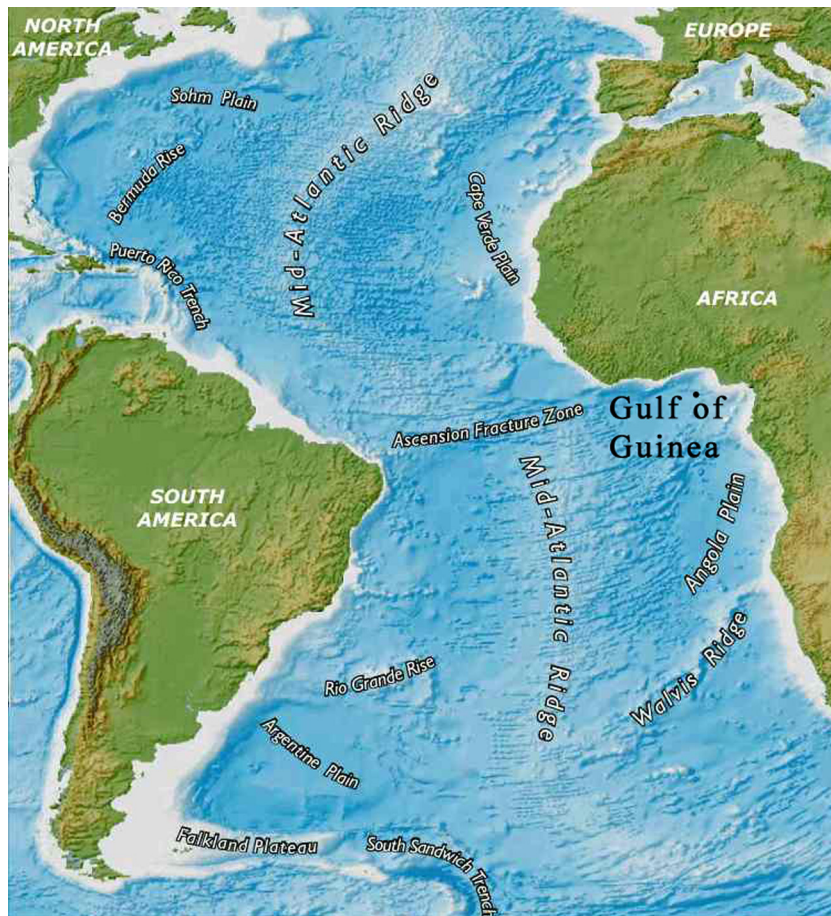


FIGURE 1.15 Map of a portion of the Atlantic Ocean that covers the equatorial belt showing the Gulf of Guinea region from where the “first discovery” of the equatorial undercurrent was made by the British oceanographer J. Y. Buchanan during the *Challenger* Expedition. (Source: <http://mccainsocialstudies.wikispaces.com/EI.+Geography.>)

Brazilian Coastal Current and that the contribution of North Atlantic water is very minor (Metcalf and Stalcup, 1967). They provided evidence on the source of the distinctive water type that makes up the Undercurrent’s core and the complex relationship between the Undercurrent and other nearby currents. Figure 1.16 provides a detailed schematic drawing of the circulation in the western equatorial Atlantic as reported by Philander (1973).

Neumann (1966) examined the Equatorial Undercurrent in the Atlantic Ocean, with special emphasis given to the sources of high-salinity water that characterizes the core of the EUC along a zonal distance of about 5,000 km. He found that the beginning, or source, of the Atlantic Equatorial Undercurrent is in the vicinity of 38°W at the confluence of two currents coming from the Northern and Southern Hemisphere, respectively. Both confluent currents are characterized by a maximum salinity in the upper thermocline. However, the branch coming from the Southern Hemisphere has a considerably higher salinity maximum. These conclusions were supported by the salinity distribution in the layer of maximum salinity at

depths between about 60 and 100 meters. Philander (1973) reports that from about 30°W to within 80 nautical miles (150 km) of the African coast, the Atlantic EUC is a permanent feature of the equatorial circulation. Its most outstanding feature is a subsurface core of water of very high salinity (usually in excess of 36.2‰). The undercurrent derives this core from the North Brazilian Coastal Current; there is no evidence of advection of high-salinity water into the undercurrent east of 35°W.

Cochrane (1963, 1965) found the high-salinity core of the Undercurrent in the western part of the ocean always a little south of the equator (near 1°S). Neumann (1966) also found evidence that the eastward extent of the Atlantic EUC varies with the season. Parachute drogue tracking of current indicated a north-south oscillation in the course of the Undercurrent with an approximate period of 2 days and 8 hours. However, different investigators found different periods of oscillation, ranging from $\frac{1}{2}$ day (Stalcup and Metcalf, 1966) to 3 days (Fedorov, 1965). However, an outstanding feature of the Atlantic EUC is the core of high-salinity water that

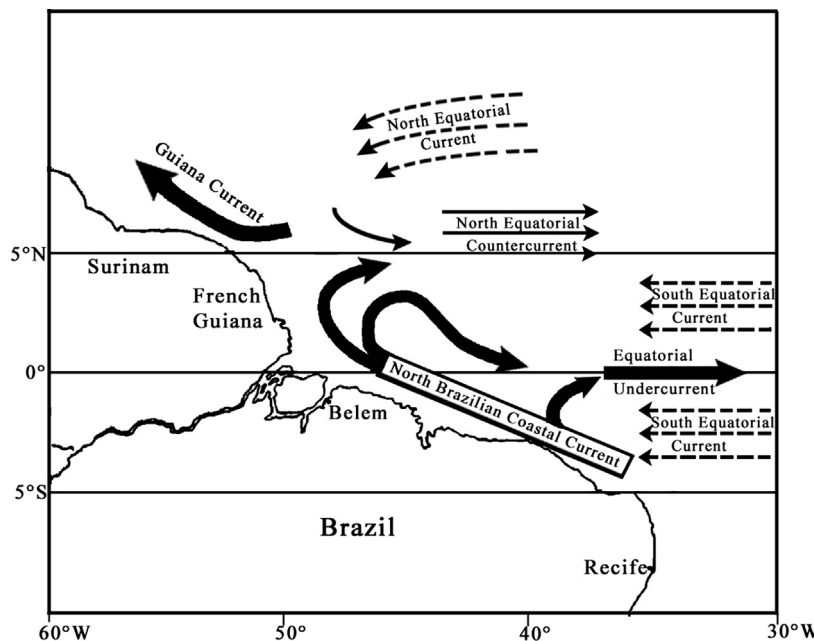


FIGURE 1.16 A schematic drawing of the circulation in the western equatorial Atlantic. (Source: Philander, 1973.)

coincides with, or is at least very close to, the core of maximum current speed. The high-salinity core is traceable far to the east into the Gulf of Guinea.

The Atlantic EUC plays a crucial role in the dynamics of the Atlantic oceans. For example, field measurements and model simulation studies by Giarolla et al. (2005) revealed the shallowing of the Atlantic EUC between January and May, concurrent with the reversal of the easterly trade winds to westerly and the deepening of the EUC from May to December.

1.4.5.2. Equatorial Undercurrent in the Pacific Ocean

It was the Japanese oceanographers who first measured an eastward subsurface equatorial current in the western Pacific around 1925. Subsequently, the undercurrent in the Pacific was *rediscovered* in August 1952 by Townsend Cromwell and Raymond Montgomery, who suggested the name *Equatorial Undercurrent*. Surprisingly, neither of these two groups was aware of Buchanan's earlier equatorial subsurface current measurements in the Atlantic Ocean way back in 1886 as well as the speculations around this current. The rediscovery of the EUC in the Pacific Ocean in 1952 inspired more comprehensive ocean surveys and dynamic theories of equatorial circulation. Although theories of the general circulation developed by Sverdrup (1947), Stommel (1948), and Munk (1950) had successfully accounted for the existence of major ocean currents such as the Gulf Stream and Kuroshio and explained the western intensification of wind-driven gyres in terms of the

sphericity of the Earth, the Equatorial *Undercurrent* had not been predicted by these theories. Thus, observation of the EUC was a “new” discovery.

Cromwell et al. (1954) made the first attempt to extensively study the EUC in the central and eastern parts of the Pacific Ocean. There arose some confusion as regards an appropriate name for the current. Shortly after Cromwell's death, Knauss and King (1958) proposed that the current be called the *Cromwell Current* after its first explorer.

During the International Geophysical Year (IGY, 1957–1958) and afterward into the 1960s, the United States, France, Japan, and the Soviet Union launched expeditions in the Pacific to determine the meridional, vertical, and zonal extent of the undercurrent and its relation to temperature, salinity, and chemical tracer distributions. Theories developed by Stommel (1960) and Charney (1960) established the central importance of the trade winds in setting up a baroclinic zonal pressure gradient to provide the source of eastward momentum for the undercurrent. Moreover, this pressure gradient eliminates singularities in the Ekman layer and so allows for a reconciliation of undercurrent dynamics and Sverdrup dynamics. It was found that in the Pacific Cromwell Current, the high-salinity core is absent or at least not well developed (Montgomery and Stroup, 1962; Knauss, 1966).

Perhaps the most dramatic observations of EUC variability in recent years were made during the 1982–1983 El Niño. The trade winds reversed over much of the western and central equatorial Pacific in late 1982, which led to a collapse of the zonal pressure gradient (Cane, 1983). Direct velocity measurements indicated the virtual disappearance

of the undercurrent from September 1982 until January 1983 at 159°W (Firing et al., 1983) and during January and February 1983 at 110°W (Halpern, 1983). Equatorial upwelling ceased as a consequence of these radical wind, current, and pressure changes, causing major disruptions in primary productivity (Barber and Chavez, 1983) and in global cycling of carbon dioxide (Gammon et al., 1986). Cessation of upwelling also led to basin-scale equatorial sea surface temperature anomalies of ~3°C. These were associated with intense atmospheric convection that maintained the most pronounced El Niño of the century (Rasmussen and Wallace, 1983).

The EUC is a quasi-permanent feature of the equatorial Pacific. Its thinness and length are remarkable. It has a meridional width of about 200–400 km, is centered on the equator in the thermocline between about 50 and 200 m depth, and extends nearly across the whole length of the basin. The EUC reaches a speed of 1 m/s in its core and transports around 30–40 Sv ($1 \text{ Sv} \equiv 10^6 \text{ m}^3/\text{s}$). Thus, the Pacific Equatorial Undercurrent, or Cromwell Current, system is characterized by a large transport of water from the western Pacific toward the east, producing a large vertical shear. An important factor in understanding the development and structure of this current system is the role of turbulence, turbulent friction, and turbulent mixing (Williams and Gibson, 1974). The EUC has strong inter-annual variations in mass transport (Picaut and Tournier, 1991; Johnson et al., 2000) and temperature (Izumo et al., 2002) and is part of both subtropical and tropical shallow meridional overturning cells (Liu et al., 1994; McCreary and Lu, 1994; Sloyan et al., 2003). The EUC feeds equatorial upwelling (Bryden and Brady, 1985) and may have strong influences on SST in the eastern Pacific and thus on El Niño Southern Oscillation (ENSO).

The EUC, the shallow meridional overturning cells feeding it, and their role in El Niño and decadal variability in the equatorial Pacific have been studied by Izumo (2005) using both *in situ* data and an ocean general circulation model. His study has evidenced how all the branches of the shallow meridional overturning cells strongly co-vary with ENSO, slowing down and even vanishing during strong El Niño events and strengthening during La Niña events, leading to important changes in zonal and meridional heat exchanges. The study reveals that mass transport variations of the different branches of the cells are indeed all very well correlated with eastern Pacific SST.

1.4.5.3. Equatorial Undercurrent in the Indian Ocean

Results obtained during the Indian Ocean expeditions have shown that an Equatorial Undercurrent exists in the Indian Ocean at least during part of the year, when winds on both sides of the equator blow toward the West

(Knauss and Taft, 1964; Swallow, 1964). Measurements in the Indian Ocean provided an important test of the theories developed to explain the EUC. The Indian Ocean is dominated by seasonally reversing monsoons and mean westerly winds along the equator. Easterlies prevail only during the northeast monsoon, which lasts from approximately December to April. Researchers therefore expected that an undercurrent and eastward pressure gradient would be present in the thermocline only during the northern winter and spring. This was confirmed independently by Soviet, British, and U.S. scientists, who found eastward subsurface flow along the equator at speeds of 50–100 cm/s during the International Indian Ocean Expedition (Knauss and Taft, 1964; Swallow, 1964). Furthermore, the zonal (i.e., parallel to the equator) pressure gradient associated with this flow reversed during the southwest monsoon, at which time the undercurrent was either absent or poorly developed.

Unlike in the Pacific and the Atlantic oceans, a distinct seasonal cycle associated with the Asian-Australian monsoon dominates the atmospheric circulation over the Indian Ocean (see Figure 1.17). Thus different oceanic structures are expected to occur in the Indian Ocean in response to such wind forcing. The undercurrent is driven by a pressure gradient and flows within the thermocline. The undercurrent in the Indian Ocean is associated with the northeast monsoon season. A subsurface salinity maximum, similar to that found in the Atlantic Ocean and associated with the Equatorial Undercurrent, is indicated also in the Indian Ocean during the Northern Hemisphere winter season. The sea level responds to both the accumulation of warm water and the wind stress. According to Wyrtki (1973), during the two months when the easterly winds blow, a slope of the sea surface of about 20 cm over a distance of 5,000 km from west to east is generated. Measurements by Luyten and Swallow (1976) in the equatorial region of the western Indian Ocean suggest a complex vertical structure in the horizontal velocity field close to the equator; this structure was found to be equatorially trapped. Based on long uninterrupted time-series measurements from a single point at (0.5°S, 73°E) in the equatorial Indian Ocean, Cane (1980) found that an undercurrent was absent in 1974.

Iskandar et al. (2009) investigated variations of subsurface zonal current in the eastern equatorial Indian Ocean by examining six-year data (December 2000 through November 2006) from an acoustic Doppler current profiler mooring at (0°S, 90°E). They found that during winter, the generation of an eastward pressure gradient, which drives an eastward flow in the thermocline, is caused primarily by upwelling equatorial Kelvin waves excited by prevailing easterly winds. The subsurface current reveals a distinct seasonal asymmetry. The maximum eastward

speed of 63 cm/s is observed in April and a secondary maximum of 49 cm/s is seen in October. The subsurface current during summer undergoes significant interannual variations; it was absent in 2003, but it was anomalously strong during 2006 (Iskandar et al., 2009).

1.5. CURRENTS OF DIFFERENT ORIGINS

Currents of different origins and of various types are a fascinating permanent feature of the oceans. Thus there

exist wind-driven currents that are confined to the surface Ekman layer, geostrophic currents that are maintained by horizontal pressure gradients, tidal currents that are present all over the ocean at all depths but change periodically, surf zone currents that result from offshore wave breaking, and so forth. Ocean currents are often complicated in structure because superimposed on the major currents that transport enormous volumes of water, there are gigantic whirls called gyres that may reach to great depths. Interestingly, currents at some regions happen to be merely the arms of such gyres.

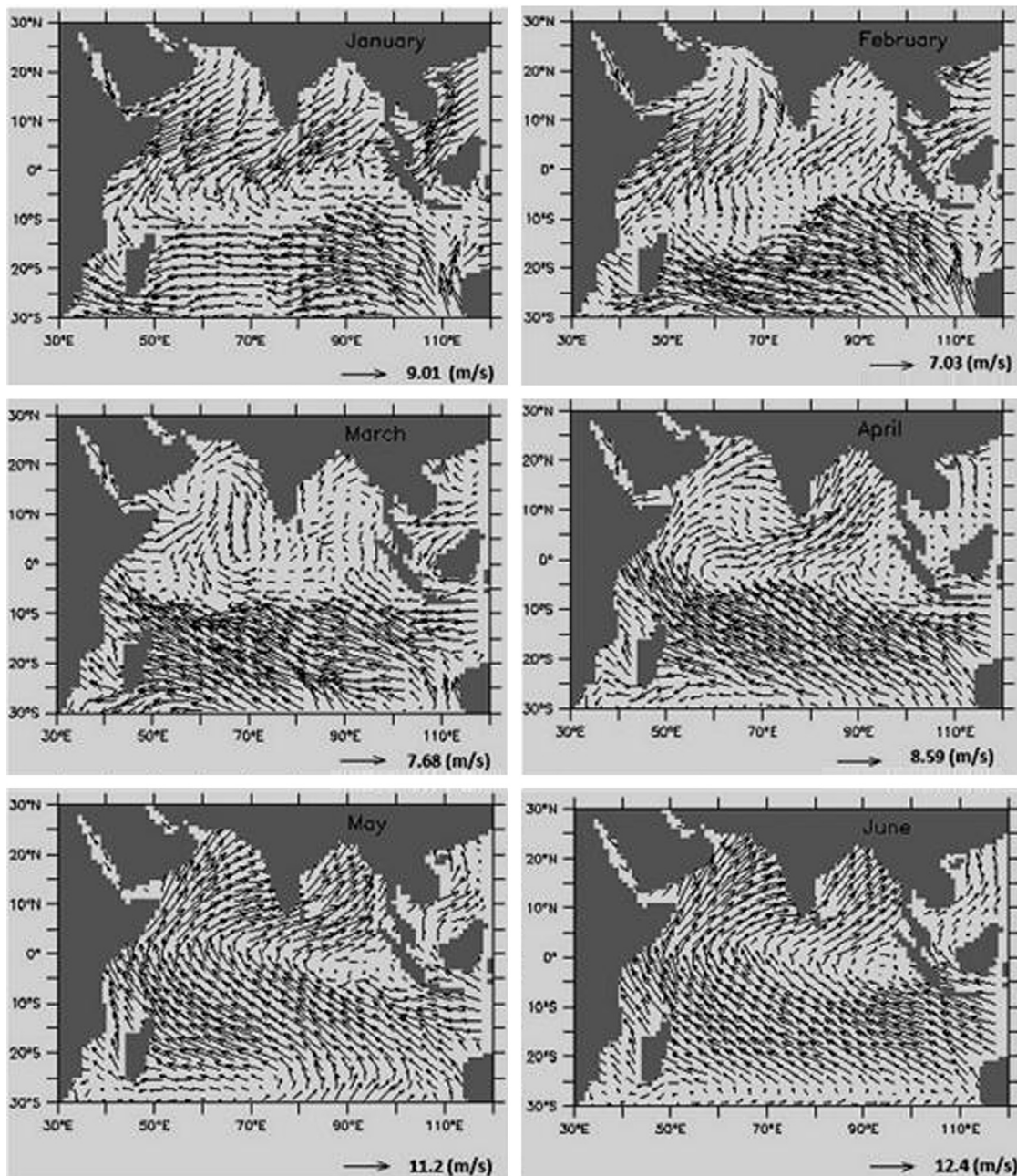


FIGURE 1.17 Pattern of European Remote Sensing (ERS) satellite-derived monthly mean sea surface wind circulation in the Indian Ocean region. (Source: Courtesy of Dr. M. R. Ramesh Kumar, Chief Scientist, National Institute of Oceanography, Goa, India.)

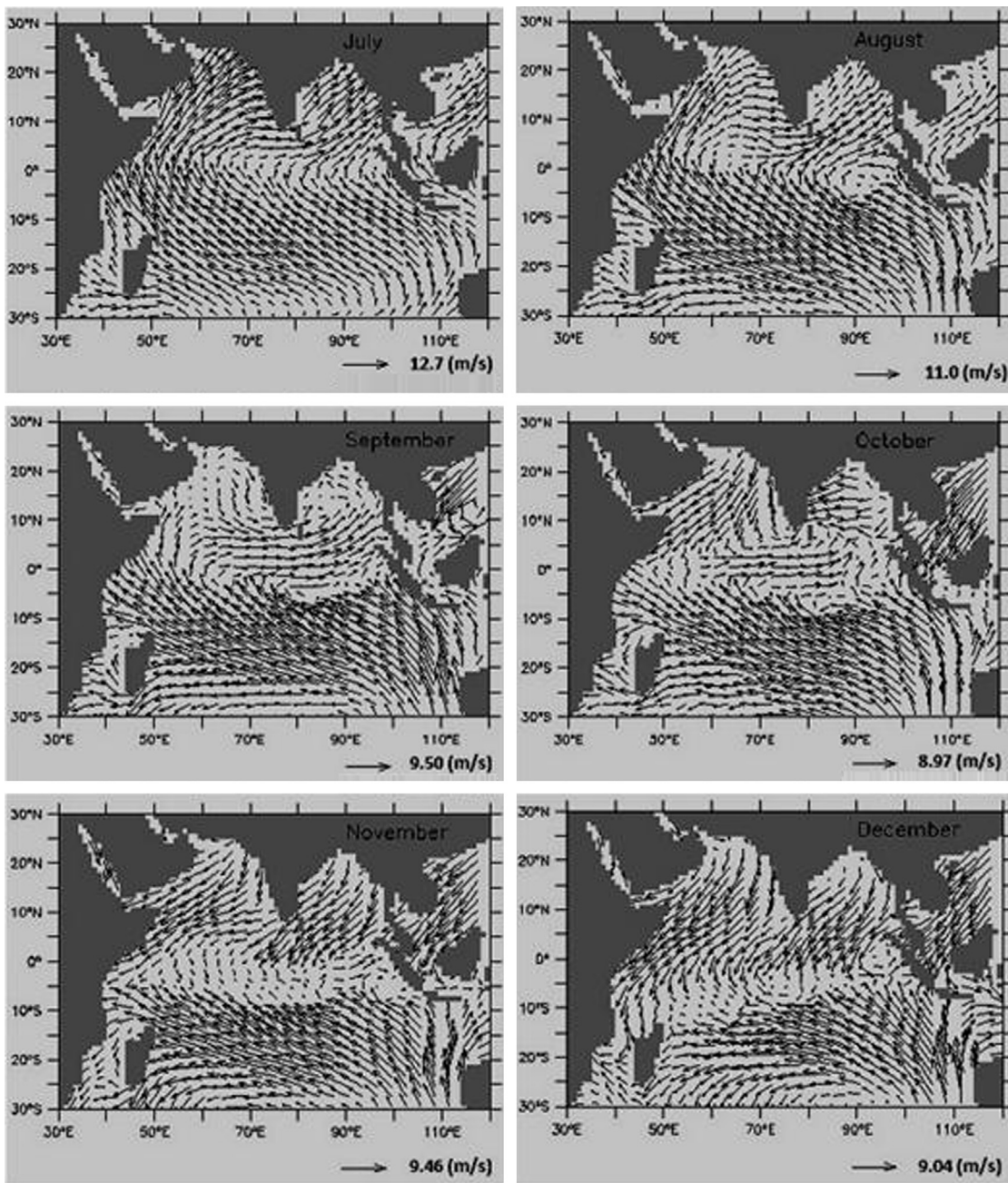


FIGURE 1.17 (Continued).

An outstanding characteristic of oceanic currents is the temporal and spatial variability of their speed and direction. Accurate observations and analysis of ocean currents have, for a long time, been a difficult task in oceanography. For a realistic understanding of any large-scale oceanic circulation feature, it is necessary to first obtain an overall picture of the temporal and spatial scales of the event as well as its variability. In the absence of such an overall picture, detailed time-series observations solely from a few selected locations are of

limited use, and can sometimes yield misleading interpretations and even lead to erroneous conclusions, when applied to large-scale events.

The modern concept of large-scale oceanic circulation features such as meanders and gyres was achieved mostly from remote monitoring of the trajectories of surface and subsurface floats over vast areas, together with remote sensing using various kinds of satellite-borne sensors. Such measurements have guided several oceanographic communities, which were indeed groping in the dark for quite some

time in the past, seeking to achieve a clearer understanding of the general features of large-scale oceanic circulation.

The 1957 joint British-American cruise in the research vessel *Aries*, sparked by Henry Stommel's ideas on deep-water movements, began to show that the deep circulation might consist of a wide spectrum of motions, some of them with velocities at least an order of magnitude faster than the mean velocities. There has since been a great volume of work on deep-water currents in open oceans.

1.5.1. Wind-Driven Current

Mixing at the surface of the oceans is important to a wide variety of concerns, including global climate and the health of marine life. Two major causes of this mixing are (1) when surface water is cooled, it becomes denser and sinks, mixing downward either to the bottom or until limited by the pre-existing stratification; and (2) the wind can mechanically stir the surface layer to some depth, usually limited by stratification. Wind also generates sea surface water motions. In the upper layers of the oceans, the currents are primarily wind-driven. When the wind blows over the ocean surface, there is transfer of momentum from air to water, part of which causes a net forward motion of the water. Generation of an Ekman spiral and Langmuir cells are two important concepts associated with wind-driven ocean currents.

1.5.1.1. Ekman Spiral

On studying the observations of wind and ice drift in the Arctic Ocean, the Norwegian oceanographer Professor Fridtjof Nansen found that the drift produced by a given wind did not follow the wind direction, as would generally have been expected, but the direction of ice drift deviated 20° to 40° to the right. Nansen hypothesized that under the influence of the Coriolis force (a force resulting from the spinning of Earth and which increases with increasing latitude of Earth), the surface water current would get progressively deflected from the wind direction. He concluded further that the water layer immediately below the surface must have a somewhat greater deviation than the latter and so on, because every water layer is put in motion by the layer immediately above it, sweeping over it like a wind. It might, therefore, be assumed *a priori* that the water current would at some depth run even in the *opposite* direction to the surface current, and there would consequently be a limit to the capability of the wind in generating currents (Kullenberg, 1954).

On Professor Nansen's suggestion, the anticipated progressive deflection (from the wind direction) of the water current in the upper layers of a large water body was given a mathematical foundation by the Swedish

researcher Vagan Walfrid Ekman. To simplify the mathematical treatment of the problem, at the same time invoking the influence of Earth's rotation and the friction in the water, Ekman imagined a large ocean of uniform depth and without differences of water density affecting the motion of the water. The influences of neighboring ocean currents and continents were also left out of the account. Finally, the curvature of the ocean surface was also disregarded within this region, and the sea surface was treated as plane. These assumptions would allow the water to freely enter into or flow from the region under consideration. Considering water as an incompressible fluid and using the equations of motion under the simplified assumptions mentioned earlier, Ekman (1905) expressed the water current velocity components u and v in the X- and Y- directions, respectively, at depth z below the sea surface, as follows:

$$u = V_o \exp\left(-\frac{\pi}{D}z\right) \cos\left(45^\circ - \frac{\pi}{D}z\right) \quad (1.1)$$

$$v = V_o \exp\left(-\frac{\pi}{D}z\right) \sin\left(45^\circ - \frac{\pi}{D}z\right)$$

In these expressions, V_o is the absolute velocity of the water at the sea surface, given by the expression:

$$V_o = \frac{T}{\sqrt{2\mu\rho\omega \sin \phi}} \quad (1.2)$$

Here, T is the tangential pressure of the wind on the sea surface, directed along the positive axis of Y (i.e., the direction of the wind velocity relative to the water); μ is the coefficient of viscosity; ρ is the density of water at the region considered; ω is Earth's angular velocity of rotation ($=7.29 \times 10^{-5}$ radian/s); ϕ is the geographical latitude of the region under consideration; D is the depth of frictional influence (i.e., depth of wind current), also known as the *Ekman depth*, expressed as $D = \pi\sqrt{(2\mu/\rho f)}$; and f is the *Coriolis parameter* (defined as twice the vertical component of the Earth's angular velocity at geographical latitude ϕ) and is given by $f = (2\omega \sin \phi)$. The velocity of the water is as a rule much smaller than that of the wind—a few hundredths of the latter. Equations 1.1 and 1.2 show that in the northern hemisphere, the drift current at the very surface will be directed 45° to the right of the velocity of the wind relative to the water. In the southern hemisphere it is directed 45° to the left. This angle further increases uniformly with the depth.

Equations 1.1 and 1.2 predict a spiral structure for the currents in the surface layers of the sea. The major elements of the Ekman spiral are the following:

- Deviation of 45° of the surface current (to the right of the wind in the northern hemisphere, and to the left of the wind in the southern hemisphere)

- Decrease of current speed with increasing depth from the sea surface
- Progressive deviation in direction of the deeper current

The just-mentioned current profile is known as the *Ekman current profile*. The direction and velocity of water current at different depths are represented by the arrows in Figure 1.18, in which the longest arrow refers to the surface, the next one to the depth $z = \pi/10a$, and the other ones to 2, 3, 4, etc. times this depth. In this,

$$a = +\sqrt{\frac{\rho \omega \sin \phi}{\mu}}$$

position at their respective depths, would appear in the form of a spiral staircase, the breadth of the steps decreasing rapidly downward. Coming back to the meaning of the terminology *depth of wind current*, it is simply the depth down to that level where the velocity of the water is directed opposite to the velocity at the surface. At depths exceeding $z = D$, the wind-driven current velocity, and consequently the friction between the water layers, is zero. Thus, D is the depth down to which the effect of the wind is noticeable. It may be noted that at the equator, the solution embodied in Equations 1.1 and 1.2 does not hold true. It has been noted that whereas the deflection increases with increasing depth from the sea surface, the magnitude of the wind-driven current decreases with increasing depth and finally vanishes at a certain depth. Thus, the deep oceans have a more or less clearly defined upper layer, which represents the portion of the ocean that is influenced by wind stress. Below this layer, there is a much larger body of water of greater density that shows little response to the prevailing atmospheric state but undergoes motion under the influence of a pressure gradient and a host of other factors unrelated to wind stress. Further, independently of any other circumstances except the geographical latitude, a wind-driven current would become practically fully developed a very short time after the rise of the generating wind—in a day or two outside the tropics.

In the initial investigations of Ekman, the very important influence of continents, differences of density of the water, and other complicating circumstances were expressly left out of accounting. In a detailed investigation, some of these restrictions, particularly the influence of continents and of neighboring currents, were examined. The calculation showed, as might be expected, a decided tendency on the part of the surface current to follow the direction of the shorelines, though with a deviation *more or less* to a direction 45° to the right of the wind (in the northern hemisphere).

Following the theoretical concepts underlying the formation of the *Ekman spiral* (named after Ekman), quantitative work by several researchers ensued to test these concepts under various oceanic environments. Thus,

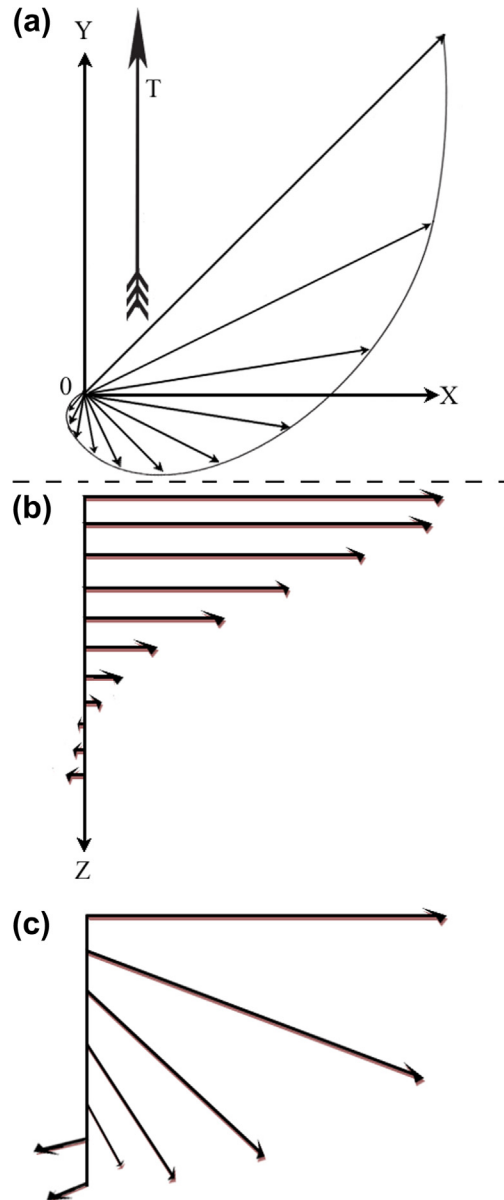


FIGURE 1.18 Schematic diagram of an Ekman spiral: (a) plan view in the horizontal plane (source: Ekman, 1905); (b) elevation view in the vertical plane; (c) isometric view.

a qualitative indication of the Ekman spiral in the deep-ocean region was observed by Katz et al. (1965). A detailed Ekman spiral structure has been measured under the polar ice by Hunkins (1966). Assaf et al. (1971) conducted field experiments in the Bermuda area to study the vertical structure of near-surface currents through aerial photography of surface-floating cards and colored plumes at different depth layers below the sea surface. The colored plumes were generated through a variety of dye injections under different wind, sea state, and thermal profile

conditions. The vertical profile of horizontal currents obtained by them contained all the major elements of the Ekman spiral.

Calculations by Ekman long ago suggested that the dominant flow direction in wind-driven shallow waters near coasts should be primarily along the coast except under winds that are nearly perpendicular to the coast. Murray (1975) conducted detailed observations (using precision theodolite) of the movement of drogues within 800 m of a long, straight, sandy shoreline, and his measurements indicated that the direction of currents driven by local winds is predominantly alongshore and that there is little dependence on wind speed. It was found that under moderate conditions, current speed is strongly controlled by the wind angle to the shoreline and, to a lesser degree, by wind speed. In the moderately stratified waters off the coast of the Florida Gulf, a subtle three-layered pattern was persistent in the coastal normal component of the velocity profile such that onshore motion was present in a near-surface and a near-bottom layer, whereas intermediate depths were characterized by offshore motion. In unstratified (i.e., well-mixed) coastal waters of Lake Superior, similar drogue experiments conducted by Saylor (1966) showed a dominant coastal parallel flow despite large wind angles to the shore. The lack of stratification in the Lake Superior data apparently results in a two-layered velocity profile in which onshore components are in the upper layer and offshore components are in the lower layer.

It must be noted that incorporation of vertical structure near the equator was not straightforward, because the Coriolis force, an important component of Ekman theory, vanishes at the equator. This led to singularities in the surface Ekman layer flow.

1.5.1.2. Langmuir Circulation

When wind blows steadily over the sea surface, lines are often visible on that surface, running roughly parallel to the wind. These lines are manifestations of a special kind of water motion known as *Langmuir circulation*. Langmuir circulation consists of a series of shallow, slow, rotating vortices at the sea surface. Irving Langmuir discovered this phenomenon after observing windrows of seaweed in the Sargasso Sea in 1938. In an exemplary series of experiments, Langmuir (1938) found these to be lines of convergence along the sea surface, with downwelling below each line. He found also that maxima in the downwind surface currents occur along these lines. Thus the mixing layer is organized into rolls of alternating sign, aligned with the wind, and water parcels follow helical paths downwind (the helix forming bands of divergence and convergence at the surface).

This form of water circulation in the surface layers of water has come to be called *Langmuir circulation* after its discoverer. Historically, this term has not implied any particular mechanism of formation, and it generally has not been used in reference to other similar structures (e.g., roll vortices in the atmosphere). The form of helical vortices set up by wind is efficient in transporting momentum, energy, and matter throughout the surface layer of water. At the convergence zones, there are commonly concentrations of floating seaweed, foam, and debris along these bands. Along the divergence zones, the sea surface is typically clear of debris because diverging currents force material out of this zone and into adjacent converging zones.

Langmuir circulation in the mixing layer in the Bermuda area has been examined by Assaf et al. (1971) based on aerial photographs of floating cards and a variety of dye injections. The *Sargassum* weeds present at the experimental site provided natural surface floats to study the Langmuir circulation pattern. As expected, the photographed lines of *Sargassum* weed were parallel to the lines of convergence of the dye patches. The experimental results showed that the maximum horizontal spacing between adjacent cells is approximately the same as the depth of the mixing layer. Faller (1969) also found that the spacing between the *Sargassum* lines was the same, on average, as the mixing depth.

Langmuir circulation is often observed to form within minutes after the onset of wind. Smith (1992) reported observations from a time period including a sudden increase in wind, followed by rapid evolution of Langmuir circulation from small to larger scale. It was found that the evolution from initially small scales to a “quasi-steady state” occurred within a time span of less than an hour. Another finding obtained from Smith’s observations is that the Langmuir circulation oriented with streaks parallel to the dominant wave direction but not absolutely uniform in that direction (i.e., irregular streaks). Theoretical aspects of Langmuir circulation have been reported by Craik and Leibovich (1976), Garrett (1976), Leibovich and Paolucci (1981), Leibovich (1983), and Leibovich et al. (1989). Based on numerous studies, Scott et al. (1969) and Gordon (1970) conclude that the most common and effective mechanism of vertical transport in the mixing layer is Langmuir circulation (and under moderate to strong winds this process dominates the other mechanisms).

1.5.2. Inertia Current

It has been known that under favorable conditions (e.g., if, for some reason, the horizontal pressure gradient as well as friction, that is, dissipative forces, become zero), the water particles in the ocean can move with a constant speed with

a constant rate of change in direction. This circulation, described in the literature as *inertia current*, must move in a circle, termed the *circle of inertia*, with constant speed. At depths below the surface Ekman layer of frictional influence, the two conditions of zero horizontal pressure gradient and zero frictional forces will be satisfied if the oceanic region under consideration is homogenous (i.e., of uniform density). It has been shown that in the Northern Hemisphere this inertia current must move around the inertia circle in a clockwise sense and in the Southern Hemisphere in a counter-clockwise sense (Neumann, 1968). When water particles move with a velocity c on a rotating Earth of angular velocity ω , the Coriolis force comes into the picture. Because the Coriolis force always acts at a right angle to the motion, the only acceleration to balance the Coriolis acceleration, $2\omega c \sin \phi$, in the absence of friction is the centrifugal acceleration, (c^2/r) , when the water moves in a circle of radius r . To maintain the inertia motion in a circle, both accelerations must be equal and must act in opposite directions, so that:

$$\frac{c^2}{r} = 2\omega c \sin \phi \quad (1.3)$$

The radius of the inertia circle, therefore, becomes

$$r = \frac{c}{2\omega \sin \phi} \quad (1.4)$$

In these expressions, ϕ is the local geographical latitude.

It can be seen from Equation 1.4 that, for a given flow speed (c), the radius (r) of the inertia circle becomes infinite at the equator ($\phi = 0^\circ$) and a minimum at the poles ($\phi = 90^\circ$). The time needed to complete a full path around the circle of inertia, known as the *inertia period* T_p , is given by the expression

$$T_p = \frac{\pi}{\omega \sin \phi} \quad (1.5)$$

This suggests that the inertia period depends only on the geographical latitude. Thus, at the poles, T_p is approximately 12 hours; at latitude 30° , T_p is approximately 24 hours; and at the equator T_p is infinite. Existence of these circulating currents in the oceans was established by direct observations as early as 1931. Currents of elliptical as well as circular shapes have since been observed at varying depths below 1,000 meters. It has been found (Neumann, 1968) that the observed inertia period of these circulating currents closely matched with the theoretically predicted periods, and their measured radius was related to the current c and the geographical latitude predicted by the equation for r . It has been noticed that some of the observed circulating currents have exhibited a translatory motion. The trajectory shape may, perhaps, change under topography-related reasons.

1.5.3. Tidal Currents in Open Seas, Estuaries, and Ridge Valleys

The periodic rise and fall of tides, in concert with astronomically induced tide-generating forces and topographically induced interactions among various tidal constituents, are associated with a periodic horizontal flow of water, known as *tidal current*. Tidal currents are strongest in restricted areas such as funnel-shaped estuaries with wide mouths and narrow heads, shallow areas, and over the sills. A decrease of cross-sectional area of the flow channel produces faster flows. In the open sea, where the direction of flow is not restricted by any barriers, the tidal current is rotary; i.e., it flows continuously, with the direction changing through 360° during the tidal period. The tendency for the rotation in direction has its origin in the deflecting force of the Earth's rotation, known as *Coriolis force*. The current speed usually varies throughout the tidal cycle, passing through two maximums in approximately opposite directions and two minimums about halfway between the maximums in time and direction. Rotary current, depicted by a series of arrows representing the speed and direction of the current, is usually known as a *current rose*. A line joining the extremities of the radius vectors will form a curve roughly approximating an ellipse. The cycle is completed in one-half tidal day or in a whole tidal day, according to whether the tidal current is of the semidiurnal or the diurnal type. A current of the mixed type will give a curve of two unequal loops each tidal day. Because of the elliptical pattern formed by the envelope joining the ends of the arrows, it is also referred to as a *tidal current ellipse*. Figure 1.19 shows a graphic representation of a rotary current in which the velocity of the current at different hours of the tidal cycle is represented by radius vectors and vectorial angles.

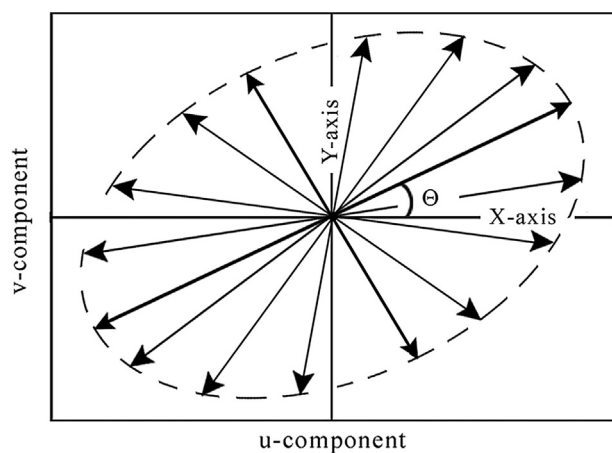


FIGURE 1.19 Graphic representation of a rotary current in which the velocity of the current at different hours of a tidal cycle is represented by radius vectors and vectorial angles. By convention, the u component is the east component and the v component is the north component.

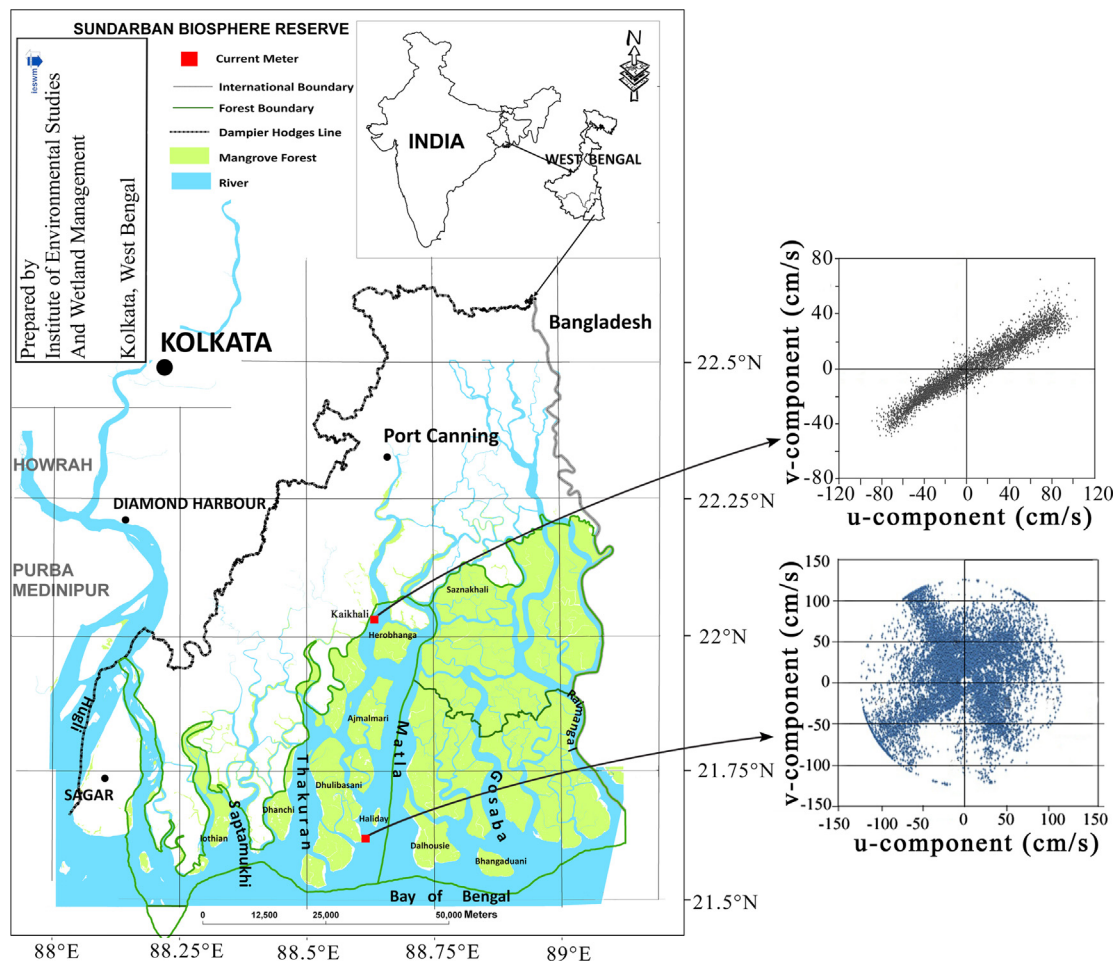


FIGURE 1.20 Graphic representations of two extreme forms of tidal current ellipses (i.e., circular and rectilinear) at two different locations in Sunderbans mangrove reserve forest delta. The tidal current circle observed at the southern station appears to have resulted from a combination of two near-rectilinear currents flowing through the two adjacent channels. (Source: Courtesy of Kakoli Sen Sarma and Somenath Bhattacharyya, Institute of Environmental Studies & Wetland Management, Kolkata, India.)

The characteristics of tidal ellipse are (1) semi-major axis, (2) semi-minor axis, (3) eccentricity (ratio of minor to major axes; positive for counter-clockwise rotation), (4) orientation, and (5) sense of rotation. With a one-year-long dataset it is possible to extract the characteristics of tidal ellipses for the main semidiurnal, diurnal, fortnightly, monthly, semiannual, and annual constituents. Depending on the regional peculiarities, tidal ellipses are often found to exhibit large spatial variability. The tidal ellipse can change from cyclonic (counter-clockwise in both hemispheres) to anticyclonic (clockwise in both hemispheres) and from rectilinear (major axis \gg minor axis) to circular (major axis = minor axis). Depending on the topographic peculiarities, the eccentricity has been found to vary considerably, both laterally and vertically; also, different tidal current constituents (e.g., M_2 , K_1 , etc.) can rotate in different directions (Marinone and Lavin, 2005). Tidal current is expected to be constant from sea surface to bottom, unless modified by stratification or bottom friction.

Figure 1.20 shows the presence of two extreme forms of tidal current ellipses (i.e., *circular* and *rectilinear*) at two different locations in Sunderbans, which is the largest delta in the world, with $10,200 \text{ km}^2$ of Mangrove Reserve Forest extending over two countries, namely India ($\sim 4,200 \text{ km}^2$) and Bangladesh ($\sim 6,000 \text{ km}^2$). In a true tidal current ellipse, the current direction must exhibit a smooth change over a full tidal circle (i.e., in the range $0\text{--}360^\circ$). Based on the concentration of the *u*-components (i.e., east components) and *v*-components (i.e., north components) of currents along two dominant directions, it can be suggested that the tidal current circle observed at the southern station results primarily from a combination of two near-rectilinear tidal currents flowing through the two adjacent channels. Plotting of tidal current ellipses of different constituents (of tidal currents) at different depths will throw more light on the character of tidal currents in a region.

There are instances in which the tidal current ellipses are not the result of the Coriolis force but are generated by

the alternating cross-shore water fluxes due to the tide. Houwman and Hoekstra (1998) have reported such a case happening at a multiple-bar system of the barrier island of Terschelling in the Netherlands. At this site, the direction of rotation of the current vector has nothing to do with the Coriolis force but is determined by the position of the coast, left or right, relative to the progressive tidal wave.

Tidal currents in the open ocean are generally weak. However, tidal currents in coastwater bodies belong to the most vigorous flow phenomena in the sea. Nonlinear instabilities give rise to a large variety of “secondary currents,” ranging from the smallest three-dimensional eddies in the dissipation range—with a scale of $\sim 10^{-3}$ m, carried along by the tidal flow (Grant et al., 1962)—to the topographically “frozen” quasi-two-dimensional residual eddies (Zimmerman, 1978; 1980) with length scales of 10^4 m. Topographic obstacles in the path of large currents give rise to production of vortex streets in the wakes of such obstacles, and the vortices are carried along by the current. Any existing quasi-two-dimensional turbulence in tidal currents must have a pronounced influence on the physical transport processes in tidal areas and hence on the total physical environment (Veth and Zimmerman, 1981).

In estuaries or straits or where the direction of water flow is more or less restricted to certain channels, the tidal current is *reversing*, i.e., it flows alternately in approximately opposite directions with a short period of little or no current, called *slack water*, at each reversal of the current. During the flow in each direction, the speed varies from zero at the time of slack water to a maximum, called *strength*, about midway between the slacks. The water current movement from the sea toward shore or upstream is the *flood current*, and the water current movement away from shore or downstream is the *ebb current*. Tidal currents may be of the semidiurnal, diurnal, or mixed type, depending on the type of tide at the location. Offshore rotary currents that are purely semidiurnal repeat the elliptical pattern each tidal cycle of 12 h and 25 min duration. If there is considerable diurnal inequality (i.e., if there is considerable difference in the two successive tidal ranges), the arrows representing the instantaneous tidal current vector describe a set of two ellipses of different sizes during a period of 24 h and 50 min (one lunar day). The difference between the sizes of the two ellipses is dependent on the diurnal inequality. In a completely diurnal rotary current, the smaller ellipse disappears and only one ellipse is produced in duration of 24 h and 50 minutes.

The magnitude of the tidal current speed varies with the tidal range (i.e., the difference between successive high-tide and low-tide elevations). Thus, the stronger *spring* and *perigean* currents occur, respectively, near the times of new and full moon and near the times of the moon’s

perigee. The weaker *neap* and *apogean* currents occur, respectively, at the times of neap and apogean tides. An important role of the fast tidal currents is to produce intense tidal mixing, which, by pumping nutrients into the surface layers, is one of the ultimate causes of a location’s biological richness.

Tidal currents in ridge valleys are particularly interesting. For instance, Garcia-Berdeal et al. (2006) have reported fascinating vertical structures of time-dependent water currents in the axial valley at Endeavour Segment of the Juan de Fuca Ridge, which lies along the divergent boundary between the Pacific and Juan de Fuca plates, approximately 400–500 km off the coasts of Washington and Oregon (Figure 1.21).

Diurnal tidal current motions are trapped to the ridge and experience an amplification of their clockwise rotary component that is attributed to the generation of anticyclonic vorticity by vortex squashing over the ridge. Whereas the across-valley water currents diminish with increasing depth, the along-valley currents are accelerated and intensified with depth. Alignment of the current flow with the along-valley direction yields a velocity vector that spirals with depth.

At the central valley site, all diurnal tidal ellipses are found to be clockwise rotary. At the central valley site, both a gradual decrease in the eccentricity of the ellipses and an amplification of the major axis with increasing depth down to 15 m above the bottom has been noticed. In addition, the orientation of the major axis of the ellipses rotates predominantly counter-clockwise with increasing depth and aligns with the along-valley direction.

In contrast, in the case of the diurnal tidal current ellipses at the Easter Island, the higher ellipses tend to be clockwise rotary and the deeper ones, counter-clockwise, although they are all rather rectilinear. The major axes of the K_1 ellipses at Easter Island (2–4 cm/s) are larger than those from the central valley record (2–3 cm/s) and do not undergo a progressive trend with depth. The ellipse orientation rotates clockwise with increasing depth and becomes aligned along the valley.

1.5.4. Rip Currents

The shallow-water coastal zone encompassing the onshore and offshore sides of the wave-breaking region (known as the *surf zone*) is one of the very energetic regions of the oceans. Changes in wave breaking owing to variations in wave height and direction along curving coastlines, irregular bathymetry, and manmade structures cause complex surf zone circulation, primarily rip currents, along with relatively weak mean alongshore currents that can change direction both across the surf zone and along a depth contour (Shepard and Inman, 1950). *Rip currents* are a generic name given to approximately shore-normal,

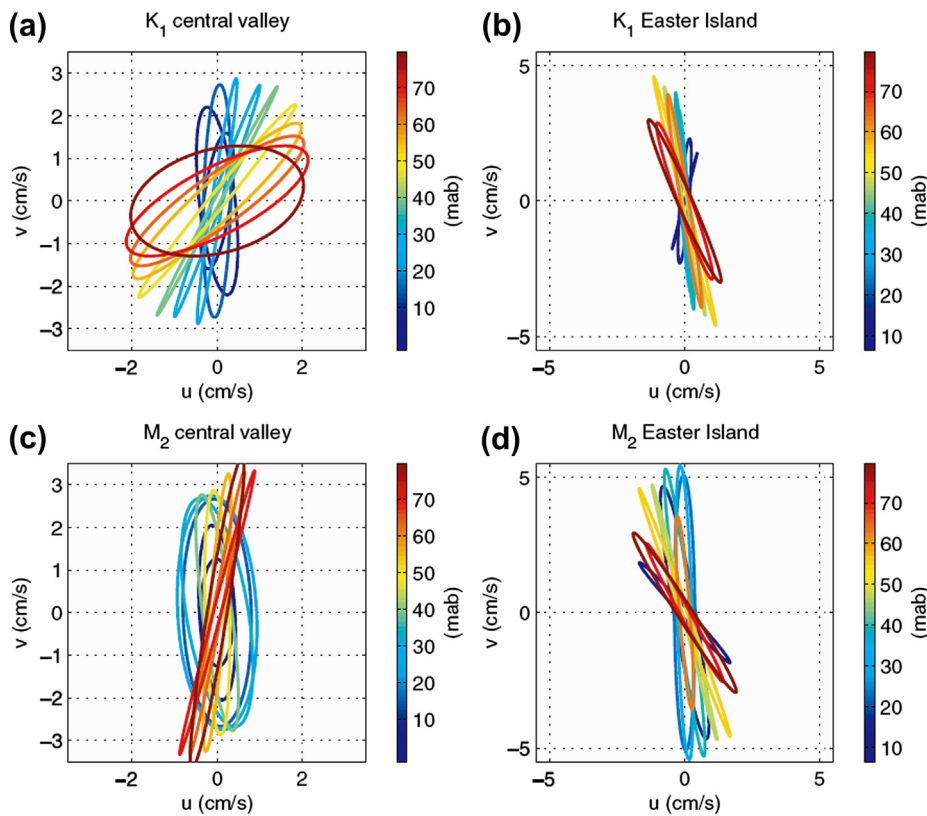


FIGURE 1.21 Observed tidal current ellipses in across-valley (u-component) and along-valley (v-component) coordinates for the diurnal (top panels) and semidiurnal (bottom panels) frequencies from the central valley (a), (c) and Easter Island (b), (d) records. Ellipses are plotted at 6.5–78.5 m above bottom (mab), in intervals of 8 m. Blue corresponds to levels closer to the bottom. Note change of velocity scale in (b) and (d). (Source: Garcia-Berdeal et al., 2006.)

strong, narrow, offshore-directed (i.e., seaward-flowing) current jets with a strong and constrained flow that originate within the surf zone, extend seaward, and broaden outside the breaking region, forming a head region once they pass beyond the surf zone (see Figure 1.22).

Figure 1.23 shows a photograph of a rip current in Monterey Bay, California. Once initiated, a rip current develops into a distinct current system consisting of three main features: (1) a *feeder region* where the currents are directed toward the center of the rip and provide the volume flux for the offshore flow, (2) the *rip neck*, which is the narrow offshore-flowing section of the rip that usually has the highest current velocities and may extend a significant distance outside the surf zone, and (3) the *rip head*, which is the seaward end of the rip current, wherein distinct vortex features such as spinning down eddies are often seen. The rip head can often be observed and clearly identified in photographic and satellite images as a mushroom-shaped feature at the offshore limit. According to Smith and Largier (1995), episodic instability plumes are often observed outside the breaker region. Outside the surf zone, Haas and Svendsen (2002) found the mean velocities to be near zero, although instantaneous velocities could be substantial. This is associated with the pulsing and unstable nature of the rip current (Haller and Dalrymple, 2001). They found that the jet flow is surface dominant

seaward of the breaking region. Therefore, the visual markers such as sediment plumes or bubbles associated with rip currents seen outside of the surf zone are surface dominated and their average propagation speed is minimal. As the rip current moves offshore into deeper water, the streamlines move closer together, creating a stronger and narrower current, which explains why even when a rip channel occurs over a gentle alongshore depression, the offshore jet is well confined (Peregrine, 1998; Kennedy and Thomas, 2004).

Although the rip neck is characterized by intense water current velocities in the offshore direction, the currents decelerate rapidly in the head region. The spatial gradients of the current velocities across the rip neck and the diverging region of the head are strong. In addition, the region of strong offshore flow is tightly constrained. In several instances, shore-perpendicular rip current trajectories have been found to swing to become oblique to the shore as a result of the complex hydrodynamics involved. In a complete rip current cell, a diffuse onshore flow in the feeder region supplies the rip necks. Examination of trajectories of freely drifting drogues deployed in the surf zone have indicated that quite often the rip current undergoes a large meander while still maintaining a coherent jet form before spreading in a head-type feature. This general circulation feature is often

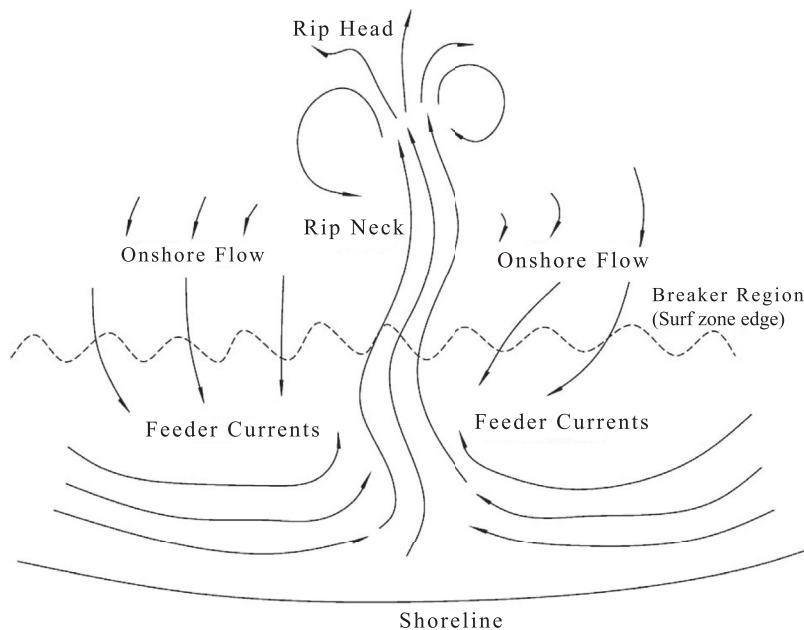


FIGURE 1.22 A schematic of a rip current. (Source: MacMahon et al., 2006.)

observed even though the rips themselves are transient in time and space. Most field observations have been for rip currents coupled to the underlying beach morphology. There have been a few observations of nonstationary rip currents, which are often referred to as *transient rip currents* (Tang and Dalrymple, 1989; Fowler and Dalrymple, 1990; Johnson and Pattiarchi, 2004). Whereas the exact arrangement in a rip system varies greatly, the law of conservation of mass alone suggests that all rip current systems must possess these three basic regions in some form.

Early qualitative observations suggested that the rip currents are coupled to the morphology, the rip currents pulsate, and the velocities increase with increasing wave height (Shepard, 1936; Shepard et al., 1941; Shepard and Inman, 1950; McKenzie, 1958; Bowman et al., 1988a,b). Later studies have increased both spatial and temporal resolution of the observations and with greater accuracies, which have quantified earlier qualitative assessments.

There are weaker and broader onshore-directed flows in the region neighboring the rip current, contributing to the alongshore-directed feeder currents that converge to the rip

FIGURE 1.23 A photograph of a rip current in Monterey Bay, California. The rip current is the dark patch. There is intense wave breaking on both sides of the rip currents with little breaking within the deeper rip channel, where bubbles are advected seaward. (Source: MacMahon et al., 2006.)



current. Early studies obtained crude estimates of rip current velocities, which include 1 m/s (Shepard and Inman, 1950), 50 cm/s (Sonu, 1972), 30 cm/s (Huntley et al., 1988), and 70 cm/s (Short and Hogan, 1994). Mega-rips are generally observed on embayed beaches with suggested velocities exceeding 2 m/s (Short, 1999), but there are no *in situ* field measurements of mega-rips. Rip currents shape the sandy shoreline and are considered to be important for transporting sediments offshore (Cooke, 1970; Komar, 1971; Short, 1999). The seaward-directed high-speed rip current flow often transports sediments, pollutants, foam, surfers, and swimmers offshore and is dreaded by beach swimmers. Based on survey results, rip currents account for more than 80% of lifeguard rescue efforts and are the number-one natural hazard in the state of Florida (MacMahan et al., 2006). More people fall victim to rip currents in Florida than to lightning, hurricanes, and tornadoes (Luschine, 1991; Lascody, 1998).

Recently there have been a significant number of laboratory and field observations to study rip currents, which has led to advances in our understanding of these systems. An overview of rip current kinematics based on these observations and the scientific advances obtained from these efforts have been synthesized by MacMahan et al. (2006). Johnson and Pattiarchi (2004) and MacMahan et al. (2006) have given brief surveys of rip currents based on available literature and their own findings from field measurements and model-based studies. It is generally agreed that the rip current flow consists of various temporal contributions, all of which have their own forcing mechanism. Accordingly, rip current flows can be partitioned in terms of the following contributions (MacMahan et al., 2006):

1. Infragravity band (i.e., period of oscillation in the range 25–250 seconds)
2. Very low-frequency band (i.e., period of oscillation in the range 4–30 minutes)
3. A mean flow based on the rip current system and wave conditions
4. Modulation associated with the slow variations in the water level due to changing tidal phase

Each of these contributes significantly to the total, and the combination results in significant flow speeds that have the potential for transporting sediment and catching beachgoers off-guard.

Longuet-Higgins (1970) showed that water circulation in the surf zone is driven primarily by breaking waves. All dynamical models of rip currents are forced by alongshore variations of wave height that result in alongshore variations in wave-induced momentum flux, termed *radiation stress* by Longuet-Higgins and Stewart (1964). When the waves break, the changes in radiation stresses generate slowly migrating rip currents traveling alongshore.

Bowen (1969) was the first to show that alongshore perturbations in bathymetry result in alongshore variations in wave height, which generate rip currents. Rip currents are most often observed to occur when the waves approach at near-normal incidence and where there are alongshore variations in bathymetry with the alongshore sandbar incised by rip channels. When adjacent pairs of wave groups offset in time and space enter the surf zone, the interaction of the generated vortices can lead to narrow, offshore-directed, quasi-steady flows. Over an alongshore homogeneous bathymetry, the circulation cells, in general, propagate slowly alongshore, simulating migrating rip currents. Thus, rip current flows are forced by the incoming wave energy but influenced by tidal elevation and the shape of the morphology.

Rip currents pulsate at various temporal scales, which have different forcing. The pulsations are composed of infragravity motions, modulations of wave group energy, shear instabilities, and tides. The summation of these flow contributions can lead to strong offshore rip currents that last for several minutes. The time-averaged pulsations are minimal outside the surf zone, yet when the pulsations occur, they are surface dominated. Data from the laboratory and the field suggest that rip current strength increases with increasing wave energy and decreasing water depths. Rip currents can occur under various bathymetric perturbations, even for beaches with subtle alongshore variations. The maximum mean current occurs inside the surf zone, where the maximum forcing is present owing to the dissipation of waves. Wave-current interaction may define the energy of a rip current system and feedback mechanisms.

Rip currents are tidally modulated such that decreases in tidal elevation increase rip current flows to a relative maximum (Sonu, 1972; Aagaard et al., 1997; Brander, 1999; Brander and Short, 2001; MacMahan et al., 2005), and the presence and danger of rip currents are often linked to lower tidal elevations. Rip currents are nonexistent at high tides (Shepard et al., 1941; McKenzie, 1958; Short and Hogan, 1994; Luschine, 1991; Lascody, 1998; Engle et al., 2002). During times of spring tides, the threat of rip currents to beachgoers and the potential influence of the rip currents transporting sediments increase until the water depth over the shoal becomes too shallow or dry. Rip currents are morphologically controlled, and therefore the mean velocity of a rip current varies for different beaches, wave forcing, and tidal elevation. Subtle bathymetric perturbations can induce significant three-dimensional flows. Laboratory and field data indicate that rip current velocity increases with increasing wave height and decreasing water depth.

The maximum mean current occurs inside the surf zone, where the maximum forcing is present owing to the dissipation of waves. Rip currents have been observed to pulsate in association with wave groups at the infragravity band, and

such infragravity rip current pulsations increase the instantaneous rip current maximum flow to over 1 m/s. Stochastically varying wave groups can further increase the rip velocity.

Numerical modeling experiments by Svendsen et al. (2000) have indicated that the total transport through the rip channel does not depend on the spacing of the rip channels, and preliminary analysis from the Nearshore Canyon Experiment (NCEX) supports this finding. In topographic rips, the extent of the feeder region is also largely independent of rip spacing and the rip is only supplied by a small local area (Svendsen et al., 2001). However, whether this is the case in transient rips is not known at present. The rip neck may be directed perpendicular or obliquely to the shore, may have a meandering shape, and may move around. The rip head is often clearly visible as a sediment-laden patch of water at the end of the narrower neck. This patch of water may persist as a coherent feature for some time after the rip flow has ceased.

Surf zone eddies associated with rip currents have been predicted theoretically and numerically by several researchers (e.g., Peregrine, 1998; Chen et al. 1999; Svendsen et al., 2000) and noted in field and laboratory observations. There exist transient rips, which are temporary features that develop in varying locations. These have a specific lifetime and subsequently decay. Rip currents are ubiquitous in the near-shore regions of several long beaches. The world-famous Calangute beach in Goa (on the west coast of India), which finds a prominent place on tourist maps, is just such a beach; it is notorious for rip current generation, leading to human casualties almost every year.

1.6. IMPLICATIONS OF OCEAN CURRENTS

Ocean currents and atmosphere interact to produce large-scale changes in climate. For example, the baroclinic transport variability of the Kuroshio Current system is considered to have an important effect on the winter climate of the Northern Hemisphere (White, 1975). The timing and strength of the Indian monsoon depend at least partially on the behavior of the Somali Current (the only known ocean current that reverses its direction in consonance with the overlying winds) off the East African Coast (Anderson and Rowlands et al., 1976; Das, 1988), as well as to a global-scale atmospheric circulation feature called the Southern Oscillation (Shukla, 1987), the temperature anomalies of the El Niño current and of the western Indian Ocean (Rameshkumar et al., 1986; Shukla, 1987), and some as-yet unknown large-scale, low-frequency forcings (Shukla, 1987). The poleward transport of heat by the oceans and the eddies shed by them also play an important role in this activity. The poleward “counter-currents”—a characteristic feature of boundary current regions—are well known for their influence on activities such as fishing

and sound ranging as well as on coastal marine climate and small-scale, near-shore circulations for which they may be a significant driving mechanism (Wickham, 1975).

Apart from their influence on climate change, ocean currents affect us in several other ways. For example, transport of large volumes of water with anomalous temperature differences is believed to be responsible for triggering unusual weather patterns affecting entire continents. As carriers of thermal energy, ocean currents have a direct influence on fish migration and weather patterns. It is well known that El Niño, a current of warm water that appears in some years off the coast of Peru, causes a rapid rise of SST in normally cool-water regions. This leads to instabilities in the overlying atmosphere, which cause excessive rainfall and damaging floods, and erosion in regions where the normal precipitation is very low. The anomalous condition also has a disastrous effect on the fishing industry due to catastrophic destruction of plankton and fish life. Finding nothing to feed on, the surviving fish move on to newer pastures. Consequently, sea birds die of hunger in large numbers (e.g., in Peru during some El Niño events) or migrate, abandoning their young ones. Interestingly, the El Niño event, at least partially, is an indirect indicator of deficient monsoon over India and may provide very useful guidance for long-range forecasting of monsoon rainfall over India (Shukla 1987a,b).

Currents within approximately a meter of the sea surface transport floating matter and, therefore, are of great importance in coastal areas, where considerable damage can be inflicted by surface-borne pollutants and spilled oil. From pollution monitoring and control perspectives as well as for determination and forecasting of oil-spill drift in the case of oil tanker accidents, knowledge of currents is of great practical interest. Surface current measurements are also important for studies related to pollutant distribution patterns and identification of suitable areas for disposal of these pollutants.

From an environmental perspective, seasonal mapping of coastal surface currents is useful to determine the most optimal outfall sites for emerging industries, harbors, thermal and nuclear power plants, and so forth. With more and more pollutant outfalls being brought to the coastal waters, such mapping procedures have become all the more important to control the spread of effluent emissions and thereby save the coastal waters from excessive pollution levels. Because a vast majority of humans’ ocean-related activities are influenced by sea surface conditions, timely information on the surface currents and their perturbations in such areas is of vital importance. The behavior of surface phenomena such as thermal plumes can be properly studied only if the coastal water current circulation patterns are known.

Radioactive emissions from nuclear power stations in Japan as a result of the damage inflicted on them by the

March 2011 Japanese tsunami and the fear of the possible spread of radioactive-contaminated water to distant locations through ocean currents were great concerns among a large section of people in Japan and the neighboring coastal nations in the days immediately after the Japanese tsunami episode. This concern is justifiable in view of the fact that tsunamis are known to generate strong water-current velocities in the coastal zones and inside partially confined water bodies such as bays and harbors (Koshimura et al., 2009), and such strong currents can quickly spread radioactive contamination offshore, facilitating further transport across the oceans. In the mid-1980s, there was considerable interest in the potential for disposal of radioactive waste either below or on the seabed. The feasibility studies included research on the interaction of radionuclides with sediment but also called for an investigation of ocean circulation around potential disposal sites. This required information on both the subthermocline mean circulation and on eddy-induced lateral mixing at these depths.

Currents and turbulence are essential factors in understanding many biological processes. Turbulence is one of the factors that regulate the supply of nutrients to the photic zone, and the nutrient supply ultimately controls the productivity of the area. The upper portion of the sea, especially the photic (light-penetrating) zone, carries zooplankton and phytoplankton, which are the dominant components at the bottom of the food chain and are responsible for the production of most of the world's oxygen. Ocean surface pollution, which destroys these vital components required for the survival and prosperity of mankind, is of serious concern. Fish eggs are borne by surface currents, which are, therefore, of concern to the fishing industry. Knowledge of surface currents is useful in understanding the distribution of fish such as salmon and tuna. The mass transport of plankton and marine invertebrates to and from the bays and shelf waters is greatly influenced by the currents of the near-shore waters. Detailed knowledge of currents is necessary to understand the transport of larval forms of oysters, crabs, and the like from the point of hatching to the point of attachment or residence.

One of the critical needs of the offshore industries is for real-time information on water currents during events such as severe storms. Near-real-time data are also highly desirable during quieter periods to aid on-site construction. Knowledge of ocean currents is essential for several ocean engineering applications such as offshore pipe laying, offshore mining (e.g., minerals, hydrocarbon deposits, polymetallic nodules), and coastal erosion control. Estimation of hydrodynamic loads required for the design of marine structures such as offshore drilling platforms, pipelines, and dock facilities also require ocean current data. With the advancement of the offshore industry to deeper waters, oil and gas operators face new environmental challenges. There

is an ever-increasing need for ocean current data for applications in the design and operation of offshore structures. Whether in the Gulf of Mexico, southeast of Brazil, offshore South Africa, or in Indonesia, the oceanic upper layer often encompasses very strong and extremely variable currents (jets, eddies, meanders, filaments, etc.). Such energetic features present major risks for marine operations and have already caused costly losses of structures over various areas of the world.

Potentially dangerous ocean current eddies have threatened several drillships. It is important to track and forecast eddies as they head toward the drilling vessel so that their effects can be minimized by careful planning of subsea operations. Eddies are fast enough to severely impact drillship operations. Tracking and forecasting the progress of eddies help reduce the delays and the harm they can cause. There is a special requirement for near-real-time observations during installation of offshore structures. For instance, drilling superintendents on exploration rigs need real-time information on ocean currents in order to assess present and upcoming stresses on marine risers, which may produce vortex-induced vibrations. In extreme cases these can cause the riser to separate from the blowout preventer stack. Other operations, such as the deployment of underwater vehicles and subsea systems, also benefit from knowledge of the ocean current regime. Real-time data measured from rigs are used not only to assist day-to-day drilling operations but also to provide valuable information for future design engineering plans.

A major component of understanding a unique system called a *hydrothermal vent field* involves characterizing near-bottom currents at mid-ocean ridges and determining the flux of heat and the dispersal of biological/chemical species associated with hydrothermal fluid. The transport of planktonic larvae by bottom currents plays a key role in the dispersal potential of vent species that have limited mobility yet are constantly faced with the challenge of colonizing new sites because of the ephemeral, unpredictable, and highly variable nature of hydrothermal vent systems. Because the highest abundances of these larvae are found close to the bottom and to their vent source communities (Mullineaux and France, 1995) and because hydrothermal venting is largely concentrated within the axial valley of the ridge, characterizing the current flow patterns in the valley is central to understanding larval dispersal mechanisms and pathways. In addition, it has been suggested that transport by near-bottom currents may be a more prevalent larval pathway than entrainment into rising plumes and dispersal within the neutrally buoyant plume, which is favored only during periods of slack tide (Kim and Mullineaux, 1998).

Abyssal currents of remarkably great widths (30 to 500 km) have been discovered and surveyed in most major ocean basins (Stommel and Arons, 1972). Bottom currents are considered major contributors that control sediment

distribution in the oceans. Deep thermohaline currents have given rise to many large sediment drifts comprising silt and clay located in a variety of places, including the foot of the continental rise (Heezen et al., 1966). There are examples where deep currents were responsible for the formation of sediment ridges several hundred km long, several tens of km in width, and as much as a km in thickness (Ewing and Edgar, 1966). In other areas, strong evidence of erosion on the deep-sea floor is indicative of the important role of currents in the distribution of oceanic sediments. Large forms such as *longitudinal triangular ripples* (LTR) and furrows occur at the sea bottom under strong currents and greatly influence abyssal sediment dynamics. Variations in deep-ocean thermohaline circulation merit investigation.

At the estuarine level, data on water currents are important to hydrodynamic numerical modeling for prediction of sediment transport and deposition along shipping channels and estuaries (Biswas and Chatterjee, 1987). Such predictions aid hydrographic surveys and are useful for selective dredging along long and complex navigation channels (e.g., Hugli River in Calcutta, India, and the Waterway to Rotterdam Port, which often branch and wend their way between the port and the sea).

Coastal current circulation measurements are needed for studies related to the dynamics of coastal waters. Current measurements have important applications for coastal surveillance, rescue operations, and proper planning for effective utilization of coastal waters. Information on surface currents is vital to assess the impact of possible offshore oil recovery operations. It is the surface currents that primarily determine whether an oil spill or leak may dissipate harmlessly at sea or do irreparable damage to the coast. A vast majority of mankind's ocean-related activities take place on or near the ocean's surface, and most coastal operations are influenced by surface conditions.

It is now our understanding that each oceanic region, however unique in individual behavior, consists of a number of "common" characteristic synoptic circulation structures and water masses. These synoptic entities, or "features," when put together in the background climatology of a particular region, interact and evolve together to generate the combined circulation variability due to various factors. A regional basin may include a set of multiscale features such as large-scale meandering currents and fronts, basin-scale and subbasin-scale gyres, mesoscale eddies, and vortices. A coastal region may include circulation structure features such as mesoscale buoyancy-driven fronts, upwelling fronts, and submesoscale eddies and fronts. Thus, the scales of motions in the oceans range from major ocean dimensions down to millimeters. As would be expected, the spectrum of motions has a wide range. During the last few decades,

there has been significant advancement of our accrued knowledge and understanding of oceanic circulation and variability in regional oceans. This has been possible due to technological advances in multiplatform at-sea and space-borne instrumentation capabilities, in the availability of highly efficient computing platforms and numerical modeling capabilities, and in model data assimilation and integration methodologies.

The oceanographer, with his inaccessible environment, has long sought to unravel all the characteristics of oceanic variabilities and statistics of fluid motion. Measurements of variabilities ranging from microscale to mesoscale are, therefore, important. Because it is impossible to develop a single technique to make measurements that could be used to describe all scales of motion, it becomes necessary to divide them into subranges and study them separately. Although studies of all scales of motions are important, a limited range of motions might be more significant to a specific problem and can be studied in depth if techniques are developed to look only at the range of interest. The opportunity to learn about a phenomenon in part offers the advantage that the complexity of instrumentation can be reduced to practically achievable bounds. The last few decades have witnessed a rapid evolution of new technologies for measuring ocean currents. These technologies and the associated problems and prospects are addressed in the following chapters.

REFERENCES

- Aagaard, T., Greenwood, B., Nielsen, J., 1997. Mean currents and sediment transport in a rip channel. *Mar. Geol.* 140, 25–45.
- Anderson, D.L.T., Rowlands, P.B., 1976. The Somali Current response to the southwest monsoon: the relative importance of local and remote forcing. *J. Mar. Res.* 34, 395–417.
- Anderson, L.T., Rowlands, P.B., 1976. The Somali current response to the southwest monsoon: the relative importance of local and remote forcing. *J. Mar. Res.* 34 (1), 395–417.
- Andrews, J.C., Scully-Power, P., 1976. The structure of an East Australian Current anticyclonic eddy. *J. Phys. Oceanogr.* 6, 756–765.
- Aoki, S., Yoritaka, M., Masuyama, A., 2003. Multidecadal warming of subsurface temperature in the Indian sector of the Southern Ocean. *J. Geophys. Res.* 108, 8081.
- Assaf, G., Gerard, R., Gordon, A.L., 1971. Some mechanisms of oceanic mixing revealed in aerial photographs. *J. Geophys. Res.* 76 (27), 6550–6572.
- Babu, M.T., Kumar, S.P., Rao, D.P., 1991. A subsurface cyclonic eddy in the Bay of Bengal. *J. Mar. Res.* 49, 403–410.
- Barber, R.T., Chavez, F.P., 1983. Biological consequences of El Niño. *Science* 222, 1203.
- Barlow, E.W., 1935. The 1910–1935 survey of the currents of the Indian Ocean and China Seas. *Mar. Observer* 12, 153–163.
- Beal, L.M., Chereskin, T.K., Lenn, Y.D., Eliot, S., 2006. The sources and mixing characteristics of the Agulhas Current. *J. Phys. Oceanogr.* 36, 2060–2074.

- Bernstein, R.L., White, W.B., 1977. Zonal variability in the distribution of eddy energy in the mid-latitude North Pacific Ocean. *J. Phys. Oceanogr.* 7, 123–126.
- Bernstein, R.L., White, W.B., 1981. Stationary and traveling mesoscale perturbations in the Kuroshio Extension Current. *J. Phys. Oceanogr.* 11, 692–704.
- Biastoch, A., Krauss, W., 1999. The role of mesoscale eddies in the source regions of the Agulhas Current. *J. Phys. Oceanogr.* 29, 2303–2317.
- Biswas, A.N., Chatterjee, A.K., 1987. Sedimentation at Auckland in the Hugli Estuary, Proc. Coastal and Port Engineering in Developing Countries. In: China Ocean Press, 2, 1309–1320.
- Boebel, O., Davis, R.E., Ollitrault, M., Peterson, R., Richard, P., Schmid, C., Zenk, W., 1999. The intermediate depth circulation of the Western South Atlantic. *Geophys. Res. Lett.* 26 (21), 3329–3332.
- Boland, F.M., 1973. A monitoring section across the East Australia Current. *CSIRO Div. Fish. Oceanogr. Tech. Pap.*, 34.
- Boland, F.M., Hamon, B.V., 1970. The East Australian Current, 1965–1968. *Deep-Sea Res.* 17, 777–794.
- Bowen, A., 1969. Rip currents: 1. Theoretical investigations. *J. Geophys. Res.* 74, 5479–5490.
- Bowman, D., Arad, D., Rosen, D., Kit, E., Goldbery, R., Slavicz, A., 1988a. Flow characteristics along the rip current system under low energy conditions. *Mar. Geol.* 82, 149–167.
- Bowman, D., Rosen, D., Kit, E., Arad, D., Slavicz, A., 1988b. Flow characteristics at the rip current neck under low energy conditions. *Mar. Geol.* 79, 41–54.
- Brander, R., 1999. Field observations on the morphodynamic evolution of a low-energy rip current system. *Mar. Geol.* 157, 199–217.
- Brander, R.W., Short, A.D., 2001. Flow kinematics of low-energy rip current systems. *J. Coast. Res.* 17 (2), 468–481.
- Brown, O.B., Bruce, J.G., Evans, R.H., 1980. Evolution of sea surface temperature in the Somali Basin during the southwest monsoon of 1979. *Science* 209, 595–597.
- Brugge, B., 1995. Near-surface mean circulation and kinetic energy in the central North Atlantic from drifter data. *J. Geophys. Res.* 100, 20543–20554.
- Bryden, H.L., Brady, E.C., 1985. Diagnostic model of the three-dimensional circulation in the upper equatorial Pacific Ocean. *J. Phys. Oceanogr.* 15, 1255–1273.
- Bryden, H.L., Beal, L.M., Duncan, L.M., 2005. Structure and transport of the Agulhas Current and its temporal variability. *Japan. J. Oceanogr.* 61, 479–492.
- Burkov, V.A., Bulatov, R.P., Neyman, V.G., 1981. Large scale features of water circulation in the world ocean. *Mar. Phys.*, 325–332.
- Cane, M.A., 1980. On the dynamics of equatorial currents, with application to the Indian Ocean. *Deep-Sea Res.* 27A, 525–544.
- Cane, M.A., 1983. Oceanographic events during El Niño. *Science* 222, 1189.
- Chao, S., McCreary, J.P., 1982. A numerical study of the Kuroshio south of Japan. *J. Phys. Oceanogr.* 12, 679–693.
- Charney, J.G., 1960. Non-linear theory of a wind-driven homogeneous layer near the equator. *Deep Sea Res.* 6, 303.
- Chen, Q., Dalrymple, R., Kirby, J., Kennedy, A., Haller, M., 1999. Boussinesq modelling of a rip current system. *J. Geophys. Res.* 104, 20,617–20,637.
- Church, J.A., J-Bethoux, P., Theocharis, A., 1998. Semienclosed seas, islands and Australia (S). In: Robinson, A.R., Brink, K.H. (Eds.). *The Sea*, vol. 11. Wiley, New York, NY, USA, pp. 79–124.
- Cochrane, J.D., 1963. Equatorial Undercurrent and related currents off Brazil in March and April 1963. *Science*. 142 (3593), 669–671.
- Cochrane, J.D., 1965. Equatorial currents of the western Atlantic. ONR Progress Report, Dept. of Oceanography and Meteorology, Texas A&M University, College Station, TX, USA. June 1965.
- Comiso, J., 2006. Arctic warming signals from satellite observations. *Weather* 61 (3), 70–76.
- Cooke, D.O., 1970. The occurrence and geologic work of rip currents off southern California. *Mar. Geol.* 9, 173–186.
- Cowen, R.K., Sponaugle, S., Paris, C.B., Lwiza, K., Fortuna, J., Dorsey, S., 2003. Impact of North Brazil Current rings on local circulation and coral reef fish recruitment to Barbados, West Indies, Interhemispheric Water Exchange in the Atlantic Ocean. In: Goni, G.J., Malanotte-Rizzoli, P. (Eds.). Elsevier Oceanographic Series, vol. 68. Elsevier, pp. 443–455.
- Cox, M.D., 1989. An idealized model of the world ocean. Part I: the global scale water masses. *J. Phys. Oceanogr.* 19, 1730–1752.
- Craik, A.D.D., Leibovich, S., 1976. A rational model for Langmuir circulation. *J. Fluid Mech.* 73, 401–426.
- Cram, R., Hanson, K., 1974. The detection by ERTS-1 of wind-induced ocean surface features in the lee of the Antilles islands. *J. Phys. Oceanogr.* 4, 594–600.
- Cromwell, T., Montgomery, R.B., Stroup, E.D., 1954. Equatorial undercurrent in the Pacific Ocean revealed by new methods. *Science*. 119, 648–649.
- Csanady, G.T., 1985. A zero potential vorticity model of the North Brazilian Coastal Current. *J. Mar. Res.* 43, 553–579.
- Dantzler, H.L., 1976. Geographic variations in intensity of the North Atlantic and North Pacific oceanic eddy fields. *Deep-Sea Res.* 23, 783–794.
- Darbyshire, J., 1964. A hydrological investigation of the Agulhas current area. *Deep-Sea Res.* 11, 781–815.
- Das, P.K., 1988. Why monsoons fail. *Science Reporter*. Council of Scientific and Industrial Research, New Delhi, India.
- Davis, R.E., 2005. Intermediate-depth circulation of the Indian and South Pacific Oceans measured by autonomous floats. *J. Physical Oceanogr.* 35, 683–707.
- de Ruijter, W.P.M., Ridderinkhof, H., Lutjeharms, J.R.E., Schouten, M.W., Veth, C., 2002. Observations of the flow in the Mozambique Channel. *Geophys. Res. Lett.* 29 (10), 1502–1504.
- de Ruijter, W.P.M., van Leeuwen, P.J., Lutjeharms, J.R.E., 1999. Generation and evolution of Natal pulses: Solitary meanders in the Agulhas Current. *J. Phys. Oceanogr.* 29 (12), 3043–3055.
- Dijkstra, H.A., de Ruijter, W.P.M., 2001. On the physics of the Agulhas Current: Steady retroflection regimes. *J. Phys. Oceanogr.* 31, 2971–2985.
- Duing, W., Mooers, C.N.K., Lee, T.N., 1977. Low frequency variability in the Florida Current and relations to atmospheric forcing from 1972 to 1974. *J. Mar. Res.* 35, 129–161.
- Duing, W., Molinari, R.L., Swallow, J.C., 1980. Somali Current: Evolution of surface current. *Science* 209, 588–590.
- Ekman, V.W., 1905. On the influence of the earth's rotation on ocean currents. *Ark. Mat. Astron. Fys.* 2, 1–53.
- Engle, J., MacMahan, J., Thieke, R.J., Hanes, D.M., Dean, R.G., 2002. Formulation of a rip current predictive index using rescue data. Florida Shore and Beach Preservation Association National Conference.
- Ewing, J., Edgar, T., 1966. Abyssal sediment (thickness). *Encyclopedia of Oceanography* 1, 6–10.
- Faller, A.J., 1969. The generation of Langmuir circulations by the eddy pressure of surface waves. *Limnol. Oceanogr.* 14, 504–513.

- Fedorov, K.N., 1965. Equatorial seiches. *Oceanology* 5 (1), 37. (English translation).
- Fernandez, E., Pingree, R.D., 1996. Coupling between physical and biological fields in the North Atlantic subtropical front southeast of the Azores. *Deep-Sea Res.* 43, 1369–1393.
- Firing, E., Lukas, R., Sadler, J., Wyrtki, K., 1983. Equatorial undercurrent disappears during 1982–1983 El Niño. *Science* 222, 1121.
- Fowler, R.E., Dalrymple, R.A., 1990. Wave group forced nearshore circulation, Proceedings of the 22nd International Conference on Coastal Engineering. Am. Soc. of Civ. Eng. Delft, the Netherlands, 729–742.
- Fratantoni, D.M., Glickson, D.A., 2002. North Brazil Current Ring generation and evolution observed with SeaWiFS. *J. Phys. Oceanogr.* 32, 1058–1074.
- Fratantoni, D.M., Richardson, P.L., 2006. The evolution and demise of north Brazil current rings. *J. Phys. Oceanogr.* 36, 1241–1264.
- Fuglister, F.C., 1955. Alternative analyses of current surveys. *Deep-Sea Res.* 2 (3), 213–229.
- Fuglister, F.C., 1960. Gulf Stream '60. Woods Hole Oceanographic Institution Report, 265–372.
- Fuglister, F.C., Worthington, L.V., 1951. Some results of a multiple ship survey of the Gulf Stream. *Tellus* 3, 1–14.
- Fyfe, J.C., Saenko, O.A., 2005. Human-induced change in the Antarctic Circumpolar Current. *J. Climate* 18, 3068–3073.
- Fyfe, J.C., 2003. Extratropical Southern Hemisphere cyclones: Harbingers of climate change. *J. Climate* 16, 2802–2805.
- Gammon, R.H., Sundquist, E.T., Fraser, P.J., 1986. History of carbon dioxide in the atmosphere, In: Report to the U.S. Congress on the CO₂ Question. U.S. Dept. of Energy, Washington, D.C., USA, 62 pp.
- Gangopadhyay, A., Robinson, A.R., Arango, H.G., 1997. Circulation and dynamics of the western north Atlantic. I. Multiscale feature models. *J. Atmos. Oceanic Technol.* 14 (6), 1314–1332.
- Gangopadhyay, A., Robinson, A.R., 2002. Feature oriented regional modeling of oceanic fronts. *Dynamics of Atmospheres and Oceans* 36, 201–232.
- Garcia-Berdeal, I., Hautala, S.L., Thomas, L.N., Johnson, H.P., 2006. Vertical structure of time-dependent currents in a mid-ocean ridge axial valley. *Deep-Sea Res. I* 53, 367–386.
- Garrett, C.J.R., 1976. Generation of Langmuir circulations by surface waves—A feedback mechanism. *J. Mar. Res.* 34, 117–130.
- Garzoli, S.L., Ffield, A., Yao, Q., 2003. North Brazil Current Rings and the variability in the latitude of retroflection, Interhemispheric Water Exchange in the Atlantic Ocean. In: Goni, G.J., Malanotte-Rizzoli, P. (Eds.). Elsevier Oceanographic Series, vol. 68, pp. 357–373. Elsevier.
- Gerdes, R., Koeberle, C., Beckmann, A., Herrmann, P., Willebrand, J., 1999. Mechanisms for spreading of Mediterranean Water in coarse-resolution numerical models. *J. Physic. Oceanogr.* 29, 1682–1700.
- Giarrolla, E., Nobre, P., Malagutti, M., Pezzi, L.P., 2005. The Atlantic Equatorial Undercurrent: PIRATA observations and simulations with GFDL modular ocean model at CPTEC. *Geophys. Res. Lett.* 32, L10617. <http://dx.doi.org/10.1029/2004GL022206>.
- Gille, S.T., 2002. Warming of the Southern Ocean since the 1950s. *Science* 295, 1275–1277.
- Godfrey, J.S., Creswell, G.R., Golding, T.J., Pearce, A.F., Boyd, R., 1980. The separation of the East Australian Current. *J. Phys. Oceanogr.* 10, 430–440.
- Goldenberg, S.B., Landsea, C.W., Mestas-Nunez, A.M., Gray, W.M., 2001. The recent increase in Atlantic hurricane activity: Causes and implications. *Science* 293, 474–479.
- Goni, G.J., Johns, W.E., 2003. Synoptic study of warm rings in the North Brazil Current retroflection region using satellite altimetry, Interhemispheric Water Exchange in the Atlantic Ocean. In: J.Goni, G., Malanotte-Rizzoli, P. (Eds.). Elsevier Oceanographic Series, vol. 68. Elsevier, pp. 335–356.
- Gordon, A.L., 1970. Vertical momentum flux accomplished by Langmuir circulation. *J. Geophys. Res.* 75, 4177–4179.
- Gordon, A.L., 1985. Indian-Atlantic transfer of thermocline water at the Agulhas Retroflection. *Science* 227, 1030–1033.
- Gordon, A.L., Lutjeharms, J.R.E., Gründlingh, M.L., 1987. Stratification and circulation at the Agulhas retroflection. *Deep-Sea Res.* 34, 565–599.
- Gouretski, V., Danilov, A., Ivchenko, V.O., Klepikov, A., 1987. Modelling of the Southern Ocean Circulation. *Hydrometeorologisher Publ.*, Leningrad, U.S.S.R.
- Grant, H.L., Stewart, R.W., Moillet, A., 1962. Turbulence spectra from a tidal channel. *J. Fluid Mech.* 12, 241–268.
- Haas, K.A., Svendsen, I.A., 2002. Laboratory measurements of the vertical structure of rip currents. *J. Geophys. Res.*, 107.
- Hall, A., Visbeck, M., 2002. Synchronous variability in the Southern Hemisphere atmosphere, sea ice, and ocean resulting from the annular mode. *J. Climate* 15, 3043–3057.
- Haller, M.C., Dalrymple, R.A., 2001. Rip current instabilities. *J. Fluid Mech.* 433, 161–192.
- Halpern, D., 1983. Variability of the Cromwell Current before and during the 1982–83 warm event. In: *Trop. Ocean Atmos. Newslett.*, 21. Univ. of Washington, Seattle, WA, USA.
- Hamon, B.V., 1965. The East Australian Current, 1960–1964. *Deep-Sea Res.* 12, 899–921.
- Hamon, B.V., Cresswell, G.R., 1972. Structure functions and intensities of ocean circulation off east and west Australia. *Aust. J. Mar. Freshwater Res.* 23, 99–103.
- Hata, K., 1974. Behavior of a warm eddy detached from the Kuroshio. *J. Meteor. Res.* 7, 295–321.
- Heezen, B.C., Hollister, C.D., Ruddiman, W.F., 1966. Shaping of the continental rise by deep geostrophic contour currents. *Science* 152, 502–503.
- Hill, A.E., Hickey, B.M., Shillington, F.A., Strub, P.T., Brink, K.H., Barton, E.D., Thomas, A.C., 1998. Eastern ocean boundaries (E). In: Robinson, A.R., Brink, K.H. (Eds.). *The Sea*, vol. 11. Wiley, New York, NY, USA, pp. 29–68.
- Holmes, J., 2009. Proc. Second Session of the Global Platform for Disaster Risk Reduction. Switzerland, Geneva, 16–19 June 2009, pp. 3–5.
- Houwman, K.T., Hoekstra, P., 1998. Tidal ellipses in the near-shore zone (−3 to −10 m): Modeling and observations. *Coastal Eng.*, 773–786.
- Hunkins, K., 1966. Ekman drift currents in the Arctic Ocean. *Deep-Sea Res.* 13, 607–620.
- Huntley, D.A., Hendry, M.D., Haines, J., Greenidge, B., 1988. Waves and rip currents on a Caribbean pocket beach, Jamaica. *J. Coast. Res.* 4, 69–79.
- Hynd, J.S., 1969. Isotherm maps for tuna fisherman. *Aust. Fish* 28 (7), 13–22.
- Ikeda, M., Johannessen, J.A., Lygre, K., Sandven, S., 1989. A process study of mesoscale meanders and eddies in the Norwegian coastal current. *J. Phys. Oceanogr.* 19, 20–35.
- Iskandar, I., Masumoto, Y., Mizuno, K., 2009. Subsurface equatorial zonal current in the eastern Indian Ocean. *J. Geophys. Res.* 114, C06005.
- Ivchenko, V.O., Richards, K.J., Stevens, D.P., 1996. The dynamics of the Antarctic Circumpolar Current. *J. Phys. Oceanogr.* 26, 753–774.
- Izumo, T., 2005. The equatorial undercurrent, meridional overturning circulation, and their role in mass and heat exchanges during El Niño events in the tropical Pacific ocean. *Ocean Dynamics* 55, 110–123.

- Izumo, T., Picaut, V., Blanke, B., 2002. Tropical pathways, equatorial undercurrent variability and the 1998 La Niña. *Geophys. Res. Lett.* 29 (22), 2080–2083.
- Jacobs, S.S., Georgi, D.T., 1977. Observations on the southwest Indian/Antarctic Ocean. *Deep-Sea Res.* 24, 43–84.
- Jarraud, M., 2009. Reducing risk in a changing climate, United Nations International Strategy for Disaster Reduction, Proc. Global Platform for Disaster Risk Reduction, 20–21.
- Jia, Y., 2000. Formation of an Azores Current due to Mediterranean overflow in a modeling study of the North Atlantic. *J. Physical Oceanogr.* 30, 2342–2358.
- Johns, W.E., Lee, T.N., Schott, F.A., Zantopp, R.J., Evans, R.H., 1990. The North Brazil Current retroflection: Seasonal structure and eddy variability. *J. Geophys. Res.* 95 (C12), 22103–22120.
- Johns, W.E., Lee, T.N., Beardsley, R.C., Candela, J., Limeburner, R., Castro, B., 1998. Annual cycle and variability of the North Brazil Current. *J. Phys. Oceanogr.* 28, 103–128.
- Johnson, D., Pattiarchi, C., 2004. Transient rip currents and nearshore circulation on a swell-dominated beach. *J. Geophys. Res.* 109, (C02026).
- Johnson, D., Pattiarchi, C., 2004. Transient rip currents and nearshore circulation on a swell-dominated beach. *J. Geophys. Res.* 109, (C02026).
- Johnson, G.C., McPhaden, M.J., Rowe, G.D., McTaggart, K.E., 2000. Upper equatorial ocean current and salinity during the 1996–1998 El Niño–La Niña cycle. *J. Geophys. Res.* 105, 1037–1053.
- Jury, M.R., Valentine, H.R., Lutjeharms, J.R.E., 1993. Influence of the Agulhas Current on summer rainfall along the southeast coast of South Africa. *J. Appl. Meteor.* 32, 1282–1287.
- Kamenkovich, V.M., Koshyakov, M.N., Monin, A.S., 1986. Synoptic eddies in the ocean, D. Reidel, the Netherlands.
- Karsten, R., Marshall, J., 2002. Constructing the residual circulation of the ACC from the observations. *J. Phys. Oceanogr.* 32, 3315–3327.
- Kase, R.H., Siedler, G., 1982. Meandering of the subtropical front southeast of the Azores. *Nature* 300, 245–246.
- Katz, B., Gerard, R., Costin, M., 1965. Response of dye tracers to sea surface conditions. *J. Geophys. Res.* 70, 5505–5513.
- Kawai, H., 1972. Hydrography of the Kuroshio Extension. In: Stommel, H., Yoshida, K. (Eds.), *Kuroshio, Its Physical Aspect*. University of Tokyo Press, Tokyo, Japan, pp. 235–352.
- Kawai, H., 1979. Rings south of the Kuroshio and their possible roles in transport of the intermediate salinity minimum and in formation of the skipjack and albacore fishing ground, *Kuroshio IV*. Proc. Fourth CSK Symp. Tokyo, 250–273.
- Kelly, K.A., Small, R.J., Samelson, R.M., Qiu, B., Joyce, T.M., Kwon, Y.-O., Cronin, M.F., 2010. Western boundary currents and frontal air–sea interaction: Gulf Stream and Kuroshio Extension. *J. Climate* 23, 5644–5667.
- Kennedy, A.B., Thomas, D., 2004. Drifter measurements in a laboratory rip current. *J. Geophys. Res.* 109, C08005.
- Kim, S.L., Mullineaux, L.S., 1998. Distribution and near-bottom transport of larvae and other plankton at hydrothermal vents. *Deep-Sea Res. II* 45, 423–440.
- Kitano, K., 1975. Some properties of the warm eddies generated in the confluence zone of the Kuroshio and Oyashio Current. *J. Phys. Oceanogr.* 5, 670–683.
- Klein, B., Siedler, G., 1989. On the origin of the Azores Current. *J. Geophys. Res.* 94, 6159–6168.
- Knauss, J.A., King, J.E., 1958. Observations of Pacific Equatorial Undercurrent. *Nature* 182, 601–602.
- Knauss, J.A., 1966. Further measurements and observations on the Cromwell Current. *J. Mar. Res.* 24 (2), 205–240.
- Knauss, J.A., Taft, B.A., 1964. Equatorial Undercurrent of the Indian Ocean. *Science* 143 (3004), 354–356.
- Knox, R.A., Anderson, D.L.T., 1985. Recent advances in the study of the low-latitude ocean circulation. *Prog. Oceanogr.* 14, 259–317.
- Komar, P.D., 1971. Nearshore cell circulation and the formation of giant cusps. *Geol. Soc. Amer. Bull.* 82, 2643–2650.
- Koshimura, S., Yanagisawa, H., Miyagi, T., 2009. Mangrove's fragility against tsunami, inferred from high-resolution satellite imagery and numerical modeling. Abstract; 24th International Tsunami Symposium (ITS-2009) and Technical Workshop on Tsunami Measurements and Real-Time Detection, held at Novosibirsk, Russia (14–16 July 2009).
- Krauss, W., Kase, R.H., 1994. Mean circulation and eddy kinetic energy in the eastern North Atlantic. *J. Geophys. Res.* 89, 3407–3415.
- Kullenberg, B., 1954. Vagn Walfrid Ekman 1874–1954: A biography by B. Kullenberg. *Journal du Conseil international pour l'exploration de la mer* 20 (2), 1–52.
- Kwon, Y.-O., Alexander, M.A., Bond, N.A., Frankignoul, C., Nakamura, H., Qiu, B., Thompson, L., 2010. Role of the Gulf Stream and Kuroshio–Oyashio systems in large-scale atmosphere–ocean interaction: A review. *J. Climate* 23, 3249–3281.
- La Fond, E.C., 1980. Upwelling. McGraw-Hill Encyclopedia of Ocean and Atmospheric Sciences, 523–525.
- Lai, D.Y., Richardson, P.L., 1977. Distribution and movement of Gulf Stream Rings. *J. Phys. Oceanogr.* 7, 670–683.
- Langmuir, I., 1938. Surface motion of water induced by wind. *Science* 87, 119–123.
- Lascody, R.L., 1998. East central Florida rip current program. National Weather Service In-house Report, 10.
- Le Traon, P.Y., Rouquet, M.C., Boissier, C., 1990. Spatial scales of mesoscale variability in the North Atlantic as deduced from Geosat data. *J. Geophys. Res.* 95, 20267–20285.
- Lee, T.N., Atkinson, L.P., Legeckis, R., 1981. Observations of a Gulf Stream frontal eddy on the Georgia continental shelf, April 1977. *Deep-Sea Research* 28A (4), 347–378.
- Lee, T.N., 1975. Florida current spin-off eddies. *Deep-Sea Res.* 22, 753–765.
- Lee, T.N., Brooks, D.A., 1979. Initial observations of current, temperature and coastal sea level response to atmospheric and Gulf Stream forcing on the Georgia shelf. *Geophys. Res. Letts.* 6, 321–324.
- Lee, T.N., Mayer, D., 1977. Low-frequency current variability and spin-off eddies on the shelf off southeast Florida. *J. Mar. Res.* 35, 193–220.
- Lee, T.N., Atkinson, L.P., Legeckis, R., 1981. Observations of a Gulf Stream frontal eddy on the Georgia continental shelf, April 1977. *Deep-Sea Res.* 28A (4), 347–378.
- Leetmaa, A., Quadfasel, D.R., Wilson, D., 1982. Development of flow field during the onset of the Somali Current, 1979. *J. Phys. Oceanogr.* 12, 1325–1342.
- Legeckis, R., 1979. Satellite observations of the influence of bottom topography on the seaward deflection of the Gulf Stream off Charleston, South Carolina. *J. Phys. Oceanogr.* 9, 483–497.
- Legeckis, R., Gordon, A.L., 1982. Satellite observations of the Brazil and Falkland Current. *Deep-Sea Res.* 29, 375–401.
- Leibovich, S., 1983. The form and dynamics of Langmuir circulations. *Annu. Rev. Fluid Mech.* 15, 391–427.
- Leibovich, S., Paolucci, S., 1981. The instability of the ocean to Langmuir circulations. *J. Fluid Mech.* 102, 141–167.

- Leibovich, S., Lele, S.K., Moroz, I.M., 1989. Nonlinear dynamics in Langmuir circulations and in thermosolutal convection. *J. Fluid Mech.* 193, 471–511.
- Lilley, F.E.M., Filloux, J.H., Bindoff, N.L., Ferguson, I.J., 1986. Barotropic flow of a warm-core ring from seafloor electric measurements. *J. Geophys. Res.* 91, 12979–12984.
- Liu, Z., Philander, S.H.G., Pacanowski, R.C., 1994. A GCM study of tropical–subtropical upper-ocean water exchange. *J. Phys. Oceanogr.* 24, 2606–2623.
- Lobel, P.S., 1978. Diel, lunar and seasonal periodicity in the reproductive behavior of the pomacanthid fish, *Centropyge potteri* and some other reef fishes in Hawaii. *Pac. Sci.* 32, 193–207.
- Lobel, P.S., 1989. Ocean current variability and the spawning season of Hawaiian reef fishes. *Environ. Biol. Fish.* 2 (3), 161–171.
- Lobel, P.S., 2011. Transport of reef lizardfish larvae by an ocean eddy in Hawaiian waters. *Dynamics of Atmospheres and Oceans* 52, 119–130.
- Lobel, P.S., Robinson, A.R., 1983. Reef fishes at sea: ocean currents and the advection of larvae. In: Reaka, M.L. (Ed.), *The Ecology of Deep and Shallow Reefs. Symposia Series for Undersea Research*, vol. 1. Office of Undersea Research, NOAA, Rockville, MD, USA, pp. 29–38.
- Lobel, P.S., Robinson, A.R., 1986. Transport and entrapment of fish larvae by ocean mesoscale eddies and currents in Hawaiian waters. *Deep-Sea Res.* 33, 483–500.
- Lobel, P.S., Robinson, A.R., 1988. Larval fishes and zooplankton in a cyclonic eddy in Hawaiian waters. *J. Plank. Res.* 10 (6), 1209–1223.
- Loder, J.W., Petrie, B., Gawarkiewicz, G., 1998. The coastal ocean off northeastern North America: a large-scale view (I, W). In: Robinson, A.R., Brink, K.H. (Eds.), *The Sea*, Vol. 11. Wiley, New York, NY, USA, pp. 125–134.
- Longuet-Higgins, M.S., 1970. Longshore currents generated by obliquely incident seawaves, 1. *J. Geophys. Res.* 75, 6790–6801.
- Longuet-Higgins, M.S., Stewart, R.W., 1964. Radiation stress in water waves, a physical discussion with applications. *Deep-Sea Res.* 11 (4), 529–563.
- Lozier, M.S., Owens, W.B., Curry, R.G., 1995. The climatology of the North Atlantic. In: *Progress in Oceanography*, 36. Pergamon, 1, 44.
- Luschine, J.B., 1991. A study of rip current drownings and weather related factors. *Natl. Weather Dig.*, 13–19.
- Luschine, J.B., 1991a. A study of rip current drownings and weather related factors. *Natl. Weather Dig.*, 13–19.
- Luther, M.E., O'Brien, J.J., 1985. A model of the seasonal circulation in the Arabian Sea forced by observed winds. *Prog. Oceanogr.* 14, 353–385.
- Lutjeharms, J.R.E., Gordon, A.L., 1987. Shedding of an Agulhas Ring observed at sea. *Nature* 325, 138–140.
- Lutjeharms, J.R.E., 1981a. Features of the southern Agulhas Current circulation from satellite remote sensing. *S. Afr. J. Sci.* 77, 231–236.
- Lutjeharms, J.R.E., 1981b. Spatial scales and intensities of circulation in the ocean areas adjacent to South Africa. *Deep-Sea Res.* 28, 1289–1302.
- Lutjeharms, J.R.E., 1988. Meridional heat transport across the subtropical convergence by a warm eddy. *Nature* 331, 251–253.
- Lutjeharms, J.R.E., 2007. Three decades of research on the greater Agulhas Current. *Ocean Science* 3, 129–147.
- Lutjeharms, J.R.E., Roberts, H.R., 1988. The Natal pulse: An extreme transient on the Agulhas Current. *J. Geophys. Res.* 93, 631–645.
- Lutjeharms, J.R.E., van Ballegooyen, R.C., 1988. The Agulhas Current retroflection. *J. Phys. Oceanogr.* 18, 1570–1583.
- Lutjeharms, J.R.E., Van Ballegooyen, R.C., 1988a. The retroflection of the Agulhas Current. *J. Phys. Oceanogr.* 18, 1570–1583.
- Luyten, J.R., Swallow, J.C., 1976. Equatorial undercurrents. *Deep-Sea Res.* 23, 999–1001.
- Luyten, J., Pedlosky, J., Stommel, H., 1983. The ventilated thermocline. *J. Phys. Oceanogr.* 13, 292–309.
- MacMahan, J.H., Thornton, E.B., Reniers, A.J.H.M., 2006. Rip current review. *Coastal Engineering* 53, 191–208.
- MacMahan, J., Thornton, E.B., Stanton, T.P., Reniers, A.J.H.M., 2005. RIPEX: Rip currents on a shore-connected shoal beach. *Mar. Geol.* 218, 113–134.
- Marinone, S.G., Lavin, M.F., 2005. Tidal current ellipses in a three-dimensional baroclinic numerical model of the Gulf of California. *Estuarine Coastal Shelf Sci.* 64, 519–530.
- Marshall, D., 1995. Topographic steering of the Antarctic Circumpolar Current. *J. Phys. Oceanogr.* 25, 1636–1650.
- Marshall, G.J., 2003. Trends in the southern annular mode from observations and reanalyses. *J. Climate* 16, 4134–4143.
- Marshall, J., Radko, T., 2003. Residual-mean solutions for the Antarctic Circumpolar Current and its associated overturning circulation. *J. Phys. Oceanogr.* 33, 2341–2354.
- Mascarenhas, A.S., Miranda, L.B., Rock, N., 1971. A study of oceanographic conditions in the region of Cabo Frio. In: Costlow, Jr., D. (Ed.), *Fertility of the Sea*, Vol. 1. Gordon and Breach, New York, NY, USA, pp. 285–308.
- Mason, S.J., 1995. Sea-surface temperature: South African rainfall associations, 1910–1989. *Int. J. Climatol* 15, 119–135.
- Matano, R.P., Palma, E.D., Piola, A.R., 2010. The influence of the Brazil and Malvinas Currents on the Southwestern Atlantic Shelf circulation. *Ocean Sci.* 6, 983–995.
- Maury, M.F., 1855. *The physical geography of the sea*. Harper & Brothers, New York, NY, USA.
- McCreary, J.P., Kundu, P.K., 1985. Western boundary circulation driven by an alongshore wind: With application to the Somali Current system. *J. Mar. Res.* 43 (3), 493–516.
- McCreary, J.P., Lu, P., 1994. Interaction between the subtropical and equatorial ocean circulations: The subtropical cell. *J. Phys. Oceanogr.* 24, 455–497.
- McKenzie, P., 1958. Rip-current systems. *J. Geol.* 66, 103–113.
- McKenzie, P., 1958a. Rip-current systems. *J. Geol.* 66, 103–113.
- McPhaden, M.J., 1986. The Equatorial Undercurrent: 100 years of discovery. *Eos* 67 (40), 762–765.
- Meehls, G.A., Stocker, T.F., Idlingstein, W.D., Gaye, A.T., Gregory, J.M., Kitoh, A., Knutti, R., Murphy, J.M., Noda, A., Raper, S.C.B., Watterson, I.G., Weaver, A.J., Zhao, Z.-C., 2007. *Climate change: The physical science basis*. Cambridge University Press, New York, NY, USA. Chap. Global Climate Projections.
- Metcalf, W.G., Voorhis, A.D., Stalcup, M.C., 1962. The Atlantic Equatorial Undercurrent. *J. Geophys. Res.* 67, 2499.
- Metcalf, W.G., Stalcup, M.C., 1967. Origin of the Atlantic Equatorial Undercurrent. *J. Geophys. Res.* 72 (20), 4959–4975.
- Mizuno, K., White, W.B., 1983. Annual and inter-annual variability in the Kuroshio Current System. *J. Phys. Oceanogr.* 13, 1847–1867.
- Montgomery, R.B., Stroup, E.D., 1962. Equatorial waters and currents at 150°W in July–August 1952. Johns Hopkins Oceanogr. Studies (No. 1), 68.
- Muller-Karger, F.E., McClain, C.R., Richardson, P.L., 1988. The dispersal of the Amazon's water. *Nature* 333, 56–59.
- Mullineaux, L.S., France, S.C., 1995. Dispersal mechanisms of deep-sea hydrothermal vent fauna. In: Humphris, S.E., Zierenberg, R.A., Mullineaux, L.S., Thomson, R.E. (Eds.), *Seafloor Hydrothermal*

- Systems: Physical, Chemical, Biological, and Geological Interactions. American Geophysical Union, Washington, DC, USA, pp. 408–424.
- Munk, J.W., 1983. Acoustic and ocean dynamics. In: Brewer, P.G. (Ed.), *Oceanography: The present and future*. Springer-Verlag, New York, Heidelberg, Berlin, pp. 109–126.
- Munk, J.W., Wunsch, C., 1979. Ocean acoustic tomography: A scheme for large scale monitoring. *Deep-Sea Res.* 26A, 123–161.
- Munk, W., 1950. On the wind-driven ocean circulation. *J. Meteorol.* 7, 79–93.
- Munk, W.H., Palmen, E., 1951. Note on the dynamics of the Antarctic Circumpolar Current. *Tellus* 3, 53–55.
- Murray, S.P., 1975. Trajectories and speeds of wind-driven currents near the coast. *J. Phys. Oceanogr.* 5, 347–360.
- Nakamura, M., 2012. Impacts of SST anomalies in the Agulhas Current System on the regional climate variability. *J. Climate* 25, 1213–1229.
- Neumann, G., 1960. Evidence for an equatorial undercurrent in the Atlantic Ocean. *Deep-Sea Res.* 6, 328–334.
- Neumann, G., 1966. The Equatorial Undercurrent in the Atlantic Ocean. Proc. Symposium on Oceanography and Fisheries Resources of the Tropical Atlantic, 1–17.
- Neumann, G., 1968. Ocean Currents. Elsevier, Amsterdam-London-New York.
- Nilsson, C.S., Cresswell, G.R., 1981. The formation and evolution of East Australian Current warm-core eddies. *Progress in Oceanography* vol. 9, 133–183. Pergamon.
- Nowlin Jr., W.D., Klinck, J.M., 1986. The physics of the Antarctic Circumpolar Current. *Rev. Geophys.* 24, 469–491.
- Oke, P.R., England, M.H., 2004. Oceanic response to changes in the latitude of the Southern Hemisphere subpolar westerly winds. *J. Climate* 17, 1040–1054.
- Olbers, D.J., Wenzel, M., Willebrand, J., 1985. The inference of North Atlantic circulation patterns from climatological hydrographic data. *Rev. Geophys.* 23, 313–356.
- Olbers, D., Wubben, C., 1991. The role of wind and buoyancy forcing of the Antarctic Circumpolar Current, Strategies for Future Climate Research. In: Latif, M. (Ed.), Max-Planck Institute for Meteorology, pp. 161–192.
- Olson, D.B., Evans, R.H., 1986. Rings of the Agulhas. *Deep-Sea Res.* 33, 27–42.
- Ou, H.W., DeRijter, W.P., 1986. Separation of an inertial boundary current from a curved coastline. *J. Phys. Oceanogr.* 16, 280–289.
- Peregrine, D., 1998. Surf zone currents. *Theor. Comput. Fluid Dyn.* 10, 295–309.
- Peregrine, D., 1998a. Surf zone currents. *Theor. Comput. Fluid Dyn.* 10, 295–309.
- Philander, S.G.H., 1973. Equatorial Undercurrent: Measurement and theories. *Rev. Geophys. Space Phys.* 11 (3), 513–570.
- Philander, S.G.H., Pacanowski, R.C., 1986. A model of the season cycle in the tropical Atlantic Ocean. *J. Geophys. Res.* 91, 14192–14206.
- Picaut, J., Tournier, R., 1991. Monitoring the 1979–1985 equatorial Pacific current transports with bathythermograph data. *J. Geophys. Res.* 96, 3263–3277.
- Pingree, R.D., 1997. The eastern subtropical gyre (North Atlantic): Flow rings, recirculations structure and subduction. *J. Mar. Biol. Assoc. United Kingdom* 77, 573–624.
- Quadfasel, D.R., Schott, F., 1983. Southward subsurface flow below the Somali Current. *J. Geophys. Res.* 88, 5973–5979.
- Rahmstorf, S., 1998. Influence of Mediterranean outflow on climate. *Nature* 397 (24), 281–282.
- Rahmstorf, S., 2006. Thermohaline ocean circulation. In: Elias, S.A. (Ed.), *Encyclopedia of Quaternary Sciences*. Elsevier, Amsterdam, the Netherlands.
- Rameshkumar, M.R., Sadhuram, Y., Rao, L.V.G., 1986. Pre-monsoon sea surface temperature anomalies in western Indian Ocean. Proc. Symposium on Long range forecasting of monsoon rainfall, held at New Delhi, India (16–18 April 1986).
- Rasmussen, E.M., Wallace, J.M., 1983. Meteorological aspects of the El Niño/Southern Oscillation. *Science* 222, 1195.
- Reason, C.J.C., 2001. Evidence for the influence of the Agulhas Current on regional atmospheric circulation patterns. *J. Climate* 14, 2769–2778.
- Reid, J.L., 1979. On the contribution of the Mediterranean Sea outflow to the Norwegian-Greenland Sea. *Deep-Sea Res.* 26, 1199–1223.
- Rhines, P.B., Young, W.R., 1982. A theory of the wind-driven circulation I: Mid-ocean gyres. *J. Mar. Res.* 40 (Suppl.), 559–596.
- Richardson, P.L., 1981. Gulf Stream trajectories measured with free-drifting buoys. *J. Phys. Oceanogr.* 11, 999–1010.
- Richardson, P.L., 1983. Eddy kinetic energy in the North Atlantic from surface drifters. *J. Geophys. Res.* 88, 4355–4367.
- Richardson, P.L., 1980. Gulf Stream ring trajectories. *J. Phys. Oceanogr.* 10, 90–104.
- Richardson, P.L., Cheney, R.E., Worthington, L.V., 1978. A census of Gulf Stream rings. *J. Geophys. Res.* 83, 6136–6144.
- Ridgway, K.R., Godfrey, J.S., 1997. Seasonal cycle of the East Australian Current. *J. Geophys. Res.* 102, 22921–22936.
- Rintoul, S.C., Hughes, C., Olbers, D., 2001. The Antarctic Circumpolar Current system. *Ocean Circulation and Climate*. In: Siedler, J.C.G., Gould, J. (Eds.), Academic Press, pp. 271–302.
- Robinson, A.R., Brink, K.H. (Eds.), 1998. *The Sea*, vol. 11. Wiley, New York, NY, USA, p. 1062.
- Robinson, A.R., Lobel, P.S., 1985. The impact of ocean eddies on coastal currents. In: Magaard, L., et al. (Eds.), *The Hawaiian Ocean Experiment Proceedings*. Hawaii Inst. Geophysics Spec. Publ, pp. 325–334.
- Robinson, A.R., Lobel, P.S., 1985. The impact of ocean eddies on coastal currents. In: Magaard, L., et al. (Eds.), *The Hawaiian Ocean Experiment Proceedings*. Hawaii Inst. Geophysics Spec. Publ, pp. 325–334.
- Roden, G.I., Taft, B.A., Ebbesmeyer, C.C., 1982. Oceanographic aspects of the Emperor seamounts region. *J. Geophys. Res.* 87, 9537–9552.
- Rossby, H.T., 1983. Eddies and the general circulation. In: Brewer, P.G. (Ed.), *Oceanography — the present and future*. Springer-Verlag, New York, Heidelberg, Berlin, pp. 137–161.
- Rossby, H.T., 1983a. Eddies and the general circulation. In: Brewer, P.G. (Ed.), *Oceanography: The present and future*. Springer-Verlag, New York, Heidelberg, Berlin, pp. 137–161.
- Rossby, H.T., Voorhis, A.D., Webb, D., 1975. A Quasi-Lagrangian study of mid-ocean variability using long range SOFAR floats. *J. Mar. Res.* 33, 355–382.
- Rossby, T., Dorson, D., Fontaine, J., 1986. The RAFOS system. *J. Atmos. Oceanic Technol.* 3, 672–679.
- Rouse, H., 1963. On the role of eddies in fluid motion. *American Scientist* 51, 285–314.
- Sætre, R., da Silva, A.J., 1984. The circulation of the Mozambique Channel. *Deep-Sea Res.* 31, 485–508.

- Sallee, J.B., Speer, K., Morrow, R., 2008. Response of the Antarctic Circumpolar Current to atmospheric variability. *J. Climate* 21, 3020–3039.
- Sarukhanyan, E.I., 1982. The three-dimensional structure of the west wind drift in the region between Africa and Antarctica. *Dokl. Akad. nauk SSSR* 250, 234–237.
- Saylor, J.H., 1966. Currents at Little Lake Harbor. U.S. Lake Survey Res. Rept. No. 1–1. Lake Survey District, Corps of Eng, Detroit, MI, USA.
- Schmid, C.H., Schafer, H., Podesta, G., Zenk, W., 1995. The Vitória eddy and its relation to the Brazil Current. *J. Phys. Oceanogr.* 25 (11), 2532–2546.
- Schmitz Jr., W.J., 1995. On the interbasin scale thermohaline circulation. *Rev. Geophys.* 33, 151–173.
- Schott, F., 1983. Monsoon response of the Somali Current and associated upwelling. *Prog. Oceanogr.* 12, 357–381.
- Schott, F., Quadfasel, D.R., 1982. Variability of the Somali Current system during the onset of the southwest monsoon, 1979. *J. Phys. Oceanogr.* 12, 1343–1357.
- Schouten, M.W., de Ruijter, W.P.M., van Leeuwen, P.J., 2002. Upstream control of Agulhas Ring shedding. *J. Geophys. Res.* 107 (C8), 3109–3120.
- Schouten, M.W., de Ruijter, W.P.M., van Leeuwen, P.J., 2002a. Upstream control of the Agulhas ring shedding. *J. Geophys. Res.* 107, 3109.
- Schouten, M.W., de Ruijter, W.P.M., van Leeuwen, P.J., Rifferinkhof, H., 2003. Eddies and variability in the Mozambique Channel. *Deep-Sea Res.* 50, 1987–2003.
- Scott, J.T., Myer, G.E., Stewart, R., Walther, E.G., 1969. On the mechanism of Langmuir circulations and their role in epilimnion mixing. *Limnol. Oceanogr.* 14, 493–503.
- Send, U., Worcester, P.F., Cornuelle, B.D., Tiemann, C.O., Baschek, B., 2002. Integral measurements of mass transport and heat content in the Strait of Gibraltar from acoustic transmissions. *Deep-Sea Res. II* 49, 4069–4095.
- Serreze, M.C., Maslanik, J.A., Scambos, T.A., Fetterer, F., Stroeve, J., Knowles, K., Fowler, C., Drobot, S., Barry, R.G., Haran, T.M., 2003. A record minimum Arctic sea ice extent and area in 2002. *Geophys. Res. Lett.* 30 (3), 1110.
- Shepard, F.P., 1936. Undertow, riptide, or “rip current”. *Science*, 84.
- Shepard, F.P., Inman, D.I., 1950. Nearshore water circulation related to bottom topography and wave refraction. *Trans. Amer. Geophys. Union* 31, 196–212.
- Shepard, F.P., Inman, D.I., 1950. Nearshore water circulation related to bottom topography and wave refraction. *Trans. Amer. Geophys. Union* 31, 196–212.
- Shepard, F., Emery, K., LaFond, E., 1941. Rip currents: A process of geological importance. *J. Geol.* 49, 337–369.
- Shojo, D., 1972. Time variation of the Kuroshio south of Japan. In: Stommel, H., Yoshida, K. (Eds.), *Kuroshio, Its Physical Aspect*. University of Tokyo Press, Tokyo, Japan, pp. 217–234.
- Short, A.D., 1999. Handbook of Beach and Shoreface Morphodynamics. Wiley, p. 379.
- Short, A.D., Hogan, C.L., 1994. Rip currents and beach hazards, their impact on public safety and implications for coastal management. In: Finkl, C.W. (Ed.), *Coastal Hazards*. *J. Coastal Res.*, Special Issue, 12, pp. 197–209.
- Shukla, J., 1987a. Inter-annual variability of monsoons. In: Fein, J.S., Stephens, P.L. (Eds.), *Monsoons*. Wiley Interscience, New York, NY, USA.
- Shukla, J., 1987b. Long-range forecasting of monsoons. In: Fein, J.S., Stephens, P.L. (Eds.), *Monsoons*. Wiley Interscience, New York, NY, USA.
- Signorini, S.R., 1978. On the circulation and the volume transport of the Brazil Current between the Cape of São Tomé and Guanabara Bay. *Deep-Sea Res.* 25, 481–490.
- Silveira, I.C.A., Lima, J.A.M., Schmidt, A.C.K., Cecopieri, W., Sartori, A., Francisco, C.P.F., Fontes, R.F.C., 2008. Is the meander growth in the Brazil Current system off Southeast Brazil due to baroclinic instability? *Dyn. Atmos. Oceans* 45, 187–207.
- Silveira, I.C.A., Calado, L., Castro, B.M., Cirano, M., Lima, J.A.M., Mascarenhas, A.S., 2004. On the baroclinic structure of the Brazil Current-Intermediate Western Boundary Current system at 22°–23°S. *Geophys. Res. Lett.* 31.
- Sloyan, B.M., Johnson, G.C., Kessler, W.S., 2003. The Pacific cold tongue: an indicator of hemispheric exchange. *J. Phys. Oceanogr.* 33 (5), 1027–1043.
- Smith, J.A., 1992. Observed growth of Langmuir circulation. *J. Geophys. Res.* 97 (C4), 5651–5664.
- Smith, J., Largier, J., 1995. Observations of nearshore circulation: Rip currents. *J. Geophys. Res.* 100, 10,967–10,975.
- Sonu, C., 1972. Field observations of nearshore circulation and meandering currents. *J. Geophys. Res.* 77, 3232–3247.
- Stalcup, M.C., Metcalf, W.G., 1966. Direct measurements of the Atlantic Equatorial Undercurrent. *J. Mar. Res.* 24 (1), 44–55.
- Stammer, D., 1997. Global characteristics of ocean variability estimated from regional TOPEX/Poseidon altimeter measurements. *J. Phys. Oceanogr.* 27, 1743–1769.
- Stock, C.A., Alexander, M.A., Bond, N.A., Brander, K.M., Cheung, W.W.L., Curchitser, E.N., Delworth, T.L., Dunne, J.P., Griffies, S.M., Haltuch, M.A., Hare, J.A., Hollowed, A.B., Lehodey, P., Levin, S.A., Link, J.S., Rose, K.A., Rykaczewski, R.R., Sarmiento, J.L., Stouffer, R.J., Schwing, F.B., Vecchi, G.A., Werner, F.E., 2011. On the use of IPCC-class models to assess the impact of climate on living marine resources. *Prog. Oceanogr.* 88, 1–27.
- Stommel, H., 1948. The western intensification of wind-driven ocean currents. *Eos Trans. AGU* 29, 202.
- Stommel, H., 1960. Wind drift near the equator. *Deep Sea Res.* 6, 298.
- Stommel, H.M., 1957. A survey of ocean current theory. *Deep-Sea Res.* 4 (3), 149–184.
- Stommel, H., Arons, A.B., 1972. On the abyssal circulation of the World Ocean, V. The influence of bottom slope on the broadening of inertial boundary currents. *Deep-Sea Res.* 19, 707–718.
- Stommel, H., Yoshida, K., 1971. Some thoughts on the Cold Eddy south of Enshunada. *J. Oceanographical Society of Japan* 27 (5), 213–217.
- Stramma, L., 1984. Geostrophic transport in the Warm Water Sphere of the eastern subtropical North Atlantic. *J. Mar. Res.* 42, 537–558.
- Stramma, L., 1992. The South Indian Ocean Current. *J. Phys. Oceanogr.* 22, 421–430.
- Stramma, L., Lutjeharms, J.R.E., 1997. The flow field of the subtropical gyre in the South Indian Ocean. *J. Geophys. Res.* 99, 14053–14070.
- Sturm, M., Voigt, K., 1966. Observations on the structure of the Equatorial Undercurrent in the Gulf of Guinea in 1964. *J. Geophys. Res.* 71 (12), 3105–3108.
- Summerhayes, C.P., Rayner, R., 2002. Operational oceanography, Oceans 2020: Science, Trends, and the Challenge of Sustainability. In: Field, J., Hempel, G., Summerhayes, C. (Eds.), Island Press, pp. 187–207.

- Svendsen, I.A., Haas, K.A., Zhao, Q., 2000. Analysis of rip current systems. Proc. Coastal Eng. 2000, Sydney, Australia. Amer. Soc. Civil Engineers, pp. 1127–1140.
- Svendsen, I., Haas, K., Zhao, Q., 2001. Analysis of rip current systems. Am. Soc. of Civ. Eng., Sydney, Australia. paper presented at *27th International Conference on Coastal Engineering*.
- Sverdrup, H.U., 1947. Wind-driven currents in a baroclinic ocean, with application to the equatorial currents of the eastern Pacific. Proc. Natl. Acad. Sci. 33, 318.
- Swallow, J.C., 1964. Equatorial Undercurrent in the western Indian Ocean. Nature 204, 436–437.
- Swallow, J.C., Worthington, L.V., 1961. An observation of a deep counter-current in the Western North Atlantic. Deep-Sea Res. 8 (1), 1–19.
- Swift, J.H., 1995. Comparing WOCE and historical temperatures in the deep southeast Pacific. International WOCE Newsletter, No. 18, WOCE International Project Office, Southampton, U.K, 15–26.
- Taft, B.A., 1972. Characteristics of the flow of the Kuroshio south of Japan. In: Stommel, H., Yoshida, K. (Eds.), *Kuroshio, Its Physical Aspect*. University of Tokyo Press, Tokyo, Japan, pp. 165–216.
- Tang, E.-S., Dalrymple, R., 1989. Nearshore Circulation: Rip Currents and Wave Groups. In: Seymour, R.J. (Ed.), Plenum, New York, NY, USA.
- The Ring Group, 1981. Gulf Stream cold-core rings: Their physics, chemistry, and biology. Science 212, 1091–1100.
- Thompson, D.W.J., Solomon, S., 2002. Interpretation of recent Southern Hemisphere climate change. Science 296, 895–899.
- Tilburg, C.E., Hurlburt, H.E., O'Brien, J.J., Shriver, J.F., 2001. The dynamics of the East Australian Current System: The Tasman Front, the East Auckland Current, and the East Cape Current. J. Phys. Oceanogr. 31, 2917–2943.
- Tomosada, A., 1978. A large warm eddy detached from Kuroshio east of Japan. Bull. Tokai Reg. Lab. 94, 59–103.
- Tranter, D.J., Carpenter, D.J., Leech, G.S., 1986. The coastal enrichment effect of the East Australian current eddy field. Deep-Sea Research 33 (11/12 A), 1705–1728.
- Ulbrich, U., Leckebusch, G.C., Pinto, J.G., 2009. Cyclones in the present and future climate: a review. Theor. Appl. Climatol.. published online, doi: 10.1007/s00704-008-0083-8.
- van Leeuwen, P.J., de Ruijter, W.P.M., Lutjeharms, J.R.E., 2000. Natal pulses and the formation of Agulhas rings. J. Geophys. Res. 105, 6425–6436.
- Veth, C., Zimmerman, J.T.F., 1981. Observations of quasi-two-dimensional turbulence in tidal currents. J. Physical Oceanogr. 11, 1425–1430.
- Von Arx, W.S., Bumpus, D.F., Richardson, W.S., 1955. On the fine structure of the Gulf Stream front. Deep-Sea Res. 3, 46–65.
- Walker, N.D., 1990. Links between South African summer rainfall and temperature variability of the Agulhas and Benguela Current systems. J. Geophys. Res. 95, 3297–3319.
- Weart, S., 2009. Ocean currents and climate. In: *The discovery of global warming*. Harvard University Press.
- Webster, T.F., 1961. A description of Gulf Stream meanders off Onslow Bay. Deep-Sea Res. 8 (2), 130–143.
- White, J., 1590. Narrative of the 1590 voyage to Virginia. In: Quinn, D. (Ed.), *The Roanoke voyages*, vol. 2. Hakluyt Society, London, England.
- White, W.B., 1975. Secular variability in the large-scale baroclinic transport of the North Pacific from 1950–1970. J. Mar. Res. 33 (1), 141–155.
- White, W.B., McCreary, J.P., 1976. On the formation of the Kuroshio meander and its relationship to the large-scale ocean circulation. Deep-Sea Res. 23, 33–47.
- White, W.B., Peterson, R.G., 1996. An Antarctic Circumpolar Wave in surface pressure, wind, temperature, and sea-ice extent. Nature 380, 699–702.
- Wickham, J.B., 1975. Observations of the California counter current. J. Mar. Res. 33 (3), 325–340.
- Wille, R., 1960. Karman vortex streets. Advances in Applied Mechanics 4, 185–196.
- Williams, R.B., Gibson, C.H., 1974. Direct measurements of turbulence in the Pacific Equatorial Undercurrent. J. Phys. Oceanogr. 4 (1), 104–108.
- Wilson, W.S., Dugan, J.P., 1978. Mesoscale thermal variability in the vicinity of the Kuroshio Extension. J. Phys. Oceanogr. 8, 537–540.
- Wolff, J.O., Olbers, D., Maier-Reimer, E., 1991. Wind-driven flow over topography in a zonal β -plane channel: A quasigeostrophic model of the Antarctic Circumpolar Current. J. Phys. Oceanogr. 21, 236–264.
- Wolff, J.O., Ivchenko, V.O., Klepikov, A., Olbers, D., 1990. The topographic influence on the dynamics of zonal fluxes in the ocean. Dokl. Acad. Nauk SSSR 313, 970–974.
- Wunsch, C., Stammer, D., 1995. The global frequency-wave-number spectrum of oceanic variability estimated from TOPEX/Poseidon altimetric measurements. J. Geophys. Res. 100, 24895–24910.
- Wyrtki, K., 1973. An equatorial jet in the Indian Ocean. Science 181, 262–264.
- Wyrtki, K., 1962. Geopotential topographies and associated circulation in the western south Pacific ocean. Aust. J. Marine Freshwater Res. 13, 89–105.
- Zenk, W., Muller, T.J., 1988. Seven-year current meter record in the eastern North Atlantic. Deep-Sea Res. 35 (8), 1259–1268.
- Zharkov, V., Nof, D., 2010. Why does the North Brazil Current regularly shed rings but the Brazil Current does not? J. Phys. Oceanogr. 40, 354–367.
- Zimmerman, J.T.F., 1978. Topographic generation of residual circulation by oscillatory (tidal) currents. Geophys. Astrophys. Fluid Dyn. 11, 35–47.
- Zimmerman, J.T.F., 1980. Vorticity transfer by tidal currents over an irregular topography. J. Mar. Res. 38, 601–630.